FREQUENCY DEPENDENT ELECTROMAGNETIC FIELDS: MODELS APPROPRIATE FOR THE BRAIN

Thesis by

Harrison Mon Fook Leong

In Partial Fulfillment of the Requirements

for the Degree of

Doctor of Philosophy

California Institute of Technology

Pasadena, California

1986

(Submitted December 27, 1985)

Acknowledgements

The bulk of my research was supported by an NRSA traineeship, grant number 5T320GM07737050061. The latter years were supported with funds from Dr. John Hestenes at JPL, NDSL loans, and Caltech loans. I thank Dr. Geoffery Fox for allowing me to participate in the Caltech parallel computation project. I am very grateful for having received this support. I hope my contributions to the happiness of mankind will far exceed this investment. I would like to recognize the personnel of Caltech; many of them have helped me achieve my ends. I wish to thank Dr. Stanley Klein for directing me toward the clutches of brainwave research and finally to Caltech. I would like to express my appreciation for Dr. Derek Fender whose patience and tolerence took me through these stormy years. I will carry his insights far into the future. I would like to thank Sandy Griffon who gave me reassurance at a critical time. Dr. Christopher Barrett gave me insights and inspiration, clarifying my relationship to science. Dr. Jay Myers and Dr. Budd Fried have given me years of friendship and a universe of ideas. I can never thank my parents enough for providing a blanket of security and encouragement...my sister too. Finally, I would like to mention my wife, Rita, who drove me to heights of emotion I never dreamed could exist (within me).

ABSTRACT

This dissertation addresses the problem of modeling electromagnetic fields in and about the brain-skull-scalp system that are generated by active neural populations. Specifically, frequency dependence of Maxwell's fields is explored for the case of a dipole-like current source embedded in a spherical conductor surrounded by a vacuum. Frequency dependence was found to be small. Loosely, the difference between frequency dependent and frequency independent fields reached approximately 1% at 10^3Hz and reached up to 16% at 10^4Hz. Frequency dependence was found to be highly dependent on conductivity, the size of the conductor, and on the phase of generated fields. These findings indicate that the degree to which the magnetic field is coupled to the electric field depends on interference patterns occuring within the conductor. Several highly distinguishable exceptions to general trends in the data were found to be consistent with this view.

Table of Contents

1. Introduction

In this dissertation I concern myself with modeling electromagnetic fields in and about the brain that arise from neurological activity. I am particularly interested in modeling electromagnetic fields observed at the human scalp-air interface. Maxwell's equations are taken to be the best available model[1-1]. Difficulties in applying the full equations to the situation dealt with here necessitate further abstractions. From among the possible formulations, I chose to compare a model where fields are assumed frequency independent with a comparable model containing frequency dependence.

1.1 Theoretical motivations

In order to clarify how the comparison pertains to modeling electromagnetic measurements, I would like to make the following digression. Optimally, one would like to ascertain the consequences of making modeling abstractions on the predictive power of the resultant model. There are two ways to do this. One way is to compare theoretical predictions with electromagnetic recordings from the system of interest. The other way is to assess the extent to which the introduction of a modeling simplification perturbs theoretical predictions from those given by the best available model. The work done here falls under the second category: the difference between predictions of frequency independent models and frequency dependent models is calculated where the model with frequency dependence is deemed a closer approximation to the best available model.

For the electromagnetic situation of interest here, the relevance of a theoretical approach is illustrated by the following two points. Experiments

1-1 I use ***available*** model to refer to models wherein all parameters of the model are not necessarily specifiable in practice.

showing the predictive power of Maxwell's equations are well known. Considering this evidence, it is very likely that inadequacies in modeling electromagnetic fields in and about the brain are a result of simplifications in the application of Maxwell's model rather than inadequacies of this model. My second point stems from considering one of the major goals behind finding a description for electromagnetic fields observed at the scalp. This goal is to characterize the sources of the observed fields. Unfortunately, at present, there is no way to characterize these sources independent of Maxwell's model. Furthermore, characterizing these sources based on the best computable Maxwell's model requires techniques that would result in damaging the brain. This means there is, at present, no way to assess the predictive power of theoretical models. The consequence is that we are not afforded the luxury of minimizing the complexity of theoretical models using cross-validation between theory and experiment. At best, predictive power can be assessed with respect to best computable models; at worst, we must maximize model complexity within domains of computability and have faith that they adequately approximate best available models. Between these two extremes, we can try to isolate the effects of certain simplifying assumptions by comparing simple models to models at a higher order of complexity. In this way, we can give support to the use of simple models. As we have seen above, this is the route pursued here with the simplifying assumption under question being frequency independence of the electromagnetic fields.

Choosing to focus on frequency dependence issues was motivated by noting that there seemed to be no simple way to assess the significance of magnetic induction when space was not assumed electromagnetically homogeneous. Making this assessment was motivated by noting that ignoring magnetic induction would significantly simplify Maxwell's model. A simple assessment with

respect to a model that uses magnetic permeability, μ, electric permitivity, ε, and conductivity, σ, to model charges and currents that would otherwise be impossible to specify has been obtained for the case of electromagnetically homogeneous media [88], i.e., where μ, ε, and σ are assumed constants independent of space and take on values appropriate for biological tissues. Unfortunately, the head system, consisting of the brain, skull, scalp, intervening tissues, and the surrounding air, is far from being electromagnetically homogeneous. Thus, the frequency dependence issue seems basic to inhomogeneous μ, ε, and σ models since it surfaces at the first stages of analysis. In contrast, at this time, all μ, ε, and σ models used to describe electric potential measurements in and about neurons [56, 57, 94], magnetic measurements about neurons [112], gross electric potentials at the surface and within the body [19, 22, 50, 51, 82, 88], and gross magnetic fields at the surface of the body [30, 52] have assumed frequency independence.

1.2 Experimental motivations

In the opening section of this dissertation, I have motivated, on theoretical grounds, investigating frequency independent models with respect to models that account for this dependence. The major question at this point is whether or not there are experimental reasons for such an investigation.

1.2.1 Experimental sufficiency of frequency independent models

Is there any evidence indicating the sufficiency of frequency independent models for describing electromagnetic data recorded at the scalp? I will briefly mention several relevant experiments.

1.2.1.1 For electric potential measurements Many investigators have used core conductor theory to successfully model electric potentials occurring within

neurons and at neural surfaces, most notably [56, 57, 91, 94]. The theory is based on Ohm's law. The theory does account for frequency dependence in the sense that capacitor/resistor circuits can exhibit frequency dependent behavior; however, magnetic induction is explicitly ignored since no inductors are used. Neuron models based on core conductor theory have been used to successfully model extracellular intracranial electric potential measurements of electric fields arising from stimulation of the olfactory bulb in rabbits [92, 93] and stimulating the medullary pyramid of cats [60, 61]: several theoretical neurons were superposed in special geometric configurations and zero frequency field equations, wherein it was assumed that the neurons were embedded in a conductor of infinite extent, were then used to make predictions. In the following list, I tabulate investigations wherein Maxwell's field equations for zero frequency and conductors of finite extent were used to model experimental observations.

1. [97] modeled electric potential measurements gathered from the surface of a half skull in an electrolytic case where electrodes had been placed on the edge and operated from 50Hz to 5kHz. He used a three-shell model for the head system: four concentric regions of constant conductivity where conductivity had only radial dependence. This model was also used to model electric potential measurements gathered from the cortical surface of humans and spider monkeys where current sources had been imposed at the surface.

2. [18] modeled electric potential measurements gathered from an electrolytic tank model of the human torso with embedded electric dipoles. This device accounted for conductivity inhomogenaities and anisotropies similar to those found in humans. They used numerical integration to solve an electric potential boundary integral equation for a torso-shaped conductor.

Source parameters were adjusted to minimize the discrepancy between theoretical predictions and potential measurements.

3. [58] compared predictions of a four-shell model to electric potential measurements gathered from the scalp and cortical surface of monkeys. These monkeys had electric dipole sources implanted within their brains. The dipoles were operated at sub-stimulation levels from 10Hz to 500Hz.

4. [103] compared predictions of a one-shell model to electric potential measurements gathered from within the brains of humans where current dipole sources had been inplanted. Dipoles were operated at substimulation levels using a square wave. (The fundamental frequency was not reported.)

5. [114] compared predictions of a finite element model of a brain, which utilized a sophisticated conductivity topology, to intracranial electric potential measurements taken from a cat brain. Electric dipoles had been implanted and activated with a damped 500Hz sine wave.

With theoretical predictions falling within estimates of experimental error, these experiments indicate the sufficiency of frequency independent models for describing electric potential measurements. An exception is data of [58] where theoretical predictions were poor along sagittal contours of the scalp. The sphericity of the head in the sagittal direction is lower than in the coronal direction; thus, inaccuracies of theoretical predictions probably stem from difficulties in mapping data from a non-spherical surface to a spherical one. In conclusion, the indications are that it is safe to assume the electric field frequency independent, other aspects of modeling being more important.

1.2.1.2 For magnetic measurements Though frequency independent models of the electric field may be sufficient to model electric field observations, does this imply sufficiency of magnetic field models based on the same assumption?

Examining Maxwell's equations reveals that the answer is no. (We would need to assume $\|\nabla\Phi\| \gg \|\frac{\partial}{\partial t}\vec{A}\|$ implies $\|\frac{\partial}{\partial t}\nabla\Phi\| \gg \|\frac{\partial^2}{\partial t^2}\vec{A}\|$.) Thus, we need experimental evidence. Two studies wherein comparisons between theoretical and experimentally observed magnetic fields are reported will be discussed below.

Electrolytic tank experiments were done ([30], Cohn and Hosaka) to observe whether or not the magnetic field component normal to the conductor surface was independent of currents induced in the conductor by an implanted current source. This hypothesis is predicted for several conductor geometries by frequency independent μ, ε, and σ models [32, 52]. The conductor used did have one of these shapes. I compare two of Cohen and Hosaka's experiments . Referring to figure 1-1, $\frac{\partial B_z}{\partial x}$ was measured along the line z=h, y=0 for a dipole current source (2mA, 0.5→1.5cm length, 3kHz) in air and submerged in a cubical electrolytic tank with the saline solution (conductivity, 3.3 mho/m) coming up 3cm above the dipole. (Other experimental manipulations involved putting insulators into the tank and using a dipole source oriented along the z axis.) Graph 1-1 shows a plot of the data where theoretical solutions for the case of a homogeneous medium, applicable for both frequency dependent and frequency independent electromagnetic fields, are drawn in to indicate data reliablility. Theoretical curves (dotted) have been normalized by setting

$$\frac{\mu_0 J}{4\pi} = \begin{cases} 2\text{x}10^5 & : h = 10\text{cm} \\ 2.3\text{x}10^4 & : h = 8\text{cm} \end{cases} \qquad (1\text{-}1)$$

where J is the magnitude of the current dipole and μ_0 is the permeability of free space.

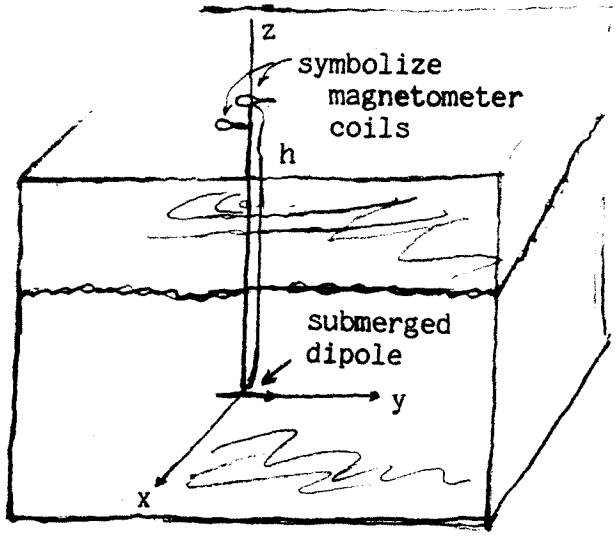

Figure 1-1

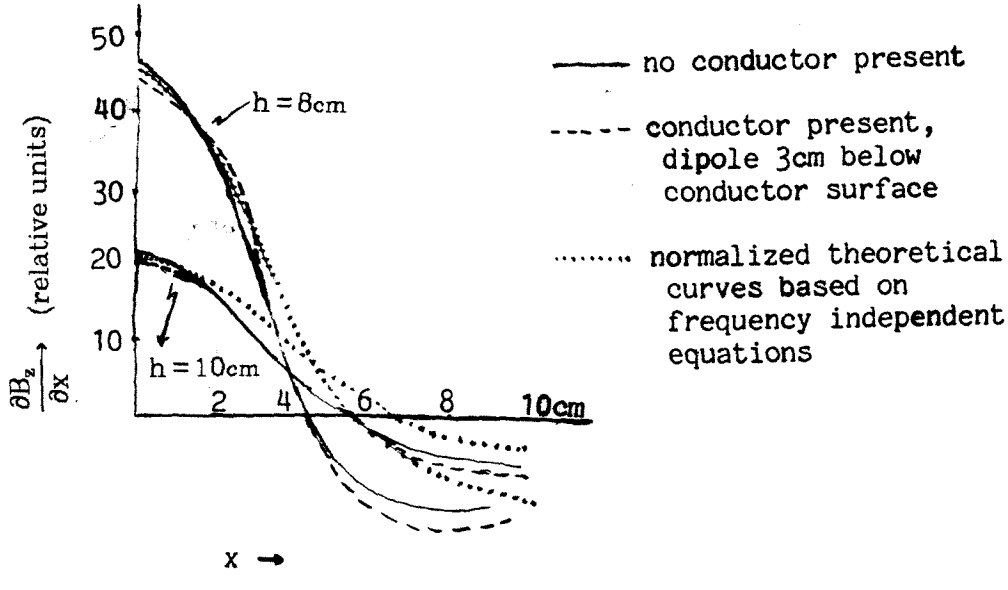

Graph 1-1

Comparing dashed and solid curves, one gathers that the imposition of the conducting medium does not result in changing $\frac{\partial B_z}{\partial x}$. It is unclear whether or not these observations would be predicted by frequency dependent equations. It can be said that, for this experiment, the frequency independent equations appear to be a sufficient model.

An effort was made to model electromagnetic fields at the scalp produced by one of the sources evoked by stimulation of the median nerve ([31], Cohn and Cuffin). The source was modeled by a current dipole. Contributions to the observed fields by, presumably, sources other than the one of interest were removed. Then, modeling parameters such as conductivity values and dipole parameters were adjusted so that theoretical predictions based on frequency independent equations optimally matched the processed data. The validity of these procedures rested on the observation that the model's dipole location did approximate the location expected for neural sources speculated to be responsible for the observed fields. Unfortunately, this experimental design does not allow one to draw conclusions about whether or not discrepancies between theory and experiment fall within experimental error.

In summary, it can be observed that no experiments have been performed where, for electromagnetic fields associated with naturally occurring sources, the accuracy of theoretical models could be assessed. However, evidence has been presented that suggests the sufficiency of frequency independent equations for modeling bioelectromagnetism as is measured by present experimental techniques.

1.2.2 Experiments of the future

With the conclusion made above, one is left wondering whether or not present technology has the sensitivity required to detect frequency

dependence in fields produced by the brain. The following discussion suggests that simultaneous measurement of both magnetic and electric fields may provide this sensitivity.

Here, I further examine results reported by Cohn and Cuffin. Consider figure 1-2. The figure illustrates electric potential contours and contours for the signed magnitude of the magnetic field's radial component that would be observable at the surface of a conductor if a current dipole existed within.

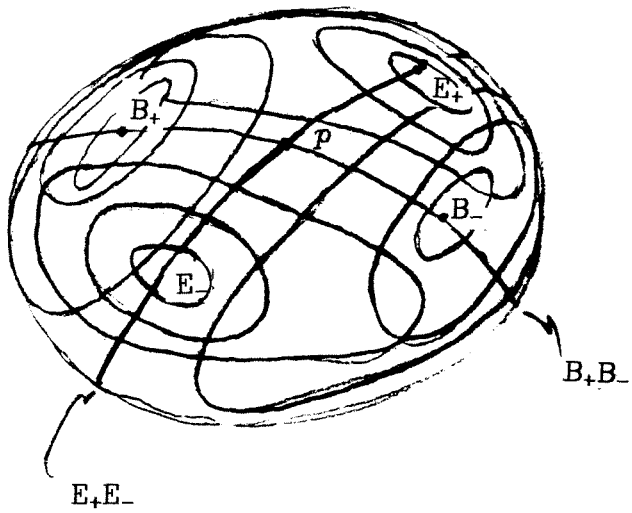

Figure 1-2

If the conductor were spherical, frequency independent equations would predict $E_+E_- \perp B_+B_-$ at point p; however, in Cohen and Cuffin's experiment, mapping observed fields at the scalp onto the surface of a sphere reveals that $E_+E_- \not\perp B_+B_-$. Deviation from perpendicular is on the order of 10°. There is no reason to believe frequency dependence is solely responsible for the observed

discrepancy. Two additional aspects of modeling must be considered: source models and the specification of μ, ε, and σ. If we can assume that source models associated with biextrema surface fields can be effectively modeled by superpositions of current dipoles, from linearity of Maxwell's equations, source models more complex than a simple current dipole would still have $E_+E_- \perp B_+B_-$; such models are explored in [34, 36]. This is the extent of current knowledge about the dependence of the fields on source models. Effects of parameters μ and ε have not been explored; in fact, for frequency independent models, ε is excluded. For σ, a study in modeling the torso by [54] shows that E_+E_- in sophisticated inhomogeneous models is rotated relative to its orientation for simpler inhomogeneous models, the simplest being a torso shaped conductor of uniform conductivity. If we take into consideration the observation that the normal component of magnetic surface fields are, based on frequency independent models, independent of conduction currents for several conductor shapes, relative rotations resulting from conductivity inhomogenaities may be indicated. It is very likely that conductor shape has something to do with observed relative rotations: to obtain comparisons of Cohen and Cuffin, note that experimental data from a nonspherical geometry had to be mapped onto a spherical geometry. The effects of doing this have not been systematically examined. Finally, observed discrepancies may exist because magnetic and electric fields were not observed simultaneously. In addition, magnetic fields were constructed from observations at single locations. It can be concluded that Cohen and Cuffin's study does not exhibit the ability to detect effects resulting from frequency dependence.

In spite of this conclusion, the study does point the way toward developing the technology that would have the sensitivity required for detecting frequency dependence in neurologically generated fields. Suppose theoretical

calculations reveal peculiarities in the relationship between magnetic and electric fields resulting from frequency dependence. Given we can surmount the problems associated with modeling σ, we may be able to detect these effects through simultaneous observation of electric and magnetic fields. Just as a balance provides the sensitivity required to weigh large and small loads, the ability to observe the relationship between the two fields may be exactly the capability that is needed.

1.3 Previous work on frequency dependent equations

Obviously, most work done on frequency dependent equations focuses on frequencies at which electromagnetic radiation occurs. However, I am strictly interested in non-radiating electromagnetic fields in and about conducting media. The area of inquiry where I have found frequency dependent equations dealt with under the appropriate conditions is eddy current analysis. Some recent work in this field has included

A. representing Maxwell's equations in terms of

   1. various potential fuctions [28, 83, 90],

   2. circuit elements where network theory is used to develop models [17, 27, 38], and

   3. current and electric or magnetic charge densities [67, 76],

B. applying finite element methods to volumn integral formulations [23, 96] and to differential equation formulations [78], both in the potential function domain, and

C. applying boundary integration methods to integral formulations in the potential domain [21, 37].

In most of these studies, the source was external to the conducting medium in

which one wishes to know the currents and magnetic field. In a few, the magnetic field at the conductor surface had to be specified. I stumbled across one study wherein the source was inside the conductor ([21, 37], Barnes and Davey). Barnes and Davey calculated the magnetic field strength arising from a dipole current source embedded 5m below the surface of a semi-infinite medium with a planar boundary. They reported values for magnetic field strength in the conductor at the depth of the dipole and in the air a height 10m above the conductor surface. They examined frequencies $1, 10^3$, and 10^5Hz and conductivities 4 and 10^3mho/m. Unfortunately, they did not report data that would allow making a comparison between the near 0Hz cases and higher frequency cases. One more point is worth mentioning: they assumed that the tangential component of $\vec{B}$ was continuous across the conductor boundary. Given a boundary condition approach to solving Maxwell's equations, this means $\vec{E}$ must be normal or 0 at the boundary. If this were true for the situation of interest here, the scalp would be an equipotential surface. In conclusion, as far as I know, there have been no previous studies on electromagnetic frequency dependence under the conditions addressed in this dissertation.

1.4 Final introductory remarks

The chapters that follow will be introduced by stating, in general terms, the stages of abstraction I will use in model development. Doing this will provide a context with which to view this work. The data to be modeled comes from electrode and magnetometer or gradiometer readings at the scalp-air interface. At certain points in the modeling process, choices will be made that cannot be traced back to their effects on answers obtained. These points separate levels of a hierarchy of models. In this context, a choice cannot be justified by claiming the resultant model produces solutions differing negligibly from those produced by the model one level up. The first model I will use associates

measurements to be modeled with the sampling of electromagnetic fields described by Maxwell's free space equations, $\vec{E}$ and $\vec{B}$. Here is the subsequent hierarchy of modeling choices:

LEVEL 2: Charges and charge movements will be separated into types and some of these will be accounted for using the functions μ, ε, and σ. This step is where characteristics of media to be dealt with will be defined such as media geometry, homogeneity, and directional dependence of properties (isotropic or anisotropic). This step is unavoidable since, in principle, it is impossible to explicitly account for all charges and their movements.

At this point, model 2 will be transformed into a domain of electromagnetic potentials: the scalar potential Φ and the vector potential $\vec{A}$. These potentials are determined by the functions μ, ε, and σ and $\vec{J}_{r(emainder)}$; $\vec{J}_r$ represents currents unaccounted for by μ, ε, and σ.

LEVEL 3: $\vec{J}_r$ will be separated into current types. Models will be chosen for current components thought mainly responsible for the dipole-like fields. The models will be used in place of $\vec{J}_r$. Significance of changes in solutions to the level 2 model resulting from this choice cannot be assessed since some $\vec{J}_r$ components are impossible to model. For example, in specifying μ, ε, and σ, the currents presumably accounted for cannot be completely represented for two reasons: 1) it is impossible to know ideal μ, ε, and σ appropriate for the model at level 1, and 2) μ, ε, and σ must be experimentally determined which implies they are known at finite precision. The component of current left in $\vec{J}_r$ associated with this incompleteness cannot be modeled. Other remainders ignored by level 3 decisions include physical processes too difficult to model and

those that are unknown.

LEVEL 4: Spacial averages will be taken which convert volumn integrals involving derivatives of μ, ε, and σ into surface integrals. This procedure is required as a result of the methodology used to define μ, ε, and σ.

LEVEL 5: Model 4 is simplified by ignoring several terms based on the experimental precision at which μ, ε, and σ are known and an assessment of relative magnitudes between terms of the equations. For some terms, the consequence of doing this can be assessed; for other terms, there is no way to predict how ignoring them will effect the model. This procedure is necessary for practical reasons. Keeping some terms would mean numerical methods could not be used to solve the equations. Ignoring other terms significantly simplifies the task of implementing numerical procedures.

LEVEL 6: Quantities will be represented by a finite number of digits. For some quantities such as surface normal vectors and distances between surface points, the effect of doing this cannot be assessed. The procedure could be viewed as another form of ignoring terms.

This list is not to be viewed as the order by which model development proceeds. It is to be used as the context with which to perceive the measures taken in the following chapters.

2. Applying Maxwell's model to the problem

2.1 Simplifying Maxwell's model

Starting with the free-space equations

$$\nabla \cdot \varepsilon_0 \vec{E} = \rho \qquad (2\text{-}1a)$$

$$\nabla \times \frac{1}{\mu_0} \vec{B} = \vec{J} + \frac{\partial}{\partial t} \varepsilon_0 \vec{E} \qquad (2\text{-}1b)$$

$$\nabla \cdot \vec{B} = 0 \qquad (2\text{-}1c)$$

$$\nabla \times \vec{E} = -\frac{\partial}{\partial t} \vec{B} \qquad (2\text{-}1d)$$

the initial step toward finding solutions is to specify the functions ρ (charge density) and $\vec{J}$ (current density). This will be done by distinguishing several forms of charge and charge movement then hypothesizing how each form contributes to ρ and $\vec{J}$. At this stage, I will attend to charges and currents that must be accounted for in terms of macroscopic properties of matter. The following discussion is based on the work of [Feynman, Hayt, Elliot, Jackson].

A distinction is made for charge and current arising from mutually bound pairs of opposite charges. Since charges of each pair move in opposite directions in response to an electric field not associated with them, each pair contributes a dipolar electric field to the imposed field and a magnetic field associated with a current filament. Examples include electrons and nuclei of atoms and macromolecules with ionic sites. I will use the labels $\rho_{p(olarization)}$ and $\vec{J}_{p(olarization)}$. Another distinction is made for current arising from nuclei and electron spins and relative motion of electrons about nuclei. These currents effect a net dipolar magnetic field that can be modulated, in direction and

magnitude, by a magnetic field not associated with them. This works mainly by modulating the dipolar field contributed by orbital electron motion. I will use the label $\vec{J}_{a(tomic)}$.

Obviously, it is unreasonable to try to explicitly model ρ_p, $\vec{J}_p$, and $\vec{J}_a$. To resolve this problem, a set of macroscopic properties can be defined such that resultant parameterized equations only have explicit dependence on current and charge densities that can be, presumably, accounted for explicitly. The consequence of doing this is that equations will no longer express relationships between quantities evaluated at a mathematical point but will express the relationship between quantities that are spacial averages; the spacial resolution defined by this average will be referred to with the label δv. Writing solutions to equations 2-1 as the superposition of solutions from the two systems

$$\nabla \bullet \varepsilon_0 \vec{E}_1 = \rho_p \qquad (2\text{-}2a)$$

$$\nabla \times \frac{1}{\mu_0} \vec{B}_1 = \vec{J}_a + \vec{J}_p + \frac{\partial}{\partial t} \varepsilon_0 \vec{E}_1 \qquad (2\text{-}2b)$$

$$\nabla \bullet \vec{B}_1 = 0 \qquad (2\text{-}2c)$$

$$\nabla \times \vec{E}_1 = -\frac{\partial}{\partial t} \vec{B}_1 \qquad (2\text{-}2d)$$

and

$$\nabla \bullet \varepsilon_0 \vec{E}_2 = \rho_{r(emainder)} \qquad (2\text{-}3a)$$

$$\nabla \times \frac{1}{\mu_0} \vec{B}_2 = \vec{J}_r + \frac{\partial}{\partial t} \varepsilon_0 \vec{E}_2 \qquad (2\text{-}3b)$$

$$\nabla \bullet \vec{B}_2 = 0 \qquad (2\text{-}3c)$$

$$\nabla \times \vec{E}_2 = -\frac{\partial}{\partial t}\vec{B}_2 \qquad (2\text{-}3d)$$

where ρ_r represents charge densities unaccounted for by ρ_p and $\vec{J}_r$, is associated with current densities unaccounted for by $\vec{J}_a$ and $\vec{J}_p$, the parameterization we need is found by investigating how electromagnetic fields of equations 2-2 depend on fields of equations 2-3. If the media of concern are non-ferromagnetic, non-ferroelectric, isotropic, and do not exhibit hysteresis, it turns out that, in the frequency domain, the dependence can be expressed as a scalar proportionality. There have been no reports indicating that media of concern here fail to met these requirements. Before writing down the relationships sought, here is the notation that will be used: $<>_{u,v(x;y)}$ implies the average over subset v, a function of variables x and parameters y, of domain u. General function notation is this: F(independent variables; parameters) where parameters may depend on independent variables. $|_c$ implies evaluation under the important conditions c or evaluation at point c. The condition, vac(uum) will be used to emphasize that a function is one at the modeling level of equations 2-1. The label for the modeling level being described at this time will be mat(ter). ${}^{\omega}F$ is used to notate $F(\omega)$, coefficients of the frequency domain. Continuing, in terms of the net fields of equations 1, the conventional notation is

$$<{}^{\omega}\vec{E}_2>_{\vec{x},\Delta v(\vec{x})}\Big|_{vac} = \frac{{}^{\omega}\varepsilon}{\varepsilon_0}<{}^{\omega}\vec{E}>_{\vec{x},\Delta v(\vec{x})}\Big|_{vac} \qquad (2\text{-}4)$$

and

$$<{}^{\omega}\vec{B}_2>_{\vec{x},\Delta v(\vec{x})}|_{vac} = \frac{\mu_0}{{}^{\omega}\mu}<{}^{\omega}\vec{B}>_{\vec{x},\Delta v(\vec{x})}|_{vac} \qquad (2\text{-}5)$$

where ε is the electric permittivity and μ is the magnetic permeability. It follows that the equations sought are derived by taking spacial averages of equations 2-3a and 2-3b at resolution δv, writing these expressions in terms of the net fields, and combining resulting expressions with spacial averages, at resolution δv, of equations 2-1c and 2-1d.

Before arriving at the final system of equations to be solved, I must deal with two more issues. First, I would like to distinguish one other type of current that can be accounted for in terms of electromagnetic fields. Distinguish $\vec{J}_{c(onductivity)}$ where $\vec{J}_{r'}=\vec{J}_r+\vec{J}_c$. $\vec{J}_c$ is associated with charges that can move indefinite distances in response to an electric field distinct from its own. When this charge movement is spacially averaged, in the frequency domain it is expressable as a tensor proportionality to the imposed electric field. At the spacial resolution required to consider the brain an electromagnetically homogeneous medium, an accurate brain model should be anisotropic in conductivity. However, at this time, I will assume all media of interest are sufficiently modeled by assuming isotropy; this simplifies the modeling process considerably since the tensor reduces to a scalar. $\vec{J}_c$ is handled by defining a parameter σ such that it can be expressed in terms of the net field:

$$<{}^{\omega}\vec{J}_c>_{\vec{x},\Delta v(\vec{x})}|_{mat} \equiv {}^{\omega}\sigma\ <{}^{\omega}\vec{E}>_{\vec{x},\Delta v(\vec{x})}|_{mat} \qquad (2\text{-}6)$$

Secondly, there is a problem with choosing a uniform spacial resolution for the equations. The discussion above indicates that the size of the region over which averages are taken is dependent on ρ and $\vec{J}$ component types, i.e., $\Delta v=\Delta v(\vec{x};\ g):g\in[\mu, \varepsilon, \sigma]$. Since all components appear at once in one of the equations, to make all equations consistent, a volume function that is single valued

at all $\vec{x}$ must be used. $\Delta v_{max}(\vec{x}) \equiv \underset{g}{MAX}\, \Delta v(\vec{x};g)$ seems a reasonable choice since, clearly, using a smaller volume would render at least one of the parameters μ, ε, and σ ill defined. In the frequency domain, the transformed equations are as follows:

$$\nabla \bullet {}^{\omega}\varepsilon <{}^{\omega}\vec{E}>_{\vec{x},\Delta v_{max}(\vec{x})} | \, mat = <{}^{\omega}\rho_r>_{\vec{x},\Delta v_{max}(\vec{x})} \tag{2-7a}$$

$$\nabla \times \frac{1}{{}^{\omega}\mu} <{}^{\omega}\vec{B}>_{\vec{x},\Delta v_{max}(\vec{x})} | \, mat = \begin{bmatrix} <{}^{\omega}\vec{J}_r>_{\vec{x},\Delta v_{max}(\vec{x})} + {}^{\omega}\sigma <{}^{\omega}\vec{E}>_{\vec{x},\Delta v_{max}(\vec{x})} | \, mat \\ + {}^{\omega}\varepsilon i\omega <{}^{\omega}\vec{E}>_{\vec{x},\Delta v_{max}(\vec{x})} | \, mat \end{bmatrix} \tag{2-7b}$$

$$\nabla \bullet <{}^{\omega}B>_{\vec{x},\Delta v_{max}(\vec{x})} | \, mat = 0 \tag{2-7c}$$

$$\nabla \times <{}^{\omega}\vec{E}>_{\vec{x},\Delta v_{max}(\vec{x})} | \, mat = -i\omega <{}^{\omega}\vec{B}>_{\vec{x},\Delta v_{max}(\vec{x})} | \, mat \tag{2-7d}$$

In subsequent text, the averaging notation and evaluation specifications used at this modeling level will be dropped. In addition, all expressions will be written in terms of the frequency domain coefficients of electromagnetic parameters and fields unless the time domain counterpart is to be emphasized where F(t) will be notated ${}^{t}F$. As a final note, ρ_p, $\vec{J}_p$, $\vec{J}_a$, and $\vec{J}_c$ are associated with actual charges in the sense that they model a specific behavior of the specified charges. Thus, these labels do not account for the actual charges though we wish this to be so for $\vec{J}_a$ and, to a large extent, ρ_p and $\vec{J}_p$. But, as will be seen in the last section of this chapter, there are behaviors of unbound charges of great interest not accounted for by $\vec{J}_c$.

2.2 Conversion to potential equations

It is known from vector calculus that equation 2-7c implies

$$ {}^{t}\vec{B} = \nabla \times {}^{t}\vec{A} \tag{2-8a} $$

and with equation 2-8a, equation 2-7d implies

$$ {}^{t}\vec{E} + \frac{\partial}{\partial t}{}^{t}\vec{A} = -\nabla {}^{t}\Phi \tag{2-8b} $$

where ${}^{t}\vec{A}$ and ${}^{t}\Phi$ are arbitrary vector and scalar fields respectively. Thus, in solving for these quantities, we are insured equations 2-7c and 2-7d are satisfied. Application of equations 2-8a and 2-8b to equation 2-7b with expansion leads to

$$ \frac{1}{\mu}\nabla^2\vec{A} = -\vec{J}_r + \nabla\frac{1}{\mu} \times \nabla \times \vec{A} + \frac{1}{\mu}\nabla(\nabla \bullet \vec{A}) + \tilde{\sigma}(\nabla\Phi + i\omega\vec{A}) \tag{2-9a} $$

where $\tilde{\sigma} \equiv \sigma + i\omega\varepsilon$. Taking the divergence of transformed equation 2-7b, using equations 2-8, and expanding leads to

$$ \nabla \bullet \tilde{\sigma}\nabla\Phi = \nabla \bullet \vec{J}_r - i\omega(\nabla\tilde{\sigma} \bullet \vec{A} + \tilde{\sigma}\nabla \bullet \vec{A}) \tag{2-9b} $$

Equation 2-7a converts to

$$ \nabla \bullet \varepsilon(\nabla\Phi + i\omega\vec{A}) = -\rho_r \tag{2-9c} $$

One more quantity needs specification. From Helmholtz's decomposition theorem, we are free to specify $\nabla \bullet \vec{A}$ having only specified $\nabla \times \vec{A}$. There are two common choices:

$$ \nabla \bullet \vec{A} = -\mu(\sigma + i\omega\varepsilon)\Phi \tag{2-10a} $$

and

$$\nabla \bullet \vec{A} = 0 \qquad (2\text{-}10b)$$

Equations 2-9 with one of equations 2-10 summarize the complete conversion of equations 2-7 to the potential domain.

A few steps can be taken to simplify this system of equations. First, note that equation 2-9c need not be dealt with further if, in the system of interest and spacial resolution assumed, the component of average charge density invariant with time is zero everywhere. In terms of equations 2-7, the reasoning behind this point is as follows: satisfying the time derivative of equation 2-7a (which is the divergence of equation 2-7b through charge conservation) implies equation 2-7a is satisfied since the constant of integration is known to be zero. The application to the system of potential equations is obvious. Another step of simplification involves the choice of gauge, equations 2-10. It would be best to use Coulomb's gauge (eq. 2-10b) since irrotational and rotational components of $\vec{E}$ would be nicely separated; this would simplify assessing the degree to which $\vec{E}$ depends on $\vec{B}$. Unfortunately, using this gauge would lead to equations with volume integrals involving Φ. In contrast, the Lorentz gauge (eq 2-10a) results in integral equations depending only on $\vec{A}$ and Φ values at the interfaces between regions of constant μ, ε, and σ; this simplifies determining values for the potentials. With this gauge, the system of equations to be solved is

$$\nabla^2\vec{A} = -\mu\vec{J}_r - \Phi\nabla\mu\tilde{\sigma} + \mu\nabla\frac{1}{\mu}\times\nabla\times\vec{A} + i\omega\mu\tilde{\sigma}\vec{A} \qquad (2\text{-}11a)$$

$$\nabla \bullet \tilde{\sigma}\nabla\Phi = \nabla \bullet \vec{J}_r - i\omega\nabla\tilde{\sigma} \bullet \vec{A} + i\omega\mu\tilde{\sigma}^2\Phi \qquad (2\text{-}11b)$$

In the next section, formulas needed to convert these equations to integral equations will be derived by examining the equation which is representative of

both of equations 2-11.

$$\nabla\bullet\,\beta\nabla\varphi_1 = \varphi_2 + \alpha^2\beta\varphi_1 \qquad (2\text{-}12)$$

2.3 Conversion to integral equations

A common trick to obtain implicit integral equations for φ_1 at some point $\vec{x}_{f(ield)}$ from equation 2-12 is to apply the divergence theorem to the divergence of

$$G(\vec{x},\vec{x}_f) = \beta(\varphi_1\nabla\frac{\tilde{e}}{R} - \frac{\tilde{e}}{R}\nabla\varphi_1) \qquad (2\text{-}13)$$

where $\vec{R} = \vec{x}-\vec{x}_f$, and $\tilde{e} = e^{\pm\sqrt{\alpha^2}R}$. (The sign will be specified shortly.) The volume over which we apply the divergence theorem is taken to be all space. This choice and choosing $\tilde{e} = e^{-\sqrt{\alpha^2}R}$ allows us to merely assume φ_1 bounded at infinity in the following sense:

$$\left|\int_{\partial V_\infty}\beta\varphi_1\sin\theta d\theta d\varphi\right| < \infty \qquad (2\text{-}14)$$

Choosing any finite volume would require stronger assumptions about the nature of φ_1 at the boundary. Choosing the (+) sign would do the same thing since, for equations 2-11, $\sqrt{\alpha^2}$ does have a non-zero real part. Proceeding with applying the divergence theorem to function G, equation 2-15 is obtained.

$$-4\pi(\beta,\varphi_1)_\infty + \lim_{\delta\to 0^+}\int_{V_\delta(\vec{x}_f)}\frac{\tilde{e}}{R}\nabla\bullet\,\beta\nabla\varphi_1 - \beta\varphi_1\nabla^2\frac{\tilde{e}}{R} - \varphi_1\nabla\beta\bullet\nabla\frac{\tilde{e}}{R} = -\int_{V_\infty-\vec{x}_f}\frac{\tilde{e}}{R}\varphi_2$$
$$-\int_{V_\infty-\vec{x}_f}\tilde{e}\varphi_1\left[\beta(\nabla^2\alpha - \|\nabla\alpha\|^2 R - 2\alpha\nabla\alpha\bullet\hat{R}) + \nabla\beta\bullet\nabla\alpha + \frac{1}{R}(\alpha+\frac{1}{R})\nabla\beta\bullet\hat{R}\right] \qquad (2\text{-}15)$$

where the definition

$$(\beta, \varphi_1)_\infty \equiv \frac{1}{4\pi}\int_{\partial V_\infty} \beta\varphi_1 \sin\theta d\theta d\varphi \qquad (2\text{-}16)$$

has been used, a δ–ball about $\vec{x}_f$, $V_\delta(\vec{x}_f)$, has been excluded, and equation 2-12 has been used to substitute for $\nabla\bullet\,\beta\nabla\varphi_1$. $V_\delta(\vec{x}_f)$ is excluded because upon differentiation, $\int_V \nabla^2 \frac{1}{R}$ is evaluated incorrectly near the singularity: equation 2-17 illustrates this point where the case $\vec{x}\neq\vec{x}_f$ corresponds to points where differentiation performs correctly.

$$\lim_{\delta\to 0^+}\int_{V_\delta(\vec{x}_f)} \nabla^2 \frac{1}{R} = \lim_{\delta\to 0^+}\int_{\partial V_\delta(\vec{x}_f)} \nabla\frac{1}{R}\bullet\, d\vec{s} \approx \begin{cases} \lim\limits_{\delta\to 0^+} -\dfrac{\hat{R}}{R^2}\bullet \int d\vec{s} = 0 & : \vec{x}\neq\vec{x}_f \\ \lim\limits_{\delta\to 0^+} -\int \dfrac{ds}{\delta^2} = -4\pi & : \vec{x}=\vec{x}_f \end{cases} \qquad (2\text{-}17)$$

How are the integrations over $V_\delta(\vec{x}_f)$ in equation 2-15 done? Noting that $\alpha^2=i\omega\mu\tilde{\sigma}$, $\beta=\tilde{\sigma}$, and given that μ, ε, and σ are experimentally determined quantities, I must clarify how electromagnetic aspects of the head system are modeled by these parameters in order to know how integrations over $V_\delta(\vec{x}_f)$ should be interpreted. The initial step is to assume the head system can be partitioned into P+1 regions, $V_{p(artition)}$, constant in μ, ε, and σ over the spacial domain. This mathematical abstraction results in discontinuities and infinite gradients at ∂V. Dealing with these characteristics requires further consideration of the modeling process used in assigning values to μ, ε, and σ. In order to reasonably consider μ, ε, and σ spacially constant throughout V_p, sample sizes on which measurements are taken must be sufficiently greater than the fine structure of the associated matter. How do we know what size is sufficient? First, a measure of sample size must be defined. Maybe a reasonable choice is the modal linear dimension through the centroid of the sample. Using this

definition, the answer is to find the minimum length, δl_p, where measurements on an arbitrary sample from V_p satisfying this resolution requirement is equal to μ, ε, and σ observed using a sample as large as V_p. Note that this means $\delta V_p \geq \Delta v_{max}(\vec{x}):\vec{x}\in V_p$. The definition also implies δV_p geometry would be an ellipsoid reducing to a spheroid for the case of isotropic μ, ε, and σ. This leads to the conclusion that at a given point of V_p, any δV_p containing the point can be used to determine μ, ε, and σ at that point except if the point is near ∂V_p. At points near ∂V_p, some choices of δV_p would encompass matter from ajacent media. If we assume the radius of curvature of ∂V_p is larger than the maximum radius of δV_p, i.e., $\frac{\delta l_p}{2}$, a surface a distance $\frac{\delta l_p}{2}$ from ∂V_p can be imagined where, for points on the side away from ∂V_p, μ, ε, and σ can be taken to be spacially constant. For points on the side toward ∂V_p, it is not obvious how μ, ε, and σ should be assigned nor is it obvious whether there is any experimental way to check the validity of a model. Because of this uncertainty, mathematical points where more than two media intersect would be extremely difficult to deal with; it is unclear how the gradient of $\mu, \varepsilon,$ or σ can be specified at such points. Consequently, equations will be developed for μ, ε, and σ models were the set of points lying on more than two V_p is the null set. In contrast, at interfaces between two media, we know gradients must be normally directed. Without assumptions about how the electromagnetic parameters vary within interfaces, using β for an example, we know that

$$\nabla\beta = 0 \quad :\vec{x}\in V_p - \partial_{\delta l_p} V_p \tag{2-18a}$$

$$\nabla\beta \neq 0 \quad :\vec{x}\in \partial_{\delta l_p - \lambda_{\beta,p}} V_p \tag{2-18b}$$

for some unknown positive indefinite constant $\lambda_{\beta,p}$ where $\partial_A B$ is used to denote the part of volume B bound by its boundary, ∂B, and the surface within B a

distance A from ∂B.

Continuing with calculating the left side of equation 2-15, the integrations will be different depending on whether $\vec{x}_f \in \partial_{\delta l_p - \lambda_p} V_p$ or $\vec{x}_f \notin \partial_{\delta l_p - \lambda_p} V_p \cup \vec{x}_f \in V_p$ or $\vec{x}_f \notin V_p$ where λ_p denotes $\underset{g\in[\alpha,\beta]}{\text{MIN}} \lambda_{g,p}$ (which is equivalent to $\underset{g\in[\mu,\varepsilon,\sigma]}{\text{MIN}} \lambda_{g,p}$). Note that just as in defining Δv_{max}, λ_p must be used because integrals involve α and β simultaneously and cannot be separated into integrals depending on only one of these parameters. Examining equation 2-15 with equations 2-18 in mind reveal that $\varphi_1|_{\vec{x}_f}$ can be expressed as a sum of φ_1 within V_p interfaces only; thus, since we are interested in electromagnetic fields at the scalp-air interface, only the case, $\vec{x}_f \in \partial_{\delta l_p - \lambda_p} V_p$, need be considered. The δ-ball integrations can be done if we can assume the quantities φ_1, β, α, and $\nabla\alpha$ are not singular at $\vec{x}_f$; the assumption implies there exists a δ such that the quantities are constant over the δ ball. Assesing the validity of the assumption requires formulating it in terms of the specific quantities we are interested in: assume $\vec{A}$, Φ, $\vec{J}_r$, $\nabla\bullet\vec{J}_r$, μ, $\tilde{\sigma}$, and $\nabla\tilde{\sigma}$ are not singular at $\vec{x}_f$. The assumption for all of these can be rationalized by saying there are no infinite forces on charged particles in the system of interest. Using this assumption, three integral types need to be calculated. They are displayed below.

$$\lim_{\delta\to 0^+} \int_{V_\delta(\vec{x}_f)} \frac{\tilde{e}}{R} = \lim_{\delta\to 0^+} -\frac{4\pi}{\alpha}\left[e^{-\alpha\delta}\left(\delta+\frac{1}{\alpha}\right)-\frac{1}{\alpha}\right] = 0 \qquad (2\text{-}19a)$$

$$\lim_{\delta\to 0^+} \int_{V_\delta(\vec{x}_f)} \nabla\frac{\tilde{e}}{R} = \lim_{\delta\to 0^+}\left[\frac{4\pi\nabla\alpha}{\alpha}\left[e^{-\alpha\delta}\left(\delta^2+\frac{2\delta}{\alpha}+\frac{2}{\alpha^2}\right)-\frac{2}{\alpha^2}\right]-\int_{V_\delta(\vec{x}_f)} \hat{R}\frac{\tilde{e}}{R}\left(\alpha+\frac{1}{R}\right)\right] \qquad (2\text{-}19b)$$

$$\lim_{\delta\to 0^+} \int_{V_\delta(\vec{x}_f)} \nabla^2\frac{\tilde{e}}{R} = \lim_{\delta\to 0^+} -\left[e^{-\alpha\delta}\nabla\alpha\bullet\int_{V_\delta(\vec{x}_f)} \hat{R} + 4\pi e^{-\alpha\delta}(\alpha\delta+1)\right] = -4\pi \qquad (2\text{-}19c)$$

Integrals involving $\hat{R}$ are zero since antiparallel vectors with the same weighting are summed. Using these results and equations 2-18, equation 2-15 is transformed to

$$4\pi(\beta\varphi_1|_{\vec{x}_f} - (\beta, \varphi_1)_\infty = -\int \frac{\tilde{e}}{R}\varphi_2 - \sum_{i=1}^{I} \int_{V_i - \vec{x}_f} \tilde{e}\varphi_1[]_{2-15} \qquad (2\text{-}20)$$

where I is the number of non-null $\partial V_{p'} \cap \partial V_{p''}$: $\{p', p'' \in [1 \to P+1]; p' \neq p''\}$ and $V_{i(ntersection)}$ corresponds to $\partial V_{p'} \cup \partial V_{p''}$: $\{\partial V_{p'} \cap \partial V_{p''} \neq 0, p' \neq p''\}$.

It is apparent from the equation that a major difficulty is the need to know $\beta|_{\vec{X}_f}$ when the variation of β in V_i is unknownable. This might be dealt with by converting equation 2-20 into an equation relating average values of φ_1 averaged in a direction normal to ∂V_p. In using this idea, volume integrals over V_i are converted to surface integrals; e.g., suppose $V_{i_1} = \partial_{\delta l_{p_1} - \lambda_{p_1}} V_{p_1} \cup \partial_{\delta l_{p_2} - \lambda_{p_2}} V_{p_2}$: $\partial V_{p_1} \cap \partial V_{p_2} \neq 0$, using f to denote some function,

$$\int_{V_{i_1}} f \approx \Sigma l_{i_1} \int_{S_{i_1}} \langle f \rangle_{\vec{x}, n_1(\vec{x})} \qquad (2\text{-}21a)$$

where $\Sigma l_{i_1} = \delta l_{p_1} - \lambda_{p_1} + \delta l_{p_2} - \lambda_{p_2}$, S_{i_1} is parallel to the surface $\partial V_{p_1} \cap \partial V_{p_2}$, and $\langle f \rangle_{\vec{x}, n_1(\vec{x})}$ denotes the spacial average of f taken over a subset of points within V_i and along a line normal to S_i at $\vec{x}$. It seems reasonable to project $\vec{x}_f$ onto the appropriate S_i. Taking $\langle R \rangle_{\vec{x}, n_1(\vec{x})}$ and $\langle \hat{R} \rangle_{\vec{x}, n_1(\vec{x})}$ places S_i half way between the two boundaries of V_i. To complete specifying the results of averaging, values for α and β, their gradients, and their laplacians must be proposed. If the averaging process is taken to be

$$\frac{1}{\|\Gamma\|}\oint_{\Gamma} f \tag{2-21b}$$

and the gradient is assumed constant along Γ (the linear approximation), using β and S_i as an example, equations 2-23 are obtained.

$$<\beta>_{\vec{x},n_1(\vec{x})} = \frac{\beta_{p_1}+\beta_{p_2}}{2} \equiv \bar{\beta} \tag{2-22}$$

$$<\nabla\beta>_{\vec{x},n_1(\vec{x})} = \frac{\beta_{p_1}-\beta_{p_2}}{\Sigma l_{i_1}}\hat{n}_{i_{p_1}}(\vec{x}) \equiv \frac{\Delta\beta_{i_1}}{\Sigma l_{i_1}}\hat{n}_{i_{p_1}} \tag{2-23}$$

$$<\nabla^2\beta>_{\vec{x},n_1(\vec{x})} = \frac{2}{R_{crv_{i_1}}}\frac{\beta_{p_{cv}}+\beta_{p_{cc}}}{\Sigma l_{i_1}} \tag{2-24}$$

where $\hat{n}_{i_1}$ is a unit vector normal to S_{i_1} directed from V_{i_1} to V_{i_2}, R_{crv_i} denotes the local radius of curvature of S_i, $\sigma_{p_{cc}}$ is the conductivity associated with the local concave side of S_i, and $\sigma_{p_{cv}}$ is that for the local convex side. The expression for the laplacian was derived by assuming, locally, $<\nabla\beta>_{\vec{x},n_{i_1}}$ could be described as a vector of constant magnitude varying in orientation as if on a sphere.

How shall λ_p be specified? Unfortunately, this parameter is not canceled out of the equations because of squared gradient magnitudes in $[]_{2\text{-}15}$ and because the location of S_i depends on it. So, to settle the issue, the previously discussed process to define the functions μ, ε, and σ must be examined. Instead of choosing one δV_p for μ, ε, and σ assignments at some point in V_p, the process could be taken to assign average values where the average is derived from measurements on all possible δV_p containing the point. At an interface $\partial V_{p'} \cap \partial V_{p''}$, this method seems very reasonable if $\delta l_{p'} = \delta l_{p''}$; but, if $\delta l_{p'} \neq \delta l_{p''}$, there could be discontinuities at $\partial V_{p'} \cap \partial V_{p''}$. In spite of this difficulty, we might

assume the method is reasonable at least for points just inside the boundaries of $\partial_{\delta l_{p'}} V_{p'} \cup \partial_{\delta l_{p''}} V_{p''}$, its validity getting worse for points closer to $\partial V_{p'} \cap \partial V_{p''}$. From this view, it follows that non-zero gradients occur just inside the boundaries of $\partial_{\delta l_{p'}} V_{p'} \cup_{\delta l_{p''}} V_{p''}$ and thus, λ_p can be taken to be zero.

2.4 Summary of the model

The mathematical model developed thus far is summarized by equations 2-25. These equations are the result of applying the integral equation formulation just developed to equations 2-11.

$$4\pi(\vec{A}|_{\vec{x}_f} - (1,\vec{A})_\infty) - \sum_{i=1}^{I} \int_{S_i - \vec{x}_f} \tilde{e}\left\{(\bar{\mu}\Delta\tilde{\sigma} + \bar{\sigma}\Delta\mu)\Phi \frac{\hat{n}_i}{R} + \frac{\Delta\mu}{\bar{\mu}} \frac{\hat{n}_i}{R} \times \nabla \times \vec{A} - \vec{A}[]_{2\text{-}15_i}\right\}$$

$$= \int_{V_\infty - \vec{x}_f} \frac{\mu\tilde{e}}{R} \vec{J}_r \qquad \text{(2-25a)}$$

$$4\pi(\tilde{\sigma}\Phi|_{\vec{x}_f} - (\sigma,\Phi)_\infty) - \sum_{i=1}^{I} \int_{S_i - \vec{x}_f} \tilde{e}\left\{i\omega\Delta\tilde{\sigma} \frac{\hat{n}_i}{R} \cdot \vec{A} - \Phi[]_{2\text{-}15}\right\} = -\int_{V_\infty - \vec{x}_f} \frac{\tilde{e}}{R} \nabla \cdot \vec{J}_r \qquad \text{(2-25b)}$$

$$[]_{2\text{-}15} = \bar{\sigma}\left[\frac{1}{2}\sqrt{\frac{i\omega}{\bar{\mu}\bar{\sigma}}}\left(\frac{\Delta\tilde{\sigma}\Delta\mu}{\delta\,\Sigma l} + \frac{2}{R_c}(\bar{\sigma}\Delta\mu + \bar{\mu}\Delta\tilde{\sigma})\right) - \frac{i\omega}{8\bar{\mu}\bar{\sigma}\,\Sigma l}\left(\frac{1}{\sqrt{i\omega\bar{\mu}\bar{\sigma}}} + R\right)(\bar{\mu}\Delta\tilde{\sigma} + \bar{\sigma}\Delta\mu)^2\right]$$

$$+ \frac{1}{4\,\Sigma l}\sqrt{\frac{i\omega}{\bar{\mu}\bar{\sigma}}}\Delta\ddot{\sigma}(\bar{\mu}\Delta\tilde{\sigma} + \bar{\sigma}\Delta\mu) + \frac{1}{R}\left(\sqrt{i\omega\bar{\mu}\bar{\sigma}} + \frac{1}{R}\right)\Delta\ddot{\sigma}\hat{n}_i \cdot \hat{R}$$

$$\ddot{\sigma} = \begin{cases} 1 & \text{for eq. 2-25a} \\ \tilde{\sigma} & \text{for eq. 2-25b} \end{cases}$$

$$\hat{n}_i = \hat{n}_{i_{in}} \quad i^{th} \text{ interface from side } \textit{in} \text{ to } \textit{out}$$

$$\Delta f \equiv f_{out} - f_{in}$$

It is important to clarify the transition between the model initially suggested for μ, ε, and σ and the model for these functions required by equations 2-25. This is done by considering equations 2-25 for ω=0:

$$4\pi(\vec{A}|_{\vec{x}_f} - (1,\vec{A})_\infty) + \sum_{i=1}^{I} \int_{S_i - \vec{x}_f} (\overline{\mu}\Delta\sigma + \overline{\sigma}\Delta\mu)\Phi \frac{\hat{n}_i}{R} - \frac{\Delta\mu}{\mu}\frac{\hat{n}_i}{R}\times\nabla\times\vec{A} = \int_{V_\infty - \vec{x}_f} \frac{\mu}{R}\vec{J}_r \quad (2\text{-}26a)$$

$$4\pi(\overline{\sigma}\Phi|_{\vec{x}_f} - (\sigma,\Phi)_\infty) + \sum_{i=1}^{I} \int_{S_i - \vec{x}_f} \Delta\sigma \frac{\hat{n}_i \bullet \hat{R}}{R^2}\Phi = -\int_{V_\infty - \vec{x}_f} \frac{\nabla\bullet\vec{J}_r}{R} \quad (2\text{-}26b)$$

It will be shown that certain requirements on the functions μ, ε, and σ are needed in order that a solution to homogeneous differential equations 2-11, at ω=0, is also a solution to homogeneous equations 2-26. Solutions must have this property since solutions to integral equations constructed from Green's functions must be solutions to the parent boundary value problem [32]. (This does not seem an obvious property of the transformation used to obtain equations 2-25. Replacing $\nabla\bullet\beta\nabla\varphi_1$ in equation 2-15 with equation 2-12 constrains solutions of equation 2-15 to be solutions of equation 2-12; it does not seem the differential equation is similarly constrained. I would also like to note that though boundary conditions have not been assumed, they are implicitly specified in the formulations presented here by specifying the electromagnetic parameters and assuming $\vec{A}$ and Φ bounded at infinity.)

Continuing, note that we can add on a vector field, $\vec{A}_{arb(itrary)}$, to $\vec{A}$ and a scalar field, Φ_{arb}, to Φ without changing solutions found for $\vec{E}$ and $\vec{B}$ so long as

$$\nabla\times\vec{A}_{arb} = 0 \quad (2\text{-}27a)$$

$$\nabla\bullet\vec{A}_{arb} = -\mu\sigma\Phi_{arb} \quad (2\text{-}27b)$$

$$i\omega\vec{A}_{arb} = -\nabla\Phi_{arb} \quad (2\text{-}27c)$$

For ω=0, equation 2-27c requires that Φ_{arb} be a spacially independent constant. We seek vector potential solutions of the form

$$\vec{A}_{arb} = C^A \hat{n} \quad : C^A = C^A(r) \tag{2-28}$$

This form satisfies equation 2-27a. Nontrivial solutions of this form exist for homogeneous equations 2-26 for the following example. Using four regions of constant μ, ε, and σ, where the three inner regions have spherical geometry, and acknowledging that equation 2-28 gives

$$(1, \vec{A}_{arb})_\infty = 0, \tag{2-29}$$

I obtain

$$\text{for } \vec{x}_f \in S_{i=1}: \begin{cases} 4\pi\left(\frac{\sigma_1+\sigma_2}{2} - \sigma_4\right)\Phi_{arb} + \left[(\sigma_2-\sigma_1)2\pi + (\sigma_3-\sigma_2)4\pi + (\sigma_4-\sigma_3)4\pi\right]\Phi_{arb} = 0 \\ 4\pi \langle C^A \rangle_{\vec{x}, n_{i=1}} \hat{n}_{\vec{x}_f} + \Phi_{arb} \mu_1 \sigma_1 \frac{4\pi}{3} R_{c_1} \hat{n}_{\vec{x}_f} = 0 \end{cases} \tag{2-30a}$$

$$\text{for } \vec{x}_f \in S_{i=2}: \begin{cases} 4\pi\left(\frac{\sigma_2+\sigma_3}{2} - \sigma_4\right)\Phi_{arb} + \left[(\sigma_3-\sigma_2)2\pi + (\sigma_4-\sigma_3)4\pi\right]\Phi_{arb} = 0 \\ 4\pi \langle C^A \rangle_{\vec{x}, n_{i=2}} \hat{n}_{\vec{x}_f} + \Phi_{arb} \dfrac{\mu_2\sigma_2(R_{c_2}^3 - R_{c_1}^3) + \mu_1\sigma_1 R_{c_1}^3}{R_{c_2}^2} \dfrac{4\pi}{3} \hat{n}_{\vec{x}_f} = 0 \end{cases} \tag{2-30b}$$

$$\text{for } \vec{x}_f \in S_{i=3}: \begin{cases} 4\pi\left(\frac{\sigma_3+\sigma_4}{2} - \sigma_4\right)\Phi_{arb} + (\sigma_4-\sigma_3)2\pi\Phi_{arb} = 0 \\ 4\pi \langle C^A \rangle_{\vec{x}, n_{i=3}} \hat{n}_{\vec{x}_f} + \Phi_{arb} \dfrac{\mu_3\sigma_3(R_{c_3}^3 - R_{c_2}^3) + \mu_2\sigma_2(R_{c_2}^3 - R_{c_1}^3) + \mu_1\sigma_1 R_{c_1}^3}{R_{c_3}^2} \dfrac{4\pi}{3} \hat{n}_{\vec{x}_f} = 0 \end{cases} \tag{2-30c}$$

which verify that, indeed, a non-trivial solution to homogeneous equations 2-26 exists.

To obtain solutions from the differential equations, the divergence theorem can be applied to equation 2-27b along with using the general forms for $\vec{A}_{arb}$ and Φ_{arb} specified above. It turns out that if $\delta l_p = 0 \forall p$ is assumed, this process gives solutions for C^A that are exactly those found for $\langle C^A \rangle_{\vec{x}, n_i}$ above. Thus, it

is observed that, with respect to the forms asssumed for $\vec{A}_{arb}$ and Φ_{arb}, contractions of V_i to S_i have resulted in an integral equation model that is equivalent to the differential model with the functions μ, ε, and σ satisfying $\delta l_p=0 \forall p$. Furthermore, when we take $\delta l_p \neq 0 \forall p$ and use a linear model for μ and σ within V_i, calculating averages $<>_{\vec{x},n_i}$ on the resulting solutions does not give answers equivalent to the integral equation solutions. In conclusion, given the necessary equivalence of integral and differential formulations, it can be inferred that contraction of V_i to S_i forces the discontinuous model for μ, ε, and σ. However, for $\omega \neq 0$, it is clear that continuous models for μ, ε, and σ need to be considered in order to estimate gradients of these quantities. In this context, I would not say that contraction to S_i results in a purely discontinuous model for μ, ε, and σ, whereupon gradients would have singularities, but the derivations above lead to a discontinuous model for μ, ε, and σ having nonsingular derivatives. Though these conclusions are drawn from analyzing a special case, I suspect this is the correct way to perceive equations 2-25. Figures 2-1 and 2-2 summarize the transformation from the initial model for μ, ε, and σ to that assumed to underlie equations 2-25.

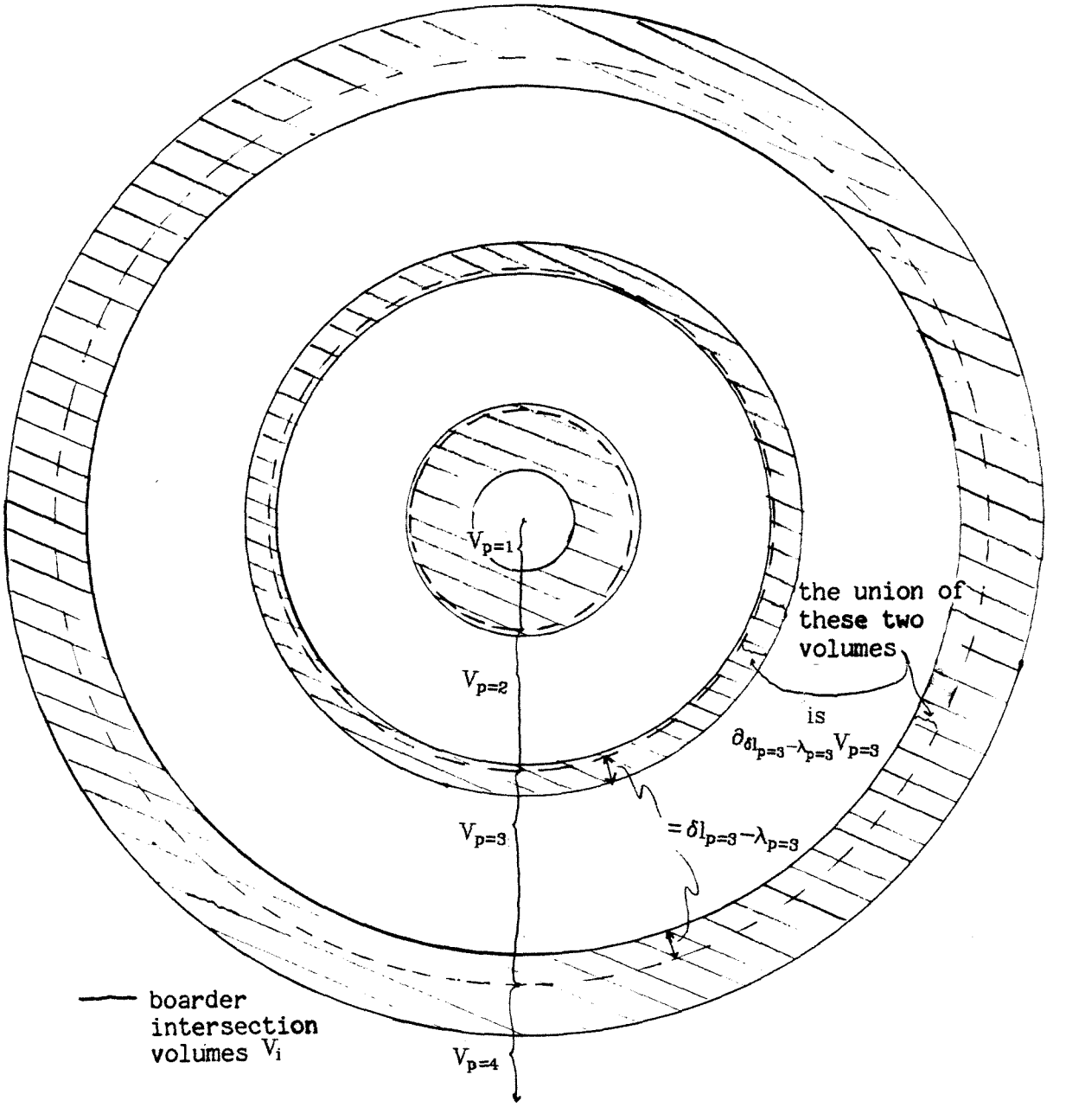

Figure 2-1 Using a spheroidal model for example, this is a slice of it showing the model before applying equation 2-21a to equation 2-20.

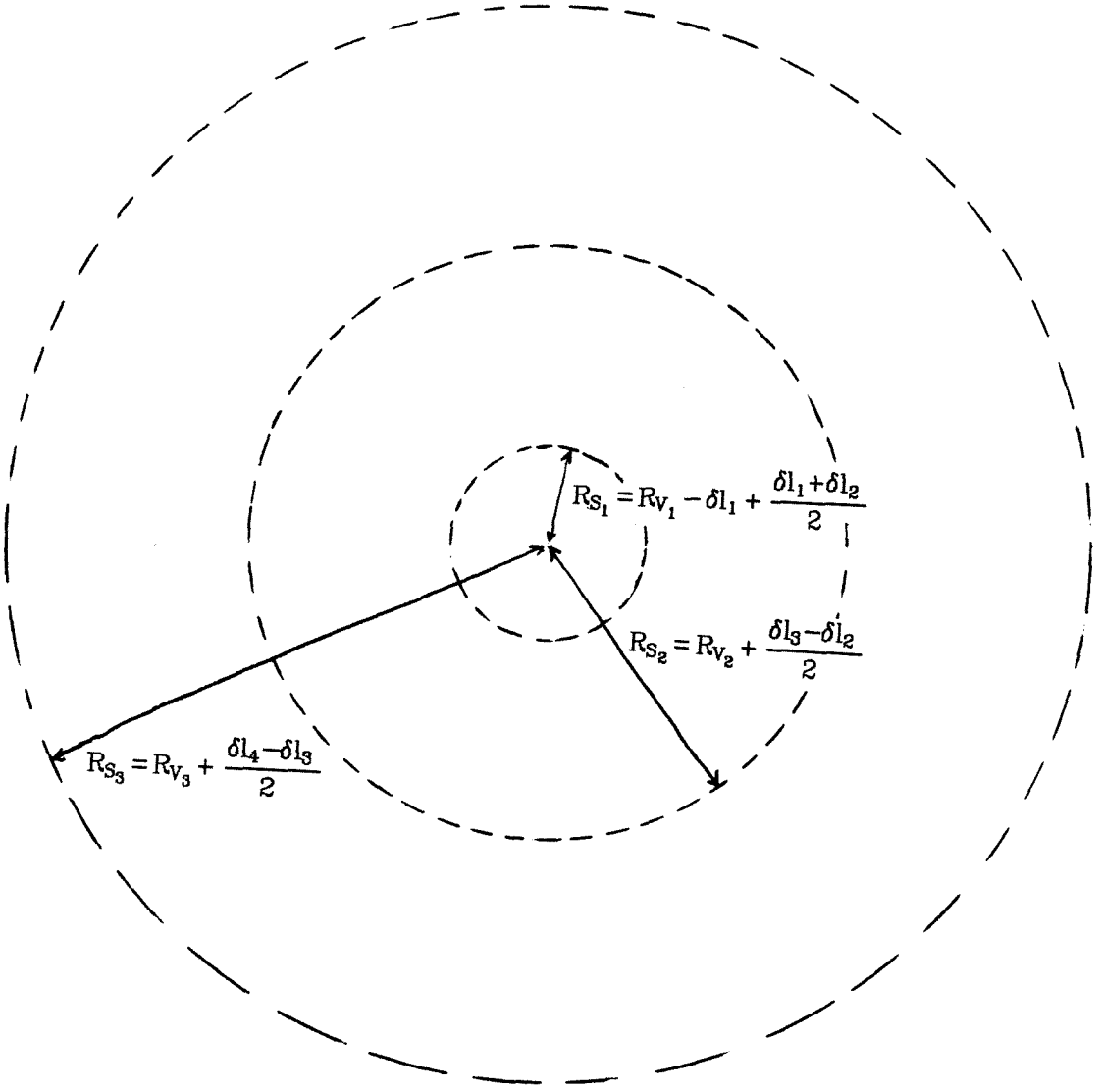

Figure 2-2 After contraction to the $\hat{S}_i$, and using equation 2-21b to compute quantities of equations 2-22 to 2-24, this discontinuous model with finite gradients is obtained.

3. Modeling $\vec{J}_r$

In this section, modeling $\vec{J}$ is completed. First I will explore the physical processes that may contribute to $\vec{J}_r$. From there, I identify the most important currents produced by the processes and then go on to speculate how these currents might be distributed. A short discussion on how neural activity might actualize such distributions follows after which mathematical models are presented. These models will lead to a way of dealing with $\vec{J}_r$ integrals. Previous work is then discussed in the context of formulations for the integrals.

3.1 Physical processes associated with $\vec{J}_r$

In order to generate reasonable models, it is of primary importance to clarify what kind of physical processes are represented by $\vec{J}_r$. The problem is to figure out which components of $\vec{J}_r$ have been left unspecified. We would like to have accounted for charge movements within atomic systems (atoms considered at rest), partially accounted for displacements of charged sites in molecular systems (molecular structures considered at rest), and partially accounted for other types of ionic movement (movement in the reference frame of the head system) through using the functions μ, ε, and σ respectively. Recalling that the reason for using μ, ε, and σ was to account for charges and currents that would be difficult to account for explicitly, contributions to $\vec{J}_r$ resulting from inaccuracies in μ, ε, and σ modeling will be dismissed from further consideration.

I will acknowledge three types of physical processes in the brain that may give rise to ionic currents unaccounted for by ε and σ. Currents generated by these processes will be given the names gating current, ion pump current, and electrodiffusive ion currents. Gating currents are associated with the opening and closing of ion channels in neuro-membrane. They are thought to consist

of spiraling H^+ movement resulting from acid-base H^+ exchanges ascending protein chains in α-helix conformation [29]. Consequent changes in protein conformations could effect movements of ionic residues which would result in a net charge flux. Ion pump currents are associated with chemical reactions transporting ions through cell membranes against concentration gradients. For squid axons and snail neurons, a net charge movement results: roughly three Na^+ are extruded per two K^+ taken in [70]. Electrodiffusive currents are associated with ion permeability changes allowing electrodiffusion of select ion species through neural membranes. This ion movement results in concentration gradients inside neurons and in intercellular clefts Differential membrane permeability for oppositely charged ionic species indicates the possibility of net current flow.

It is clear that none of these three current types can be associated with producing a dipolar electric field proportional to $\vec{E}$ and, thus, could not be modeled by ε. For σ, note that the dependence of these currents on local electric fields is non-linear. All are driven by electrical forces nontrivially coupled to other determining factors: for gating and ion pump currents it is chemical stability (highly specific local electric field dependence and quantum mechanical stability), for electrodiffusive currents it is diffusion (statistical movement of mobil particles). Thus, these currents cannot be totally accounted for by $\sigma\vec{E}$.

One final note-- if any of the three current types have components describable by a scalar proportionality to the local electric or magnetic field, it could still be true that these components are not accounted for by μ, ε, or σ. This would be true if, upon averaging over the region containing the currents with resolution Δv_{max}, it is found that there are net currents described by a proportionality constant significantly different from μ, ε, or σ. In this sense, some

current sources can be viewed as large inaccuracies of the μ, ε, and σ model in local regions containing non-zero current flow. Contributions to $\vec{J}_r$ resulting from inaccuracies of the μ, ε, and σ model were mentioned previously in this section. At that point of my discussion I was referring to global inaccuracies whereas in the present context, I am referring to inaccuracies over a region of space much smaller than the size of the medium of interest.

3.2 Identifying the important processes

Having distinguished the processes assumed to account for most of $\vec{J}$, assessing the importance of a particular process or component of the associated current involves recognizing that, for application to evoked potential research, $\vec{J}$ represents two types of averages. One of these stems from the need for signal averaging to obtain electromagnetic scalp field data that have the characteristic dipolar structure. Thus, $\vec{J}$ represents an average over sources occurring during each experimental trial. This means we are only interested in those currents that would survive this averaging process. In each trial, presumably a particular subset of neural activity is brought into being. It follows that gating and electrodiffusive currents are of interest, both being completely coupled to neural activity. However, ionic pump currents are loosely coupled to neural activity so their contribution to $\vec{J}$ is expected to be partially attenuated by signal averaging. The other average has been expressed in equations 2-7; $\vec{J}$ is a spacial average. For my purposes, an average over regions at least large enough to contain a neuron and many surrounding glial cells is required. Thus, gating currents can be assumed to make no net contribution if, perceiving a neuron as a network of tubes, ionic channels are assumed to be distributed symetrically about tube axes. In case there are gating currents associated with chemically mediated channels at synapses, this also means active synapses are assumed to have an axially symetric

distribution about a neuron. The reasoning used to eliminate gating currents from further consideration is another reason to assume ion pump currents make no net contribution since neuron and glial cell membranes are geometrically closed surfaces with uniform pump distributions [70, 2]. It is concluded that electrodiffusive currents are the only significant contributors to $\vec{J}_r$.

3.2.1 On electrodiffusive currents

Three types are distinguished: neural membrane currents (purely radial), intraneural (mainly axial), and extraneural currents. Arguments similar to those for gating currents eliminate the first of these from further consideration. For the other two, I will first discuss the possibility of axial contributions then will consider the possibility of radial contributions.

3.2.1.1 Axial contributions In considering axial contributions, note that extraneural and intraneural electrodiffusive currents derive from membrane electrodiffusive current; thus, if currents are confined to neuron-glial clefts, their contributions to $\vec{J}_r$ cancel upon averaging assuming diffusion coefficients are the same for extra and intraneural media. In addition, under certain circumstances, axial components of these two currents may not exist even though membrane currents do. This would happen when the propagation of an action potential quickly eliminates axial concentration gradients over the length of a neuron or when the space-time distribution of synaptic activity effects the same. However, there are reasons to believe the two currents do make a net axial current contribution. Of extraneural K^+ currents, 75% flows through glial cells [44, 45, 46, 47] and other ions, which are mainly confined to extracellular spaces [68, 69, 80], can flow through glial-glial clefts intersecting neuron-glial clefts. This means extraneural currents could have a substantial radial component from which it follows that intraneural axial flows would only

be partially canceled. Summarizing, because neurons are closed volumns in comparison to neuron-glial clefts, it seems net axial contributions could exist along any of the constituent tubes of a neuron except axons where action potential propagation mitigates against the build up of axial concentration gradients. It seems reasonable to say that an active neuron associated with a source contributes a component of current to $\vec{J}_r$ that is oriented in the direction of an average over the directions of its constituent tubes excluding action potential producing axons.

3.2.1.2 Radial contributions For the radial component of electrodiffusive currents, the existence of a net contribution is dependent on ion concentration distributions at a scale larger than the single neuron system analysed above. For a single neuron system with a homogeneous extraneural ion concentration environment, the radial component would be expected to have axial symetry. Thus, if significant radial currents occurred only within grain size Δv_{max}, no net contribution to $\vec{J}_r$ would result. But with other neurons contributing to the extraneural ion distribution along with the existence of anisotropic ion mobility, radial components could be biased such that they have a net contribution to $\vec{J}_r$ despite averaging.

3.3 Current distributions for dipolar fields

Now that the important currents have been identified, we need to know what distributions of these currents are responsible for observed dipole-like electromagnetic fields at the scalp. Examining intracranial measurements of electric potentials supports hypothesizing standard charge and current dipole models. Potential measurements within the superior olivary nucleus of cats have been made during the application of auditory stimuli [43]. This data is reproduced in figure 3-1.

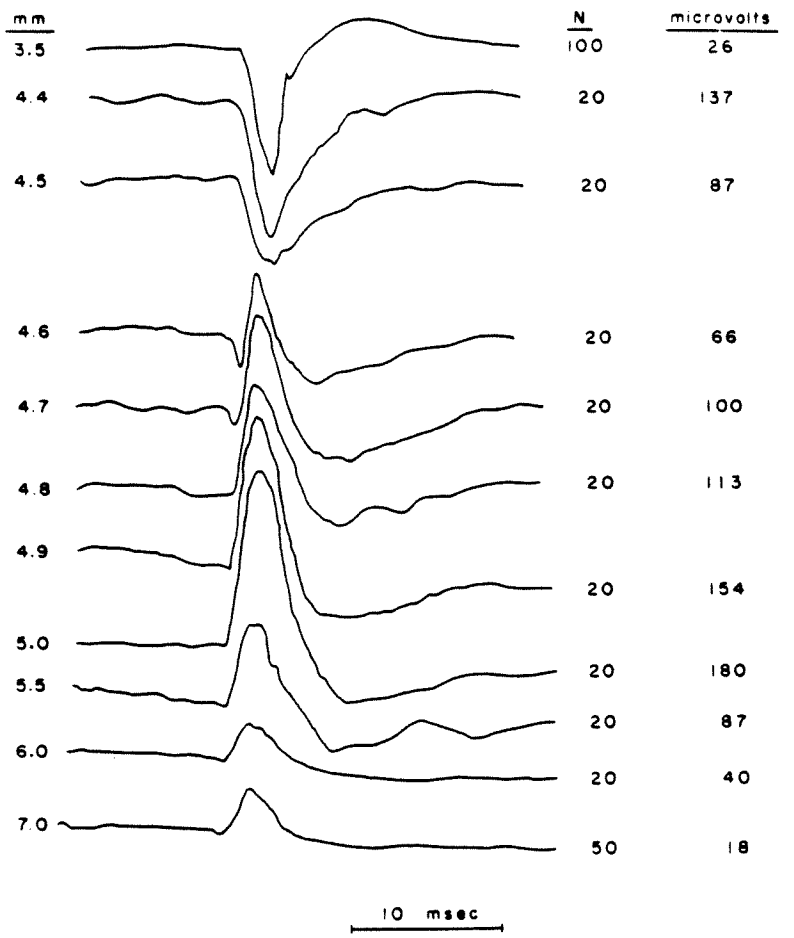

FIG. 3-1 Click-evoked potentials recorded from various points in the superior olivary complex of the cat

The variation of potentials with electrode depth certainly have the form expected of a dipole source. The amplitude of extrema as a function of distance for the deepest four points is compared with an inverse square law in table 3-1, giving further support to the dipole model.

TABLE 3-1

depth (mm)	peak height	$\frac{A}{r^2}$ prediction
5	180	177
5.5	87	78
6	40	43
7	18	19

Several intracranial studies where current source density analysis [81] has been applied to potential measurements in visual cortex of cats [77] and monkeys [79, 109] also support the dipole model. Current source density analysis is the name given to estimating $\nabla\bullet\vec{J}_r$ from numerically estimating $\nabla^2\Phi$: for $\omega=0$, taking the divergence of equation 2-7b, combining this with equation 2-8b, and attending to regions where σ is a locally spacially independent quantity,

$$\sigma\nabla^2\Phi = \nabla\bullet\vec{J}_r \tag{3-1}$$

Using a smoothed gate function for a crude model of $\vec{J}_r$,

$$\vec{J}_r = \left(\text{Amp-m}\right)\hat{j} \tag{3-2}$$

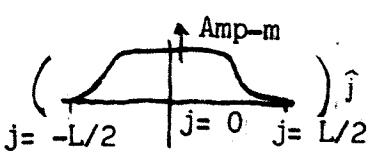

we get

$$\nabla\bullet\vec{J}_r = \tag{3-3}$$

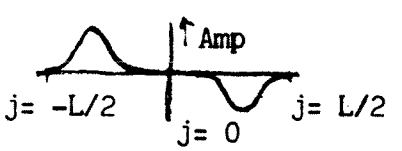

and this form is observed in the literature.

What about the size of the source? Since equation 3-2 is the simplest form for $\vec{J}_r$ that will account for the data, we will adopt it as a model. With this model, current source density analysis data cited above suggest that L is on the order of 0.5mm, five times the length of a typical cortical pyramidal cell. It is important to note that these data were generated by estimating $\nabla^2\Phi$ using one-dimensional data. Thus, with respect to the model expressed by equation 3-2, the estimate of L is a minimum.

3.3.1 Actualization of dipoles

From the size estimates above, it is obvious that the dipole sources must result from small populations of neurons. I can imagine two mechanisms that would give rise to $\vec{J}_r$ of the general form expressed by equation 3-2. One possibility follows directly from ideas of the section on identifying important currents. It was mentioned that each active neuron could make a net contribution to $\vec{J}_r$ in a direction parallel to the neuron axis. Thus, the dipole source can be considered to be the net contribution of a population of similarly oriented neurons. Many people have postulated this model [92, 93, 115]. The other possibility I will propose does not depend so much on the anatomy of the relevant neuro-population and can result in a source orthogonol to neuro-axes. Consider a region of high neuro-activity a distance L from a region of low activity, both regions flanked by moderate activity. This distribution of neuro-activity would result in an asymmetric electrodiffusion of extracellular Na^+ toward the very active region, mainly coming from the region of low activity (assuming there is a dense matrix of randomly oriented extracellular clefts such that significant flows orthogonol to neuron axes can exist). Certainly, this mechanism can also account for dipole sources that are parallel to neuro-

axes: a column of neurons in series where, at one end of the column, neurons are excited that result in inhibition of neurons further down in the series could result in the required topology of neuroactivity. This mechanism is probably more likely to result in observable sources than that which would result in dipoles orthogonol to neuro-axes since ion conductivities along neuro-axes are much higher [81].

3.4 The mathematical model

The remaining task is to come up with mathematical models for $\vec{J}_r$. The discussion in the previous sections support approximating the source with a tube of current density:

$$\vec{J}_r = \frac{J_{rl(inear)\,d(ensity)}(j,t)}{A_{cr(oss\,section)}}\hat{j} \;:\; J_{rld} = \begin{cases} \text{positive indefinite} & j\in[-L/2, L/2] \\ & t\in[t_0, t_f] \\ 0 & \text{elsewhere} \end{cases} \tag{3-4}$$

where the coordinate system is defined in figure 3-2 below.

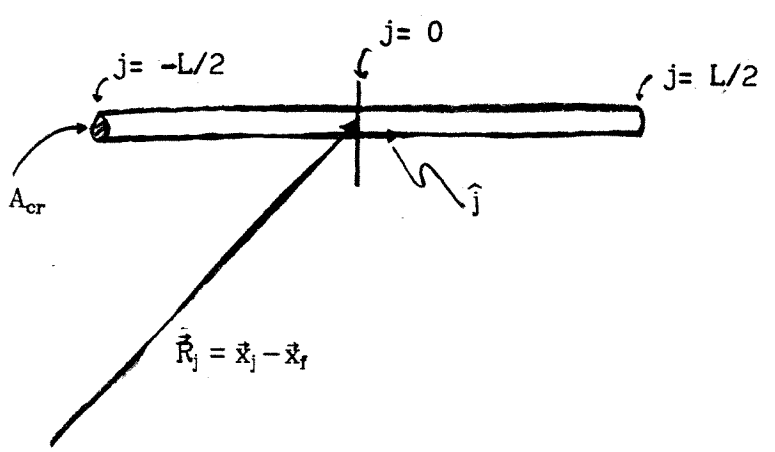

figure 3-2

There are problems with specifying the spacial distribution of $\vec{J}_r$ in more detail and specifying how $\vec{J}_r$ changes in time. We see that because the sources have a diffusional component, the spacial distribution of a source is tightly coupled to its time course. This time course depends on membrane currents. Modeling these currents is a very involved process [84, 85, 86]. It seems that dealing with this complexity would be fruitless for our purposes since the space-time distribution of membrane current is tightly coupled to the space-time distribution of local neural activity; certainly, this dependence suggests a wide range of time characteristics for membrane current. This means that in the fourier domain, we are obliged to study all possible phases at several frequencies. In conclusion, the time dependence of $\vec{J}_r$ is dealt with by writing each fourier coefficient as

$$\omega\vec{J}_r = \frac{|J_{rld}(j,\omega)|}{A_{cr}} e^{i\theta_{FT}}\hat{j} \qquad (3\text{-}5)$$

and then examining solutions for various choices of θ_{FT} at each ω.

The spacial dependence of $\vec{J}_r$ can be dealt with by using the Taylor expansion for $\frac{e^{-(Re+iIm)R}}{R}$ in terms of j of figure 3-2 and then expressing integrations in terms of $\int_{-L/2}^{L/2} |J_{rld}|$. The required ability to integrate $\vec{J}_r$ and $\nabla\bullet\ \vec{J}_r$ with various powers of j restricts us to a zeroth order expansion for integrating $\vec{J}_r$ and a first order expansion for integrating $\nabla\bullet\ \vec{J}_r$. Before writing down integrations of the source integrals of equations 2-25, preliminary results requiring special details are presented for the purpose of clarifying key underlying assertions. Two factors underlie the integrations involving $\nabla\bullet\ \vec{J}_r$: first, there is no net charge in the head system so for any source,

$$\int_{\substack{\text{region}\\ \text{containing}\\ \text{source}}} \nabla\bullet\, {}^{t}\vec{J}_r = 0 \quad \forall t \tag{3-6}$$

When this is combined with the orthogonality of fourier basis functions, $e^{i\omega t}$, we have

$$\int_{\substack{\text{region}\\ \text{containing}\\ \text{source}}} \nabla\bullet\, {}^{\omega}\vec{J}_r = 0 \quad \forall \omega \tag{3-7}$$

Second, the source model of equation 3-2 asserts

$${}^{t}\vec{J}_r|_{L/2,-L/2} = 0 \quad \forall t \tag{3-8}$$

at the tube ends. Again, with the orthogonality of $e^{i\omega t}$ we obtain

$${}^{\omega}\vec{J}_r|_{L/2,-L/2} = 0 \quad \forall \omega \tag{3-9}$$

Using the above relations,

$$\int_{-L/2}^{L/2} j\nabla\bullet\,(|J_{rld}|\hat{j}) = -\int_{-L/2}^{L/2} |J_{rld}| \tag{3-10}$$

$$\int_{-L/2}^{L/2} j^2\nabla\bullet\,(|J_{rld}|\hat{j}) = -2\int_{-L/2}^{L/2} j|J_{rld}| \tag{3-11}$$

This last equation is needed in order to obtain estimates of the uncertainty arising from neglecting terms of the Taylor series. Acknowledging that $|J_{rld}|\geq 0$, other expressions for this purpose are

$$\left|\int_{-L/2}^{L/2} j^2\nabla\bullet\,(|J_{rld}|\hat{j})\right| \leq L\int_{-L/2}^{L/2} |J_{rld}| \tag{3-12}$$

and

$$\left| \int_{-L/2}^{L/2} j\,|J_{rld}| \right| \le \frac{L}{2} \int_{-L/2}^{L/2} |J_{rld}| \qquad (3\text{-}13)$$

since the integrals on the left are maximal if $|J_{rld}|$ is zero over half the tube. These inequalities, along with Lagrange's form for the remainder of Taylor series, are used to specify uncertainties. Magnitudes of first and second order remainders are maximized at j= L/2. In summary, equations 3-14 are obtained. Considering integral equations for $\vec{A}$ and Φ and the formulas above, the term $\int_{-L/2}^{L/2} |J_{rld}|$ is observed to be simply a scaling factor.

$$\int_{-L/2}^{L/2} \frac{e^{-\eta R_j}}{R_j} |J_{rld}|\,\hat{j} = \hat{j} \left(\int_{-L/2}^{L/2} |J_{rld}| \right) e^{i\theta_{FT}} \left\{ \frac{e^{-\eta R_j}}{R_j} \pm \frac{L}{2} \frac{e^{-\eta \sqrt{}}}{\sqrt{^2}} \frac{(2R_j - L)}{2} \left(\frac{1}{\sqrt{}} + \eta \right) \right\} \qquad (3\text{-}14a)$$

$$\int_{-L/2}^{L/2} \frac{e^{-\eta R_j}}{R_j} \nabla \bullet (|J_{rld}|\,\hat{j}) = \hat{j} \left(\int_{-L/2}^{L/2} |J_{rld}| \right) e^{i\theta_{FT}} \left\{ \begin{array}{l} \dfrac{\hat{R}_j \bullet \hat{j}}{R_j} e^{-\eta R_j} \left(\dfrac{1}{R_j} + \eta \right) \\ \pm \dfrac{L}{2} \dfrac{e^{-\eta \sqrt{}}}{\sqrt{^2}} \left[\left(\eta + \dfrac{1}{\sqrt{}} \right) \left[\dfrac{3(2R_j - L)^2}{4\sqrt{^2}} - 1 \right] \right. \\ \qquad \left. + \dfrac{(2R_j - L)^2}{4\sqrt{}} \eta^2 \right] \end{array} \right\}$$

$$\sqrt{} \equiv \sqrt{R_j^2 + (L/2)^2 - R_j L} \qquad (3\text{-}14b)$$

$$\eta \equiv \sqrt{\omega \bar{\mu}} \left(\sqrt{\frac{-\bar{\varepsilon}\omega + \sqrt{\bar{\varepsilon}^2\omega^2 + \bar{\sigma}^2}}{2}} + i \sqrt{\frac{\bar{\varepsilon}\omega + \sqrt{\bar{\varepsilon}^2\omega^2 + \bar{\sigma}^2}}{2}} \right)$$

To close this section, I would like to compare equations 3-14 with sources other workers have used. Previous investigators have used point charge

dipoles in studies of electric fields alone [25, 36, 42, 51] and point current dipoles in studies of both magnetic fields alone [30, 52, 53, 113] and combined fields [21, 31, 35, 37, 98]. With $i_{p(oint)}$ symbolizing current density for these point sources, point charge dipoles give

$$\int_V \frac{\nabla\bullet \vec{J}_r}{R_j} = \frac{\hat{j}\bullet \hat{R}_j}{R_j^2} i_p L \tag{3-15}$$

Point current dipoles give

$$\int_V \frac{\vec{J}_r \times \hat{R}_j}{R^2_j} = \frac{i_p L \hat{j}\times \hat{R}_j}{R^2_j} \tag{3-16a}$$

$$\approx \frac{\vec{J}_r \times \hat{R}_j}{R^2_j} A_{cr} L \tag{3-16b}$$

$$\Rightarrow \int_V \frac{\vec{J}_r}{R_j} = \frac{\hat{j}}{R_j} i_p L \tag{3-16c}$$

These are to be compared with the magnitudes of the corresponding ω=0 fourier coefficients: ignoring uncertainties,

$$\left| \int_V \frac{\nabla\bullet \vec{J}_r|_{\omega=0}}{R_j} \right| = \frac{|\hat{R}_j\bullet \hat{j}|}{R_j^2} \int_{-L/2}^{L/2} |J_{rld}| \tag{3-17}$$

$$\left\| \int_V \frac{\vec{J}_r|_{\omega=0}}{R_j} \right\| = \frac{1}{R_j} \int_{-L/2}^{L/2} |J_{rld}| \tag{3-18}$$

Thus, we see that i_p is defined such that

$$\int_{-L/2}^{L/2} |J_{rld}| = i_p L \tag{3-19}$$

4. Simplifying the model

I choose to examine the simplest head model: space is divided into a spherical region, wherein μ, ε, and σ take on values appropriate for gray matter, white matter, cerebral spinal fluid, bone, or scalp, and the region external to the sphere is air. This reduces equations 2-25 by setting I=1 and making $S_{i=1}$ a sphere. Simplifying the equations further involves defining criteria with which the importance of each term of the equations can be assessed and then neglecting terms judged unimportant.

4.1 Simplification of multiplicative constants

Spacially independent constants that can be move outside integrals can be simplified using criteria based on uncertainties [4-1] in calculated solutions. Three sources of uncertainty are distinguished:

- Uncertainties in parameters μ, ε, σ, Σl, and R_c.
- Uncertainties resulting from numerical methods used to solve the equations.
- Uncertainties associated with source modeling.

The first of these is the type of uncertainty used to justify neglecting terms in space-independent factors multiplying integrals of equations 2-25. Considering

$$A = A_{main} + \delta_A \tag{4-1a}$$

$$A_{main} = \tilde{A}_{main} \pm A_{main?} \tag{4-1b}$$

and the form

4-1 Of course this is not absolute uncertainty but is uncertainty with respect to the accuracy of the model defined by equations 2-25 with I=1 and $S_{i=1}$ a sphere. In this section, this is to be the view of uncertainty.

$$F_{i=i_0}|_{\vec{x}_f} = \sum_i A_i \int K_i(\vec{x}, \vec{x}_f) F_i(\vec{x}) \tag{4-2}$$

obviously, the contribution to $F_{i=i_o}|_{\vec{x}_f}$ resulting from δ_A can be neglected if

$$|\delta_A| < A_{main?} \tag{4-3}$$

Using this reasoning and I=1 in equations 2-25,

$$\bar{\mu}\Delta\tilde{\sigma} + \tilde{\sigma}\Delta\mu \approx \bar{\mu}\Delta\tilde{\sigma} \quad : \begin{cases} |\Delta\mu| < \bar{\mu}(\sigma_{in?} + \sigma_{out?}) \\ |\Delta\mu| < \bar{\mu}\omega(\varepsilon_{in?} + \varepsilon_{out?}) \end{cases} \tag{4-4a}$$

$$\frac{\Delta\tilde{\sigma}\Delta\mu}{\Sigma l} + \frac{2}{R_c}(\tilde{\sigma}\Delta\mu + \bar{\mu}\Delta\tilde{\sigma}) \approx \frac{2\bar{\mu}\Delta\tilde{\sigma}}{R_c} \quad : \begin{cases} (\frac{1}{\Sigma l} + \frac{2}{R_c})\bar{\sigma}\,|\Delta\mu| < \frac{2}{R_c}\bar{\mu}(\sigma_{in?} + \sigma_{out?}) \\ (\frac{R_c}{2\ \Sigma l} + 1)\bar{\varepsilon}\,|\Delta\mu| < \bar{\mu}(\varepsilon_{in?} + \varepsilon_{out?}) \end{cases} \tag{4-4b}$$

$$\sqrt{i\omega\bar{\mu}\tilde{\sigma}} \approx \sqrt{\frac{\omega\bar{\mu}\bar{\sigma}}{2}}(1+i) \quad : \bar{\varepsilon}\omega + \frac{\bar{\varepsilon}^2\omega^2}{2\bar{\sigma}} < \sigma_{in?} + \sigma_{out?} \tag{4-4c}$$

$$\frac{1}{\sqrt{i\omega\bar{\mu}\tilde{\sigma}}} \approx \frac{1}{\sqrt{2\omega\bar{\mu}\bar{\sigma}}}(1-i) \quad : \bar{\varepsilon}\omega + \frac{\bar{\varepsilon}^2\omega^2}{2\bar{\sigma}} < \sigma_{in?} + \sigma_{out?} \tag{4-4d}$$

$$\sqrt{\frac{i\omega}{\bar{\mu}\tilde{\sigma}}} \approx \sqrt{\frac{\omega}{2\bar{\mu}\bar{\sigma}}}(1+i) \quad : \bar{\varepsilon}\omega + \frac{\bar{\varepsilon}^2\omega^2}{2\bar{\sigma}} < \sigma_{in?} + \sigma_{out?} \tag{4-4e}$$

$$\frac{i\omega}{\bar{\mu}\tilde{\sigma}} \approx \frac{\omega}{\bar{\mu}\bar{\sigma}}(\frac{\bar{\varepsilon}\omega}{\bar{\sigma}} + i) \quad : \bar{\varepsilon}^2\omega^2 < 2\bar{\sigma}(\sigma_{in?} + \sigma_{out?}) \tag{4-4f}$$

$$\left.\begin{array}{l} \bar{\sigma} \approx \dfrac{\sigma_{in}}{2} \\ \bar{\varepsilon} \approx \dfrac{\varepsilon_{in}}{2} \\ \bar{\mu} \approx \mu_0 \\ \Delta\sigma \approx -\sigma_{in} \\ \Delta\varepsilon \approx -\varepsilon_{in} \end{array}\right\} \textit{obvious criteria} \tag{4-4g}$$

leaving

$$4\pi(\vec{A}\,|_{\vec{x}_f} - (1,\vec{A})_\infty \approx \int_{S-\vec{x}_f} -\mu_0\tilde{\sigma}_{in}\tilde{e}\frac{\hat{n}}{R}\Phi + \frac{\Delta\mu}{\mu_0}\tilde{e}\frac{\hat{n}}{R}\times\nabla\times\vec{A} - \tilde{e}F_{\vec{A}}\vec{A} + \mu_0\int_{V_\infty-\vec{x}_f}\frac{\tilde{e}}{R}\vec{J}_r \quad (4\text{-}5a)$$

$$4\pi\left(\frac{\tilde{\sigma}_{in}}{2}\Phi\,|_{\vec{x}_f} - (\sigma,\Phi)_\infty\right) \approx \int_{S-\vec{x}_f} -i\omega\tilde{\sigma}_{in}\tilde{e}\frac{\hat{n}}{R}\bullet\vec{A} - \tilde{e}F_\Phi\Phi - \int_{V_\infty-\vec{x}_f}\frac{\tilde{e}}{R}\nabla\bullet\vec{J}_r \quad (4\text{-}5b)$$

where, after using the criterion

$$\frac{(\bar{\varepsilon}\omega)^2}{\bar{\sigma}} + 2\bar{\varepsilon}\omega < \frac{1}{2}(\sigma_{in?} + \sigma_{out?}) \quad (4\text{-}6)$$

in addition to those above,

$$F_{\vec{A}} = \varepsilon\omega\delta_1 - \sqrt{\omega\mu_0\sigma_{in}}\left(\frac{1}{R_c} + \frac{1}{4\Sigma l}\right) + i\left[\sigma_{in}\delta_1 - \sqrt{\omega\mu_0\sigma_{in}}\left(\frac{1}{R_c} + \frac{1}{4\Sigma l}\right)\right] \quad (4\text{-}5c)$$

$$F_\Phi = \varepsilon_{in}\omega\delta_1 - \frac{\sigma_{in}\sqrt{\omega\mu_0\sigma_{in}}}{2}\left(\frac{1}{R_c} - \frac{1}{4\Sigma l}\right) - \sigma_{in}\frac{\hat{n}\bullet\hat{R}}{R}\left(\frac{1}{R} + \frac{\sqrt{\omega\mu_0\sigma_{in}}}{2}\right) - i\left[\frac{\sigma_{in}}{2}\delta_1 + \frac{\sigma_{in}\sqrt{\omega\mu_0\sigma_{in}}}{2}\left(\frac{1}{R_c} - \frac{1}{4\Sigma l}\right)\right] \quad (4\text{-}5d)$$

$$\delta_1 \equiv \frac{\omega\mu_0}{4\Sigma l}R$$

Note that equations 4-4 are not applied to all terms of equations 2-25 in which

the left hand sides of equations 4-4 are involved but are applied only when the reasoning for neglect summarized by equations 4-1 to 4-3 is applicable. Table 4-1 displays the data on which criteria are evaluated. Graph 4-1 displays curves used to estimated some values of table 4-1. Calculations of the most stringent criteria for various frequencies are shown in table 4-2.

TABLE 4-1[1] Electromagnetic parameter data for biological tissues

media	$\varepsilon\omega$ (farad/m/sec)	Hz	$\sigma(\Omega m)^{-1}$	Hz	$\mu(\Omega sec/m)$
air[2]	5.57(-11)xHz		0		$4\pi x10^{-7}$
brain	2.5(-3) white 1.1(-3) gray 1.9(-2) 5.6(-2) ±30%	10^3[3] 10^5 10^6	.12→.22 =>.17±29%	$0\rightarrow10^6$	$\frac{\mu_0}{1+\mu_0(7x10^{-6})}$[4]
CSF	1.6(-4)[5]	10^3	1.53→1.56 =>1.55±1.2%	$0\rightarrow10^6$	"
scalp	7.8(-3) ±29%[6]	10^3	.34→.43±30%	$0\rightarrow10^6$	"
skull	5.6(-5) 1.3(-3) 4.8(-3) ±50%	10^3 10^5 10^6	1.3(-2) ±21% 1.7(-2) ±19%	10^3 10^6	"

1 [49, 66, 100, 101, 104, 105]
2 air values assumed approximately those for a vacuum.
3 10^3 Hz values extrapolated from values at higher frequencies, see graph 4-1.
4 the only value available for media of the head, human blood.
5 using blood data for an estimate.
6 using liver values for and estimate. Liver has higher permittivities than all other tissues for which there is data. Using this value would be a conservative estimate of $\varepsilon\omega$ neglegibility.

Graph 4-1

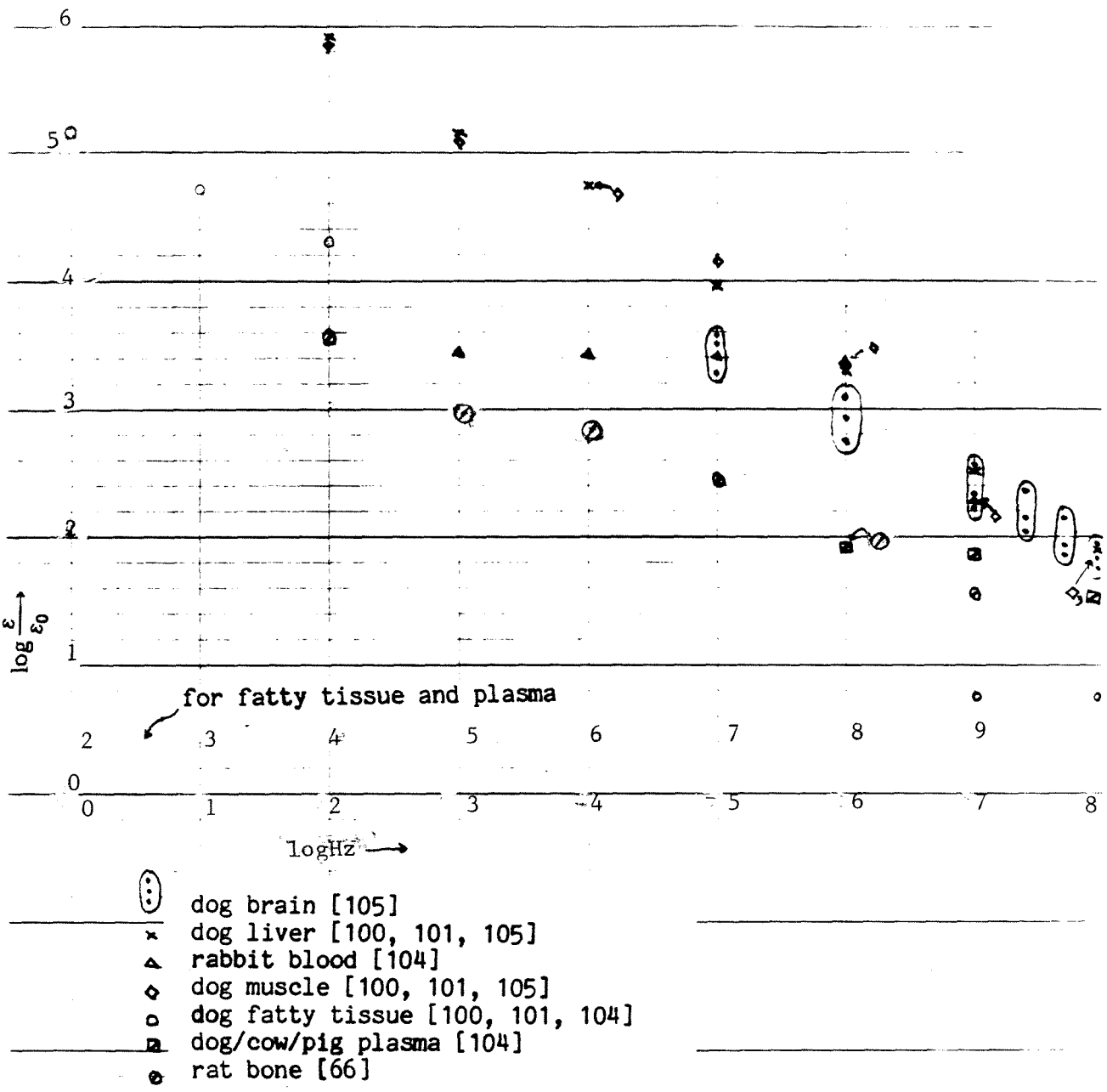
6
5
4
3
2
1
0
$\log \frac{\varepsilon}{\varepsilon_0}$
for fatty tissue and plasma
0 1 2 3 4 5 6 7 8
2 3 4 5 6 7 8 9
logHz
dog brain [105]
dog liver [100, 101, 105]
rabbit blood [104]
dog muscle [100, 101, 105]
dog fatty tissue [100, 101, 104]
dog/cow/pig plasma [104]
rat bone [66]

TABLE 4-2 Additional neglect criteria

criterion	numerical estimate at highest frequency where criterion is fulfilled		Hz
$(\frac{R_c}{(2\delta l_{sum}}+1)\lvert\Delta\mu\rvert\left[\frac{\frac{\sigma_{in}+\sigma_{out}}{2}}{\frac{\varepsilon_{in}+\varepsilon_{out}}{2}}\right] < \bar{\mu}\left[\begin{matrix}\sigma_{in?}+\sigma_{out?}\\ \varepsilon_{in?}+\varepsilon_{out?}\end{matrix}\right]$			
$< \mu_0\left[\begin{matrix}\sigma_{in}\\ \varepsilon_{in}\end{matrix}\right]\frac{1}{4}(25\%)$	1.3(-14) < 1.2(-6)		
$(\frac{R_c}{2\delta l_{sum}}+1)2\lvert\Delta\mu\rvert < \mu_0$	(R_c = .12m, δl_{sum} = .0001m)		
$2\bar{\varepsilon}\omega + \frac{(\bar{\varepsilon}\omega)^2}{\bar{\sigma}} < \sigma_{in}\frac{1}{4}(25\%)$	3.17(-3) < 3.25(-3)	(skull)	10^5
	.029 < .042	(brain)	8×10^4

4.2 Neglecting some space-dependent terms

Justifying further simplification is difficult. Remaining terms that might be assumed to result in negligible contributions to solutions are space-dependent, integrands are indefinite with respect to sign, and assessment of significance requires calculating integrals of unknown functions. The first two problems can be circumvented by using the triangle inequality. For the second problem, as far as I can see, we must resort to estimating integrals using $\omega=0$ solutions for $\vec{A}$ and Φ; this means negligibility cannot be shown but can only be supported. This restriction is somewhat lifted in dealing with the term $\frac{\hat{n}}{R}\times\nabla\times\vec{A}$. I will attend to this term first.

Ignoring the term $\frac{\hat{n}}{R}\times\nabla\times\vec{A}$ can be supported by comparing it with the smallest term involving $\frac{\hat{n}}{R}\Phi$. Measurements of electromagnetic fields at the scalp suggest

$$\left\|\frac{\Delta\mu}{\mu_0^2}\nabla\times{}^t\vec{A}\right\|_{max} = \left\|\frac{\Delta\mu}{\mu_0^2}{}^t\vec{B}\right\|_{max} \ll |{}^t\Phi|_{average}(\varepsilon\omega)|_{\omega_0} \qquad (4\text{-}7)$$

where μ is assumed independent of time and $(\varepsilon\omega)|_{\omega_0}$ is, by definition, independent of time. With $\|\vec{B}_{max}\|$ on the order of 10^{-13}tesla at the scalp surface [113], $\|\frac{\Delta\mu}{\mu_0^2}\vec{B}\|_{max}$ is on the order of 10^{-18}Amp/m. In scalp potential studies, where $\underset{\gamma}{MIN}\int_{p_1\to p_2,\,\gamma}\vec{E}\cdot d\vec{l}$ [4-2] is measured, Φ_{avrg} is on the order of 10^{-6}Volts under the assumption that the contribution of $\vec{A}$ to $\vec{E}$ is not dominant [36, 39]. In order

4-2 Scalp potential experiments measure, between points p_1 and p_2, $\underset{\gamma}{MIN}\int_{p_1\to p_2,\,\gamma}\vec{E}\cdot d\vec{l}$ which is proportional to the minimum energy necessary to move a charge between p_1 and p_2 where γ is a path in the medium ($\vec{E}$ may be non-conservative). The principle of least action [41] is an explanation for measuring devices determining this and is the basis for specifying minimization over γ.

to make the comparison of equation 4-7, a minimum value for $(\varepsilon\omega)|_{\omega_o}$ must be found. The minimum is at ω_o=0 but this minimum does not do us any good. Table 4-4, presented later in this section, shows that $\varepsilon\omega$ is a monotonic increasing function of ω for the frequencies of interest here (certainly < 10^6Hz); given this, I choose to examine frequencies at or above 10Hz since this is the lowest frequency for which I have found data for biological media. For frog muscle, $(\varepsilon\omega)|_{10Hz} \approx 1.4x10^{-3}$Amp/Volt–meter and it can be seen that the two terms of equation 4-7 differ by nine orders of magnitude. Then, from Parseval's relation, for, at worst, most frequencies within the bandwidth observed in the experiments, we can assert

$$\left\| \frac{\Delta\mu}{\mu_0^2} \nabla \times {}^{\omega}\vec{A} \right\|_{max} \ll |{}^{\omega}\Phi|_{average}(\varepsilon\omega)|_{\omega_0} \qquad (4\text{–}8)$$

Finally, to support ignoring the term involving $\nabla\times\vec{A}$, we must assume that

$$\int \frac{\hat{n}}{R}\Phi > 10^{-9}|\Phi|_{average} \qquad (4\text{–}9)$$

for most $\vec{x}_f$. This is certainly true for ω=0 solutions.

To proceed with simplification from this point, neglecting a term must be based on the following reasoning: considering equation 4-2,

$$K_i(\vec{x}, \vec{x}_f) = K_{i_{main}}(\vec{x}, \vec{x}_f) + \delta_{K_i}(\vec{x}, \vec{x}_f) \qquad (4\text{–}10)$$

and

$$\int_{Numerical} K_i(\vec{x}, \vec{x}_f)F_i(\vec{x}) = \int_{Actual} K_iF_i \pm \int_{?} K_iF_i \qquad (4\text{–}11)$$

terms involving the δ_{k_i} can be neglected if

$$\left|\sum_i A_i \int \delta_{K_i} F_i\right| \leq \sum_i |A_i| \int_? K_i F_i \qquad (4\text{-}12)$$

where the $\int_?$ represent some of the uncertainties introduced by numerical methods and uncertainties introduced by source modeling. Another way to justify neglecting terms involving the δ_{k_i} is to show that

$$\left|\sum_i A_i \int \delta_{K_i} F_i\right| \ll \text{MIN}\left(\left|F_{i=i_0}|_{\vec{x}_f}\right|, \left|A_i \int K_{i_{main}} F_i\right|\right) \qquad (4\text{-}13)$$

for most $\vec{x}_f$. Since we can only evaluate these criteria for ω=0 solutions, it seems that under these conditions, the criteria are untenable. To see this, suppose we wish to test neglecting the term $\int \Phi$, i.e. $K_{main}=0$, δ_K=1 for this integral. The observation that $\int \Phi|_{\omega=0}=0$ while $\int \left|\Phi|_{\omega=0}\right|$ is large compared to other integrations in equation 2-25b indicates that small perturbations from ω=0 solutions could result in $\int \Phi|_{\omega\neq 0}$ becoming a significant factor in the equations. This means evaluating criterion 4-12 or 4-13 based on ω=0 solutions could justify neglecting $\int \Phi|_{\omega\neq 0}$ erroneously. Given this analysis of the situation, it would be more convincing to neglect terms under the criterion

$$\sum_i |A_i| \, |\delta_{K_i}|_{max} \int |F_i| \leq \sum_i |A_i| \int_? K_i F_i \qquad (4\text{-}14)$$

where the triangle inequality has been applied to equation 4-12. It will be observed that under this criterion, given the accuracy of the best numerical integrators in integrating ω=0 solutions and the interval of frequencies I wish to study, not much simplification can be achieved. So, in order to examine the significance of terms in the equations, the absolute integrations $\int \left|K_i F_i\right|$ will be examined. Such an examination does not show which terms are most impor-

tant in determining $F_{i=i_o}|_{\vec{x}_f}$ since some integrals could be identically 0 for all $\vec{x}_f$, e.g., $\int\Phi$ for $\omega=0$ solutions mentioned above and $\int\vec{A}$ for $\omega=0$ solutions with centric source, but we will use the measure as an indicator. To give a bit of support for this, I refer back to the example used in support of the claim that criteria expressed by equations 4-12 and 4-13 were untenable. Let us suppose the converse of the example, i.e., suppose $\int\left|\Phi|_{\omega=0}\right|$ was insignificant with respect to other terms of the equations while $\int\Phi|_{\omega=0}=0$; obviously, small perturbations from $\omega=0$ solutions would still result in an insignificant contribution to the equations.

To simplify equations using the measure just discussed, we must choose a way of breaking up the equations into a series of sums. Equations 4-16 summarize the current state of the equations and serve to display how I have subdivided the terms; with writing

$$\tilde{e}=1-e_{re}+ie_{im} \tag{4-15}$$

I hope to have separated the minor from the major terms.

$$4\pi\left[\vec{A}\big|_{\vec{x}_f} - (1,\vec{A})_\infty\right]_{\substack{re\\im}} \approx$$

$$\int_{S_\infty - \vec{x}_f} \left\{ \frac{\hat{n}}{R}\mu_0 \left[\Phi_{\substack{re\\im}} (\varepsilon_{in}\omega e_{im} - (1+e_{re})\sigma_{in}) - \begin{bmatrix} -\Phi_{im} \\ \Phi_{re} \end{bmatrix} (\sigma_{in} e_{im} + (1+e_{re})\varepsilon_{in}\omega) \right] \right.$$

$$+ \sqrt{\omega\mu_0\sigma_{in}} \left(\frac{1}{R_c} + \frac{1}{4\Sigma l} \right) \left[\begin{bmatrix} -\vec{A}_{im} \\ \vec{A}_{re} \end{bmatrix} (1+e_{re}+e_{im}) + \vec{A}_{\substack{re\\im}} (1-e_{re}-e_{im}) \right]$$

$$\left. + R\frac{\omega\mu_0}{4\Sigma l} \left[\vec{A}_{\substack{re\\im}} (\sigma_{in}\varepsilon_{im} - (1+e_{re})\varepsilon_{in}\omega) - \begin{bmatrix} -\vec{A}_{im} \\ \vec{A}_{re} \end{bmatrix} (\varepsilon_{in}\omega e_{im} + (1+e_{re})\sigma_{in}) \right] \right\}$$

$$+ \hat{j} \left[\mu_0 \int_{-L/2}^{L/2} |J_{rld}| \right] \left[\pm \frac{L(2R_j - L)}{4\sqrt{\ }^2} e^{-Re\sqrt{\ }} \left[\begin{bmatrix} \cos \\ \sin \end{bmatrix} (\sqrt{\ }) \right] \left(\frac{1}{\sqrt{\ }} + Re \right) + \left[\begin{matrix} -\sin \\ \cos \end{matrix} (\sqrt{\ }) \right] Im \right]$$

$$\frac{1}{R_j} \begin{bmatrix} (1+e_{re})\cos\theta_{FT} + e_{im}\sin\theta_{FT} \\ (1+e_{re})\sin\theta_{FT} - e_{im}\cos\theta_{FT} \end{bmatrix}$$

(4-16a)

$$\begin{bmatrix} f_1 \\ f_2 \end{bmatrix}(x) \equiv \begin{bmatrix} f_1(\theta_{FT} - Im\, x) \\ f_2(\theta_{FT} - Im\, x) \end{bmatrix}$$

$$Re \equiv \sqrt{\omega\bar{\mu}} \sqrt{\frac{-\bar{\varepsilon}\omega + \sqrt{\bar{\varepsilon}^2\omega^2 + \bar{\sigma}^2}}{2}} \qquad Im \equiv \sqrt{\omega\bar{\mu}} \sqrt{\frac{\bar{\varepsilon}\omega + \sqrt{\bar{\varepsilon}^2\omega^2 + \bar{\sigma}^2}}{2}}$$

$$\sqrt{\ } \equiv \sqrt{R_j^2 + (L/2)^2 - R_j L}$$

$$\left(2\pi\sigma_{in}\Phi\big|_{\vec{x}_f} - 4\pi(\sigma,\Phi)_\infty\right)_{\substack{re\\im}} + 2\pi\varepsilon_{in}\omega\begin{bmatrix}-\Phi_{im}\\ \Phi_{re}\end{bmatrix} \approx$$

$$\int_{S-\vec{x}_f} \Bigg[\frac{\hat{n}\cdot\hat{R}}{R^2}\sigma_{in}\left(\Phi_{\substack{re\\im}}(1+e_{re}) + \begin{bmatrix}-\Phi_{im}\\ \Phi_{re}\end{bmatrix} e_{im}\right) + \frac{\hat{n}\cdot\hat{R}}{R}\frac{\sigma_{in}\sqrt{\omega\mu_0\sigma_{in}}}{2}\left(\Phi_{\substack{re\\im}}(1+e_{re}) + \begin{bmatrix}-\Phi_{im}\\ \Phi_{re}\end{bmatrix} e_{im}\right)$$
$$+ R\frac{\omega\mu_0}{4\Sigma l}\left(-\Phi_{\substack{re\\im}}\left(\frac{\sigma_{in}}{2}e_{im} + (1+e_{re})\varepsilon_{in}\omega\right) + \begin{bmatrix}-\Phi_{im}\\ \Phi_{re}\end{bmatrix}\left(\frac{\sigma_{in}}{2}(1+e_{re}) - \varepsilon_{in}\omega e_{im}\right)\right)$$
$$+ \frac{\sigma_{in}\sqrt{\omega\mu_0\sigma_{in}}}{2}\left(\frac{1}{R_c} - \frac{1}{4\Sigma l}\right)\left(\Phi_{\substack{re\\im}}(1+e_{re}-e_{im}) + \begin{bmatrix}-\Phi_{im}\\ \Phi_{re}\end{bmatrix}(1+e_{re}+e_{im})\right)$$
$$+ \omega\frac{\hat{n}}{R}\cdot\left(\vec{A}_{\substack{re\\im}}(\sigma_{in}e_{im} + (1+e_{re})\varepsilon_{in}\omega) + \begin{bmatrix}-\vec{A}_{im}\\ \vec{A}_{re}\end{bmatrix}(\varepsilon_{in}\omega e_{im} - (1+e_{re})\sigma_{in})\right) \Bigg]$$

$$-\left(\int_{-L/2}^{L/2} |J_{rId}|\right)\left(\frac{\hat{R}_j\cdot\hat{j}}{R_j}\left(\begin{bmatrix}(1+e_{re})\cos\theta_{FT} + e_{im}\sin\theta_{FT}\\ (1+e_{re})\sin\theta_{FT} - e_{im}\cos\theta_{FT}\end{bmatrix}\left(\frac{1}{R_j} + Re\right) + \begin{bmatrix}e_{im}\cos\theta_{FT} - (1+e_{re})\sin\theta_{FT}\\ e_{im}\sin\theta_{FT} + (1+e_{re})\cos\theta_{FT}\end{bmatrix} Im\right)\right.$$
$$\left. \pm\frac{L}{2}\begin{bmatrix}\cos\\ \sin\end{bmatrix}(\sqrt{\ }) \frac{e^{-Re\sqrt{\ }}}{\sqrt{\ }^2}\left(\frac{(2R_j-L)^2}{4\sqrt{\ }}\left(\frac{3}{\sqrt{\ }}(Re + \frac{1}{\sqrt{\ }}) + Re^2 - Im^2\right) - (Re + \frac{1}{\sqrt{\ }})\right)\right.$$
$$\left. \begin{bmatrix}-\sin\\ \cos\end{bmatrix}(\sqrt{\ }) \frac{Im\, e^{-Re\sqrt{\ }}}{\sqrt{\ }^2}\left(\frac{(2R_j-L)^2}{4\sqrt{\ }}\left(\frac{3}{\sqrt{\ }} + 2Re\right) - 1\right)\right)$$

(4-16b)

Simplification of these equations will be carried out through estimating absolute integrations averaged over $\vec{x}_f$ and magnitudes of terms not involving integration also averaged over $\vec{x}_f$. These estimates will be used in

$$\frac{\sum \text{average for minor terms}}{\underset{\text{all terms}}{\text{MAX (average)}}} \leq 10^{-2} \quad : \quad \frac{\text{average for major term}}{\underset{\text{all terms}}{\text{MAX (average)}}} > 10^{-2} \tag{4-17}$$

i.e., the sum of the estimates for terms judged minor must be two orders of magnitude smaller than the largest estimate where all estimates for terms judged major are individually larger than 1% of the maximum.

Here are some details I need in order to carry out calculations. Anticipating that terms involving e_{re} and e_{im} will be neglectable, I choose to take an upper limit of these quantities using

$$\int |f_1 f_2| \leq |f_1|_{max} \int |f_2| \tag{4-18}$$

For the frequencies of interest, e_{re} and e_{im} are increasing functions of R_c, σ, ε, and ω. I will take $R_{c_{max}}$=0.12m, σ_{max}=1.56$(\Omega m)^{-1}$ (CSF), and ε appropriate for various ω. It turns out that, for ω=0 solutions,

$$\Phi_{re} : \Phi_{im} = \vec{A}_{re} : \vec{A}_{im} = \vec{J}_{re} : \vec{J}_{im} = \cos\theta_{FT} : \sin\theta_{FT} \tag{4-19}$$

so that with a neglect scheme based on these solutions, under the case $\theta_{FT}=\frac{\pi}{4}$, several terms could be judged ignorable that could not be so judged if θ_{FT}=0 or $\frac{\pi}{2}$. Given that the full range of θ_{FT} is $[0,2\pi)$, a consideration of equations 4-16 shows that examining the case θ_{FT}=0 is sufficient to reveal the terms that must be retained. The choice of value for $\int_{-L/2}^{L/2} |J_{rld}|$ is unimportant since this simply sets a multiplicative constant embedded in both $\vec{A}$ and Φ. The value

5 Amp-m is used. For δl_{max}, the value 10^{-4}m is used so the values reported for absolute integrations associated with $\int\Phi$ and $\int\vec{A}$ can be smaller by an order of magnitude since $\Sigma l \in [10^{-4}m, 10^{-3}m]$ for the head system. Table 4-3 shows calculations for radial sources ($\hat{j}$ along the z axis) at eccentricity 0.8. For lower eccentricities and tangentially oriented sources ($\hat{j}$ normal to z axis) the numbers are of the same order except for the integration errors. These errors are approximately two orders of magnitude lower for eccentricities 0.4 and 0.0.

TABLE 4-3 Average magnitudes of terms of equations 4-16 using absolute integrations, $\theta_{FT}=0$, radial source at eccentricity 0.8, $\Sigma l = .0001\text{m}$, and $\int_{-L/2}^{L/2} |J_{rld}| = 5\text{Ampm}$.

term involving:	magnitude estimate	integration error or source uncertainty
$\int \frac{\hat{n}}{R}\Phi$	coordinates: x 1.9(−5), y 1.9(−5), z 3.8(−5); $\left\lvert \begin{matrix} \varepsilon_{in}\omega e_{im} - \sigma_{in} - \sigma_{in} e_{re} \\ \sigma_{in} e_{im} + \varepsilon_{in}\omega + \varepsilon_{in}\omega e_{re} \end{matrix} \right\rvert_{max}$ (real / imaginary)	7.5(−8), 7.5(−8), 4.3(−7)
$\int \vec{A}$	$\begin{matrix} 9.2(-7) \\ 9.2(-7) \\ 2.1(-6) \end{matrix} \left\lvert \begin{matrix} e_{im} - e_{re} - 1 \\ 1 + e_{im} + e_{re} \end{matrix} \right\rvert_{max}$	$\begin{bmatrix} 9.1(-11) \\ 9.3(-11) \\ 1.3(-9) \end{bmatrix} \sqrt{\text{Hz}}$
$\int R\vec{A}$	$\begin{matrix} 3.4(-10) \\ 3.4(-10) \\ 7.7(-10) \end{matrix} \left\lvert \begin{matrix} \sigma_{in} e_{im} - \varepsilon_{in}\omega(1+e_{re}) \\ \varepsilon_{in}\omega e_{im} + \sigma_{in}(1+e_{re}) \end{matrix} \right\rvert_{max}$	
$\vec{J}_r$	$\begin{matrix} 0 \\ 0 \\ 5.2(-2) \end{matrix} \left\lvert \begin{matrix} 1+e_{re} \\ e_{im} \end{matrix} \right\rvert_{max}$	$\left.\begin{matrix} 0 \\ 0 \\ 2.1(-7) \end{matrix}\right\}\text{Hz}=0 \quad \left.\begin{matrix} 0 \\ 0 \\ 2.6(-7) \end{matrix}\right\}\text{Hz}=10^6$
$\vec{A}$	$\begin{matrix} 9.0(-6) \\ 9.0(-6) \\ 3.2(-5) \end{matrix} \left\lvert \begin{matrix} 1+e_{re} \\ e_{im} \end{matrix} \right\rvert_{max}$	

TABLE 4-3 continued for equation 4-16b.

term involving:	magnitude estimate	integration error or source uncertainty
$\int \frac{\hat{n}\cdot\hat{R}}{R^2}\Phi$	$310\left\lvert\begin{matrix}1+e_{re}\\ e_{im}\end{matrix}\right\rvert_{max}$	2.0
$\int \frac{\hat{n}\cdot\hat{R}}{R}\Phi$	$6.0(-2)\left\lvert\begin{matrix}1+e_{re}\\ e_{im}\end{matrix}\right\rvert_{max}\sqrt{Hz}$	
$\int R\,\Phi$	$.33\left\lvert\begin{matrix}\varepsilon_{in}\omega(1+e_{re})+e_{im}\\ \frac{\sigma_{in}}{2}(1+e_{re})-\varepsilon_{in}\omega e_{im}\end{matrix}\right\rvert_{max}$ Hz	.032 Hz
$\int\Phi$	$200\left\lvert\begin{matrix}1+e_{re}-e_{im}\\ 1+e_{re}+e_{im}\end{matrix}\right\rvert_{max}\sqrt{Hz}$	$.16\sqrt{Hz}$
$\int \frac{\hat{n}}{R}\cdot\vec{A}$	$1.2(-5)\left\lvert\begin{matrix}(1+e_{re})\varepsilon_{in}\omega+\sigma_{in}e_{im}\\ \varepsilon_{in}\omega e_{im}-(1+e_{re})\sigma_{in}\end{matrix}\right\rvert_{max}$ Hz	$1.8(-9)$Hz
$\nabla\cdot\vec{J}_r\frac{\hat{j}\cdot\hat{R}_j}{R_j^2}$	$217\left\lvert\begin{matrix}1+e_{re}\\ e_{im}\end{matrix}\right\rvert_{max}$	$2.9\lvert_{Hz=0}$ $3.8\lvert_{Hz=10^6}$
$\nabla\cdot\vec{J}_r\frac{\hat{j}\cdot\hat{R}_j}{R_j}$	$.0035\left\lvert\begin{matrix}1+e_{re}-e_{im}\\ 1+e_{re}+e_{im}\end{matrix}\right\rvert_{max}\sqrt{Hz}$	
Φ	$195\left\lvert\begin{matrix}\sigma_{in}\\ \varepsilon_{in}\omega\end{matrix}\right\rvert_{max}$	

Suppose we wish to neglect all terms involving e_{re} and e_{im}. Considering reported integration errors, source term uncertainties, and e_{re} and e_{im} shown in table 4-4, this cannot be justified based on equation 4-14 unless frequencies fall below approximately 100Hz. Using the criteria expressed by equation 4-17, larger neglect intervals can be obtained. Table 4-5 lists several terms and the frequency intervals within which they can be neglected. Obviously, some of these intervals are absurd, specifically the unbounded ones.

TABLE 4-4 Maximum estimates for quantities shown using $\sigma_{in} = 1.56(\Omega m)^{-1}$

Hz	e_{re}	e_{im}	$\varepsilon_{in}\omega$ (1)
1	4.2(-4)	4.2(-4)	
5	9.4(-4)	9.4(-4)	
10	1.3(-3)	1.3(-3)	2.2(-4)
50	2.9(-3)	2.9(-3)	4.4(-4)
100	4.2(-3)	4.1(-3)	5.6(-4)
500	9.4(-3)	9.3(-3)	1.1(-3)
10^3	1.3(-2)	1.3(-2)	1.8(-3)
10^4	4.2(-2)	4.0(-2)	5.6(-3)
10^5	1.2(-1)	1.0(-1)	1.4(-2)
$8x10^4$	1.3(-1)	1.2(-1)	2.1(-2)

1 using ε_{in} appropriate for brain tissue, lower frequencies extrapolated from values at higher frequencies, see graph 4-1.

TABLE 4-5 Frequency domains for justifiable neglect using equation 4-17.

term(s) involving:	frequency domain (Hz)
e_{re}, e_{im}	$0 \rightarrow 500$
$\varepsilon_{in}\omega\int\frac{\hat{n}}{R}\Phi$	$0 \rightarrow \infty$[1]
$\int R\vec{A}$	$0 \rightarrow 10^4$
$\vec{J}^r$	$6.2\text{x}10^6 \rightarrow \infty$
$\vec{A}$	$2.3\text{x}10^8 \rightarrow \infty$
$\int\frac{\hat{n}\bullet\hat{R}}{R^2}\Phi$	$2.4\text{x}10^4 \rightarrow \infty$
$\int\frac{\hat{n}\bullet\hat{R}}{R}\Phi$	$0 \rightarrow \infty$
$\frac{\sigma_{in}}{2}\int R\Phi$	$0 \rightarrow 60$
$\varepsilon_{in}\omega\int R\Phi$	$0 \rightarrow 10^{3}$[1]
$\int\frac{\hat{n}}{R}\bullet\vec{A}$	$0 \rightarrow \infty$
$\nabla\bullet\vec{J}_r\frac{\hat{R}_j\bullet\hat{j}}{R_j^2}$	$1.1\text{x}10^4 \rightarrow \infty$
$\nabla\bullet\vec{J}_r\frac{\hat{R}_j\bullet\hat{j}}{R_j}$	$0 \rightarrow 5\text{x}10^5$
$\sigma_{in}\Phi$	$2.4\text{x}10^4 \rightarrow \infty$
$\varepsilon_{in}\omega\Phi$	$0 \rightarrow \infty$

1 thus, $\sigma_{in}e_{im}$ is limiting factor for this term, i.e., 500Hz limit.

Assuming the intervals valid up to 500Hz, equations 4-20 are obtained.

$$4\pi(\vec{A}|_{\vec{x}_f}-(1,\vec{A})_\infty)_{\substack{re\\im}} \approx \mu_0\left(\int_{-L/2}^{L/2}|J_{rld}|\right)\frac{\hat{J}}{R_j}\begin{bmatrix}\cos\theta_{FT}\\ \sin\theta_{FT}\end{bmatrix}$$

$$+\int_{S-\vec{x}_f}\sqrt{\omega\mu_0\sigma_{in}}\left(\frac{1}{R_c}+\frac{1}{4\ \Sigma l}\right)\begin{bmatrix}1 & -1\\ 1 & 1\end{bmatrix}\vec{A}_{\substack{re\\im}}-\frac{\hat{n}}{R}\mu_0\sigma_{in}\Phi_{\substack{re\\im}} \qquad (4\text{-}20a)$$

$$(2\pi\sigma_{in}\Phi-4\pi(\sigma,\Phi)_\infty)_{\substack{re\\im}}+2\pi\varepsilon_{in}\omega\begin{bmatrix}0 & -1\\ 1 & 0\end{bmatrix}\Phi_{\substack{re\\im}} \approx -\left(\int_{-L/2}^{L/2}|J_{rld}|\right)\frac{\hat{R}_j\bullet\hat{J}}{R_j^2}\begin{bmatrix}\cos\theta_{FT}\\ \sin\theta_{FT}\end{bmatrix}$$

$$+\int_{S-\vec{x}_f}\left\{\frac{\sigma_{in}\sqrt{\omega\mu_0\sigma_{in}}}{2}\left(\frac{1}{R_c}-\frac{1}{4\ \Sigma l}\right)\begin{bmatrix}1 & -1\\ 1 & 1\end{bmatrix}+R\frac{\omega\mu_0}{4\ \Sigma l}\frac{\sigma_{in}}{2}\begin{bmatrix}0 & -1\\ 1 & 0\end{bmatrix}+\frac{\hat{n}\bullet\hat{R}}{R^2}\sigma_{in}\begin{bmatrix}1 & 0\\ 0 & 1\end{bmatrix}\right\}\Phi_{\substack{re\\im}} \qquad (4\text{-}20b)$$

Before closing this section, I would like to present an alternative view of justifying negligibility. It is easiest to do this by example. Consider the terms $\varepsilon\omega\int\frac{\hat{n}}{R}\Phi$ and $\int\frac{\hat{n}}{R}\bullet\vec{A}$. Using the criterion expressed by equation 4-17 meant that these terms were neglected based on a comparison between integrals involving $\vec{A}$ and integrals involving Φ respectively. Doing this might be questioned since we do not know how the relationship between $\vec{A}$ and Φ evolves as ω increases from 0. This serves to illustrate one assumption that underlies the neglect analysis: for frequencies of interest, the relationship between $\vec{J}, \nabla\bullet\vec{J}, \vec{A}$, and Φ, as defined by criteria for neglect, remains approximately the same as that for solutions at ω=0. If this assumption is not made, there are

still some terms that can be neglected without relying on cross-function comparisons. Under this restriction, these would be the equations for a peak frequency of 500Hz:

$$4\pi(\vec{A}|_{\vec{x}_f}-(1,\vec{A})_\infty)_{\substack{re\\im}} \approx \mu_0\left(\int_{-L/2}^{L/2}|J_{rld}|\right)\frac{\hat{\vec{J}}}{R_j}\begin{bmatrix}\cos\theta_{FT}+e_{im}\sin\theta_{FT}\\ \sin\theta_{FT}-e_{im}\cos\theta_{FT}\end{bmatrix}$$

$$+\int_{S-\vec{x}_f}\sqrt{\omega\mu_0\sigma_{in}}\left(\frac{1}{R_c}+\frac{1}{4\Sigma l}\right)\begin{bmatrix}1 & -1\\ 1 & 1\end{bmatrix}\vec{A}_{\substack{re\\im}}-\frac{\hat{\vec{n}}}{R}\mu_0\begin{bmatrix}\sigma_{in} & -\sigma_{in}e_{im}-\varepsilon_{in}\omega\\ \sigma_{in}e_{im}+\varepsilon_{in}\omega & \sigma_{in}\end{bmatrix}\Phi_{\substack{re\\im}} \quad (4\text{-}21a)$$

$$(2\pi\sigma_{in}\Phi-4\pi(\sigma,\Phi)_\infty)_{\substack{re\\im}}+2\pi\varepsilon_{in}\omega\begin{bmatrix}0 & -1\\ 1 & 0\end{bmatrix}\Phi_{\substack{re\\im}} \approx -\left(\int_{-L/2}^{L/2}|J_{rld}|\right)\frac{\hat{\vec{R}}_j\cdot\hat{\vec{J}}}{R_j^2}\begin{bmatrix}\cos\theta_{FT}+e_{im}\sin\theta_{FT}\\ \sin\theta_{FT}-e_{im}\cos\theta_{FT}\end{bmatrix}$$

$$+\int_{S-\vec{x}_f}\left\{\frac{\sigma_{in}\sqrt{\omega\mu_0\sigma_{in}}}{2}\left(\frac{1}{R_c}-\frac{1}{4\Sigma l}\right)\begin{bmatrix}1 & -1\\ 1 & 1\end{bmatrix}+R\frac{\omega\mu_0}{4\Sigma l}\frac{\sigma_{in}}{2}\begin{bmatrix}0 & -1\\ 1 & 0\end{bmatrix}+\frac{\hat{\vec{n}}\cdot\hat{\vec{R}}}{R^2}\sigma_{in}\begin{bmatrix}1 & 0\\ 0 & 1\end{bmatrix}\right\}\Phi_{\substack{re\\im}}$$

$$+\int_{S-\vec{x}_f}\left\{\omega\frac{\hat{\vec{n}}}{R}\cdot\begin{bmatrix}\sigma_{in}e_{im}+\varepsilon_{in}\omega & \sigma_{in}\\ -\sigma_{in} & \sigma_{in}e_{im}+\varepsilon_{in}\omega\end{bmatrix}\vec{A}_{\substack{re\\im}}\right. \quad (4\text{-}21b)$$

5. Alternative formulations

Before describing the methods used to find solutions to equations 4-20 or 4-21, alternative methods to obtain an assessment of the degree of electromagnetic coupling will be discussed.

5.1 Alternative potentials

I start with alternatives to compressing Maxwell's equations. One alternative is to use an electric vector potential and a magnetic scalar potential [28]

$$\frac{1}{\mu}\vec{B} = \vec{T} + \nabla\Omega \qquad (5\text{-}1)$$

This formulation has proven useful for solving eddy current problems where quasi-static approximations are assumed ($\varepsilon\omega$=0,$\tilde{e}$=1) along with assuming the continuity of $\frac{1}{\mu}\vec{B}$ at conductor/air interfaces ([21, 37] Davey and Barnes). I too have made the quasi-static approximation in equation 4-20 and 4-21 but incompletely so. In addition, I have not assumed the boundary condition. In these circumstances, $\vec{T}$ and Ω equations are implicitly coupled:

$$\nabla^2\vec{T} - i\omega\mu\tilde{\sigma}\vec{T} = -\nabla\times\vec{J}_r - \nabla\tilde{\sigma}\times\vec{E} + i\omega\Omega\nabla\tilde{\sigma}\mu \qquad (5\text{-}2a)$$

$$\nabla\bullet\ \mu\nabla\Omega - i\omega\mu^2\tilde{\sigma}\Omega = -\nabla\mu\bullet\ \vec{T} \qquad (5\text{-}2b)$$

(Implicit coupling is independent of gauge choosen for $\vec{T}$.) In contrast, the problem solved by Davey and Barnes (obtaining the magnetic field for an electric dipole source embedded in a semi-infinite conductor for frequencies less than 10^5Hz) the term $\nabla\sigma\times\vec{E}$ disappears. This happens because the continuity of $\frac{1}{\mu}\vec{B}$ is derivable from equation 2-7b, with ω=0, only if $\vec{E}$ is normal to the conductor/air interface since there are no $\vec{J}_r$ contributions there. In

conclusion, there would be no advantage in using the potentials $\vec{T}$ and Ω for the problem with which we are concerned. Though there are an infinite number of ways to define potentials, the potentials $\vec{T}$, Ω, $\vec{A}$, and Φ are those that I have observed to be used in practice. Suffice it to say that with respect to this set, I have chosen the more convenient formulation.

5.2 Numerical differentiation

The next major methodological alternative is to use numerical differentiation instead of converting to integral equations. I decided against this alternative on the assumption that boundary integral methods would be more economical since I only wished to study fields at the scalp/air interface. However, it is not clear that this is true. I have observed that an overwhelmingly large proportion of time is spent setting up the discretized equations in comparison to finding solutions to them. A comparison between boundary integral methods (projection method) and finite element methods magnetostatic problems [102] reports setup cost for integral formulations to be the square of the cost for differential equation formulations. Thus, though the order of the discretized formulation is much larger for differential methods, it is unclear which of the two methods is best.

Integral and differential methods have been compared for the solution of the ω=0 scalar potential equation [87]. Computational expense was not reported. However, with respect to the average deviation of computed from actual solutions (they examined a spherical conductor for which there are analytical solutions), differential methods performed slightly better than integral methods. Keeping in mind that computational cost and the accuracy of numerical solutions are functions that depend both on the particular problem being solved and the particular numerical integral and differential

methods used, it would be foolish to conclude from their data that numerical integration methods were inferior. In further support of this, it will be seen below that the numerical integration methods they used perform poorly with respect to techniques used in this dissertation. Similar comments can be made of a similar study [55] wherein potentials on the surface of an infinite cylindrical conductor with an embedded centrally located dipole were sought. Computational cost assessments did not include setup costs and the simplicity of the problem undermines generalization of results. I conclude that there is, at present, insufficient data to suggest which method is to be preferred.

5.3 Alternative solutions to integral equations

In this section, I will explore alternative methods of finding solutions to Fredholm equations of the second kind.

5.3.1 Analytical solutions

Equations 4-20 or 4-21 can be converted into a Fredholm integral equation of the second kind for which there is a series solution [89]. I will detail the conversion of equations 4-21 since all subsequent developments can be easily reduced to forms appropriate for equations 4-20. The goal is to reduce the system to the form

$$F(\vec{x}_f) = J(\vec{x}_f) + \int_{\Omega} K(\vec{x}_f, \vec{x})\, F(\vec{x})\, d\vec{x} \qquad (5\text{-}3)$$

This can be done by taking Ω to consist of a collection of nested surfaces infinitesimally close together [95]. In addition, equation 4-21b must be solved for $\Phi_{\substack{re \\ im}}|_{\vec{x}_f}$. The solution is summarized by equations 5-4. Simplifications similar to those of section 4 have been used and $\omega \neq 0$ has been assumed.

For the record, I have displayed equations appropriate for equations 4-20 in equations $5-4a_0$ and $5-4b_0$.

$$\vec{A}_{im}^{re}|_{\vec{x}_f} = \frac{\mu_0}{4\pi}\left(\int_{-L/2}^{L/2} |J_{rld}|\right)\frac{\hat{j}}{R_j}\begin{bmatrix}\cos\theta_{FT}+e_{im}\sin\theta_{FT}\\ \sin\theta_{FT}-e_{im}\cos\theta_{FT}\end{bmatrix}$$
$$+\int_{S-\vec{x}_f}\frac{\sqrt{\omega\mu_0\sigma_{in}}}{4\pi}\left(\frac{1}{R_c}+\frac{1}{4\Sigma l}\right)\begin{bmatrix}1 & -1\\ 1 & 1\end{bmatrix}\vec{A}_{im}^{re}-\frac{\hat{n}}{R}\frac{\mu_0}{4\pi}\begin{bmatrix}\sigma_{in} & -\sigma_{in}e_{im}-\varepsilon_{in}\omega\\ \sigma_{in}e_{im}+\varepsilon_{in}\omega & \sigma_{in}\end{bmatrix}\Phi_{im}^{re} \quad (5\text{-}4a)$$

$$\Phi_{im}^{re}|_{\vec{x}_f} = -\frac{1}{2\pi\sigma_{in}^2}\left(\int_{-L/2}^{L/2} |J_{rld}|\right)\frac{\hat{R}_j\bullet\hat{j}}{R_j^2}\begin{bmatrix}\sigma_{in} & \varepsilon_{in}\omega\\ -\varepsilon_{in}\omega & \sigma_{in}\end{bmatrix}\begin{bmatrix}\cos\theta_{FT}+e_{im}\sin\theta_{FT}\\ \sin\theta_{FT}-e_{im}\cos\theta_{FT}\end{bmatrix}$$
$$+\int_{S-\vec{x}_f}\left\{\frac{\sqrt{\omega\mu_0\sigma_{in}}}{4\pi}\left(\frac{1}{R_c}-\frac{1}{4\Sigma l}\right)\begin{bmatrix}1 & -1\\ 1 & 1\end{bmatrix}+R\frac{\omega\mu_0}{4\Sigma l}\frac{1}{4\pi\sigma_{in}}\begin{bmatrix}\varepsilon_{in}\omega & -\sigma_{in}\\ \sigma_{in} & \varepsilon_{in}\omega\end{bmatrix}+\frac{\hat{n}\bullet\hat{R}}{R^2}\begin{bmatrix}\sigma_{in} & \varepsilon_{in}\omega\\ -\varepsilon_{in}\omega & \sigma_{in}\end{bmatrix}\right\}\Phi_{im}^{re}$$
$$+\int_{S-\vec{x}_f}\frac{\omega}{2\pi}\frac{\hat{n}}{R}\bullet\begin{bmatrix}e_{im} & 1\\ -1 & e_{im}\end{bmatrix}\vec{A}_{im}^{re} \quad (5\text{-}4b)$$

$$\vec{A}_{im}^{re}|_{\vec{x}_f} = \frac{\mu_0}{4\pi}\left(\int_{-L/2}^{L/2} |J_{rld}|\right)\frac{\hat{j}}{R_j}\begin{bmatrix}\cos\theta_{FT}\\ \sin\theta_{FT}\end{bmatrix}$$
$$+\int_{S-\vec{x}_f}\frac{\sqrt{\omega\mu_0\sigma_{in}}}{4\pi}\left(\frac{1}{R_c}+\frac{1}{4\Sigma l}\right)\begin{bmatrix}1 & -1\\ 1 & 1\end{bmatrix}\vec{A}_{im}^{re}-\frac{\hat{n}}{R}\frac{\mu_0\sigma_{in}}{4\pi}\Phi_{im}^{re} \quad (5\text{-}4a_0)$$

$$\Phi_{im}^{re}|_{\vec{x}_f} = -\frac{1}{2\pi\sigma_{in}^2}\left(\int_{-L/2}^{L/2} |J_{rld}|\right)\frac{\hat{R}_j\bullet\hat{j}}{R_j^2}\begin{bmatrix}\sigma_{in} & \varepsilon_{in}\omega\\ -\varepsilon_{in}\omega & \sigma_{in}\end{bmatrix}\begin{bmatrix}\cos\theta_{FT}\\ \sin\theta_{FT}\end{bmatrix}$$
$$+\int_{S-\vec{x}_f}\left\{\frac{\sqrt{\omega\mu_0\sigma_{in}}}{4\pi}\left(\frac{1}{R_c}-\frac{1}{4\Sigma l}\right)\begin{bmatrix}1 & -1\\ 1 & 1\end{bmatrix}+R\frac{\omega\mu_0}{4\Sigma l}\frac{1}{4\pi}\begin{bmatrix}0 & -1\\ 1 & 0\end{bmatrix}+\frac{\hat{n}\bullet\hat{R}}{R^2}\frac{1}{2\pi}\right\}\Phi_{im}^{re} \quad (5\text{-}4b_0)$$

For the problem at hand, we need eight surfaces, S_k, $k\in[1\rightarrow 8]$. In cartesian coordinates,

$$F(\vec{x}_f) = \begin{cases} A_x^{re}(\vec{x}_f) & \vec{x}_f \in S_1 \\ . & . \\ . & . \\ . & . \\ A_z^{im}(\vec{x}_f) & \vec{x}_f \in S_6 \\ \Phi^{re}(\vec{x}_f) & \vec{x}_f \in S_7 \\ \Phi^{im}(\vec{x}_f) & \vec{x}_f \in S_8 \end{cases} \tag{5-5a}$$

$$J(\vec{x}_f) = \left(\int_{-L/2}^{L/2} |J_{rld}|\right) \begin{cases} \dfrac{\mu_0}{4\pi}\dfrac{\hat{J}\bullet\vec{x}}{R_j}(\cos\theta_{FT} + e_{im}\sin\theta_{FT}) & \\ . & \vec{x}_f \in S_1 \\ . & . \\ . & . \\ \dfrac{\mu_0}{4\pi}\dfrac{\hat{J}\bullet\vec{z}}{R_j}(\sin\theta_{FT} - e_{im}\cos\theta_{FT}) & \vec{x}_f \in S_6 \\ -\dfrac{1}{2\pi\sigma_{in}^2}\dfrac{\hat{R}_j\bullet\hat{J}}{R_j^2}\left(\sigma_{in}(\cos\theta_{FT}+e_{im}\sin\theta_{FT})+\varepsilon_{in}\omega(\sin\theta_{FT}-e_{im}\cos\theta_{FT})\right) & \vec{x}_f \in S_7 \\ -\dfrac{1}{2\pi\sigma_{in}^2}\dfrac{\hat{R}_j\bullet\hat{J}}{R_j^2}\left(-\varepsilon_{in}\omega(\cos\theta_{FT}+e_{im}\sin\theta_{FT})+\sigma_{in}(\sin\theta_{FT}-e_{im}\cos\theta_{FT})\right) & \vec{x}_f \in S_8 \end{cases}$$

(5-5b)

$$
K(\vec{x}_f, \vec{x}) = \begin{cases}
\dfrac{\sqrt{\omega\mu_0\sigma_{in}}}{4\pi}\left[\dfrac{1}{R_c} + \dfrac{1}{4\Sigma l}\right] & \vec{x}_f \in S_1 \quad \vec{x} \in S_1 \\
0 & \vec{x} \in S_2, S_3, S_5, S_6 \\
-\dfrac{\sqrt{\omega\mu_0\sigma_{in}}}{4\pi}\left[\dfrac{1}{R_c} + \dfrac{1}{4\Sigma l}\right] & \vec{x} \in S_4 \\
-\dfrac{\hat{n}\cdot\hat{x}}{R}\dfrac{\mu_0\sigma_{in}}{4\pi} & \vec{x} \in S_7 \\
\dfrac{\hat{n}\cdot\hat{x}}{R}\dfrac{\mu_0}{4\pi}(\sigma_{in}e_{im} + \varepsilon_{in}\omega) & \vec{x} \in S_8 \\
\vdots & \vdots \\
0 & \vec{x}_f \in S_8 \quad \vec{x} \in S_1, S_2, S_4, S_5 \\
\dfrac{\sqrt{\omega\mu_0\sigma_{in}}}{4\pi}\left[\dfrac{1}{R_c} + \dfrac{1}{4\Sigma l}\right] & \vec{x} \in S_3, S_6 \\
-\dfrac{\hat{n}\cdot\hat{z}}{R}\dfrac{\mu_0}{4\pi}(\sigma_{in}e_{im} + \varepsilon_{in}\omega) & \vec{x} \in S_7 \\
-\dfrac{\hat{n}\cdot\hat{z}}{R}\dfrac{\mu_0\sigma_{in}}{4\pi} & \vec{x} \in S_8 \\
\dfrac{\omega}{2\pi}\dfrac{\hat{n}\cdot\hat{x}}{R}e_{im} & \vec{x}_f \in S_7 \quad \vec{x} \in S_1 \\
\dfrac{\omega}{2\pi}\dfrac{\hat{n}\cdot\hat{y}}{R}e_{im} & \vec{x} \in S_2 \\
\dfrac{\omega}{2\pi}\dfrac{\hat{n}\cdot\hat{z}}{R}e_{im} & \vec{x} \in S_3 \\
\dfrac{\omega}{2\pi}\dfrac{\hat{n}\cdot\hat{x}}{R} & \vec{x} \in S_4 \\
\dfrac{\omega}{2\pi}\dfrac{\hat{n}\cdot\hat{y}}{R} & \vec{x} \in S_5 \\
\dfrac{\omega}{2\pi}\dfrac{\hat{n}\cdot\hat{z}}{R} & \vec{x} \in S_6 \\
\dfrac{\sqrt{\omega\mu_0\sigma_{in}}}{4\pi}\left[\dfrac{1}{R_c} - \dfrac{1}{4\Sigma l}\right] + R\dfrac{\omega\mu_0}{4\Sigma l}\dfrac{\varepsilon_{in}\omega}{4\pi\sigma_{in}} + \dfrac{\hat{R}\cdot\hat{n}}{R^2}\dfrac{1}{2\pi} & \vec{x} \in S_7 \\
-\dfrac{\sqrt{\omega\mu_0\sigma_{in}}}{4\pi}\left[\dfrac{1}{R_c} - \dfrac{1}{4\Sigma l}\right] - R\dfrac{\omega\mu_0}{4\Sigma l}\dfrac{1}{4\pi} + \dfrac{\hat{R}\cdot\hat{n}}{R^2}\dfrac{\varepsilon_{in}\omega}{2\pi\sigma_{in}} & \vec{x} \in S_8 \\
-\dfrac{\omega}{2\pi}\dfrac{\hat{n}\cdot\hat{x}}{R} & \vec{x}_f \in S_8 \quad \vec{x} \in S_1 \\
-\dfrac{\omega}{2\pi}\dfrac{\hat{n}\cdot\hat{y}}{R} & \vec{x} \in S_2 \\
-\dfrac{\omega}{2\pi}\dfrac{\hat{n}\cdot\hat{z}}{R} & \vec{x} \in S_3 \\
\dfrac{\omega}{2\pi}\dfrac{\hat{n}\cdot\hat{x}}{R}e_{im} & \vec{x} \in S_4 \\
\dfrac{\omega}{2\pi}\dfrac{\hat{n}\cdot\hat{y}}{R}e_{im} & \vec{x} \in S_5 \\
\dfrac{\omega}{2\pi}\dfrac{\hat{n}\cdot\hat{z}}{R}e_{im} & \vec{x} \in S_6 \\
\dfrac{\sqrt{\omega\mu_0\sigma_{in}}}{4\pi}\left[\dfrac{1}{R_c} - \dfrac{1}{4\Sigma l}\right] + R\dfrac{\omega\mu_0}{4\Sigma l}\dfrac{1}{4\pi} - \dfrac{\hat{R}\cdot\hat{n}}{R^2}\dfrac{\varepsilon_{in}\omega}{2\pi\sigma_{in}} & \vec{x} \in S_7 \\
\dfrac{\sqrt{\omega\mu_0\sigma_{in}}}{4\pi}\left[\dfrac{1}{R_c} - \dfrac{1}{4\Sigma l}\right] + R\dfrac{\omega\mu_0}{4\Sigma l}\dfrac{\varepsilon_{in}\omega}{4\pi\sigma_{in}} + \dfrac{\hat{R}\cdot\hat{n}}{R^2}\dfrac{1}{2\pi} & \vec{x} \in S_8
\end{cases}
\tag{5-5c}
$$

giving us the form 5-3 where

$$\vec{x}_f \in \Omega \ : \Omega = \bigcup_{k=1}^{\infty} S_k \tag{5-6}$$

and S_k are nested infinitesimally close to S of equations 5-4. The applicability of Fredholm's solutions depend on the behavior of J and K. The following integrals must be bounded:

$$\int_{\Omega} J d\vec{x}_f \tag{5-7a}$$

$$\int_{\Omega} K d\vec{x}_f \tag{5-7b}$$

$$\int_{\Omega}\int_{\Omega} |K|^2 d\vec{x} d\vec{x}_f \tag{5-7c}$$

The first of these is obviously bounded since the sources are within the surfaces S_k. The second integral is bounded since, for S_k having spherical geometry,

$$\int_{\text{Sphere}-\vec{x}_f} \frac{\hat{n}}{R} = \frac{4\pi}{3}\hat{x}_f \tag{5-8a}$$

and for any closed surface S,

$$\int_{S-\vec{x}_f} \frac{\hat{n}\bullet\,\hat{R}}{R^2} = 2\pi \tag{5-8b}$$

The third integral is not bounded since we have

$$\int_{\text{Sphere}-\vec{x}_f} \left(\frac{\hat{n}\bullet\,\hat{R}}{R^2}\right)^2 = 2\pi \ln(1-\cos\theta)\Big|_{\theta=0}^{\pi} \tag{5-8c$_0$}$$

and

$$\int_{\text{Sphere}-\vec{x}_f} \left(\frac{\hat{n}}{R}\right)^2 = \pi \mathbf{R} \begin{bmatrix} \frac{3}{2} \\ \frac{3}{2} \\ \ln(1-\cos\theta)\Big|_{\theta=0}^{\pi} - 2 \end{bmatrix} \qquad (5\text{-}8c_1)$$

$$\mathbf{R} = \text{either of} \begin{cases} \begin{bmatrix} r & \frac{-x_f y_f}{r} & \frac{-x_f z_f}{r} \\ 0 & \frac{z_f}{r} & \frac{-y_f}{r} \\ x_f & y_f & z_f \end{bmatrix} & r \equiv \sqrt{z_f^2 + y_f^2} \quad r \neq 0 \\ \begin{bmatrix} \frac{z_f}{r} & 0 & \frac{-x_f}{r} \\ \frac{-x_f y_f}{r} & r & \frac{-y_f z_f}{r} \\ x_f & y_f & z_f \end{bmatrix} & r \equiv \sqrt{z_f^2 + x_f^2} \quad r \neq 0 \end{cases}$$

Although these integrals are unbounded, it is still possible to apply Fredholm's solution if we can construct a kernel that has the mentioned properties provided that it is related to the original kernel by the following algorithm:

$$K_i(\vec{x}, \vec{y}) = \int_\Omega K_{i-1}(\vec{x}, \vec{s})\, K(\vec{s}, \vec{y})\, d\vec{s} \quad : K_{i=1} = K, i \in [2, \infty) \qquad (5\text{-}9)$$

Kernels so constructed are called iterated kernels. Unfortunately, for our kernels, the required integrations are horrendous; for example, finding the first iterated kernel for $\vec{x}_{f_1}, \vec{x}_{f_2} \in S_3$ requires finding

$$k_2(\vec{x}_{f_1}, \vec{x}_{f_2}) =$$

$$\int_\varphi \int_\theta \frac{\cos\theta \sin\theta \, d\theta \, d\varphi}{\left[(x_{f_1} - \sin\theta\cos\varphi)^2 + (y_{f_1} - \sin\theta\sin\varphi)^2 + (z_{f_1} - \cos\theta)^2\right]^{\frac{1}{2}} \left[(x_{f_2} - \sin\theta\cos\varphi)^2 + (y_{f_2} - \sin\theta\sin\varphi)^2 + (z_{f_2} - \cos\theta)^2\right]^{\frac{1}{2}}} \qquad (5\text{-}10)$$

Further integrations would be required in order to construct $K_2(\vec{x}, \vec{y})$ such that

$\int |K_2(\vec{x},\vec{y})|^2 d\vec{x}d\vec{y}$ can be evaluated for boundedness. It is obvious that the amount of algebraic manipulation required is formidable. Symbolic manipulation programs (MACSYMA, SMP) were unable to give a usable form for equation 5-10; required iterated kernels may be impossible to find. Without bounded iterated kernels, we can proceed no further in the application of Fredholm's solutions to our problem.

5.3.2 Numerical methods

Here, numerical methods to solve equations of the form 5-3 are discussed. There are three major catagories which have been widely investigated [9]:

- Projection methods involve linearly expanding the unknown function in terms of a set of basis functions, integrating these basis functions with the kernel, and solving the resulting linear system of equations for the coeffecients.
- Nystrom methods involve choosing a set of points at which the unknown function is to be evaluated and discretizing integrals in terms of these function values. The resulting linear system of equations is solved for this vector.
- Product integration methods are similar to the Nystrom method. The difference is that the chosen set of points is used only to construct the linear system of equations; they are not used as points at which integrands are evaluated in numerical integrations. Optimal integration rules, i.e., points of evaluation and associated weights determined by a class of integrating functions, are used to approximate integrations. A set of interpolating functions are used to transform the numerical integration rule back into the point location domain for variables of the linear system.

Nystrom methods are known to perform poorly for integrations involving singular integrands. However, of the three methods, this method is the simplest to implement. The particular implementation used by all biopotential researchers was tried. I discuss my findings in the next section.

It is unclear which of the two other methods is best. I will present an analysis of computational cost for each of these methods. In doing this, details enabling a comprehensive comparison will be brought out. Using the notation of equation 5-3, for projection methods, let

$$f(\vec{x}_n) \approx \sum_{l=1}^{L} a_l u_l(\vec{x}_n) \tag{5-11}$$

Inserting this into equation 5-3 gives

$$\sum_{l=1}^{L} a_l u_l(\vec{x}_f) = J(\vec{x}_f) + \sum_{l=1}^{L} a_l \int_{\Omega} K(\vec{x}_f, \vec{x}) u_l(\vec{x}) d\vec{x} \tag{5-12}$$

To construct a square system matrix for coefficients a_l, we must choose L $\vec{x}_f$'s. For our problem, the integration must be done numerically [13, 14, 15]. Let this integration be

$$\int_{\Omega} f = \sum_{n=1}^{N_j} w_n(\vec{x}_n) f(\vec{x}_n) \tag{5-13}$$

Estimate $L^2(N_{(pro)j(ection)}+1)+L\times L+E_j$ to be proportional to the computational cost of solution where, at L $\vec{x}_f$'s, L integrations involving N_j terms must be done, L terms must be summed to obtain f at each $\vec{x}_f$, a L×L linear system of equations must be solved, and E_j represents the costs involved in evaluating functions u_l at various $\vec{x}_f$'s. For product integration let the interpolator be

$$f(\vec{x}_n) = \sum_{i=1}^{I_n} w_{i,n} f(\vec{x}_{i,n}) \qquad (5\text{-}14)$$

and the integration rule be expressed by equation 5-13 with N_j replaced by $N_{(pro)d(uct\ integration)}$. Taking $\tilde{I}$ to be the number of distinct $\vec{x}_i$, estimate $\tilde{I}N_d\langle I_n\rangle_n + \tilde{I}\times\tilde{I} + E_d$ to be proportional to the computation cost: $\tilde{I}$ integrations of order N_d must be performed through the use of an interpolator of average order $\langle I_n\rangle_n$, an $\tilde{I}\times\tilde{I}$ linear system of equations must be solved, and E_d represents the computational costs involved in evaluating weights for interpolation. Before discussing the computational cost comparison, note that it is clear from equations 5-11 and 5-14 that the two methods end up providing the same amount of information about the unknown function. Thus, it is sufficient to compare the two by making extimates of implementation costs. However, making this comparison is not possible in general since terms of the expressions for computational cost are dependent on the specific methods chosen and integrations involved:

- L depends on how well the u_l approximate the unknown function. A major factor involved is whether or not functions u_l satisfy the parent differential equation and boundary condition.
- E_j is u_l specific.
- N_j depends on the kernels, functions u_l, and Ω.
- $\tilde{I}$ and $\langle I_n\rangle_n$ depend on the spacial frequencies of the unknown function over Ω and on how well interpolating functions locally fit the unknown function respectively.
- E_d is interpolator specific.
- N_d depends on kernels, the unknown function, and Ω.

For N_j and N_d, I speculate that they should be approximately equal since, on Ω, the unknown function is expected to be smoother than the singular kernels. Efficient u_l should also have this degree of smoothness. For L and $\tilde{I}$, it might be expected that L is less than $\tilde{I}$ since, for product integration, there must be a set of distinct $\vec{x}_i$ large enough to cover Ω at a reasonable density whereas the projection method is not similarly constrained. However, for irregular conductor shapes such as those encountered in biological applications, L and $\tilde{I}$ may move closer to equality since there are no basis fuctions, u_l, specifically applicable for such shapes and interpolation requires only a local fit of interpolating functions to the unknown function. In addition, it may be desirable to solve an over determined system of equations for coefficients a_l. There are two reasons for this:

1. Suppose L is small in the sense that L points would cover Ω sparsely. Constraining solutions with only L equations may be insufficient to have equation 5-11 yield good approximations for solutions at other points of Ω.

2. Again, suppose L is small. If only L equations were used to constrain solutions, it may be that the number of basis functions required to achieve convergence would be deceptively small because of sparse sampling.

In conclusion, it is not at all obvious which method is best. Since product integration was a natural extension of the simple Nystrom methods I implemented first, the decision was to give this method a go.

5.3.2.1 Experience with Nystrom methods I will now discuss my experience with integration schemes constructed by, typically, representing the surface of integration with a set of triangles; this type of scheme will be referrd to as (TR). These methods can be characterized as follows: assume F constant over

N_p subregions of $\Omega, \Delta\Omega_n$, and estimate $w_n(\vec{x}_n)$ of equation 5-13 by $\int_{\Delta\Omega_n} K(\vec{x}_n,\vec{x})d\vec{x}$. My particular implementation of the method involved selecting a set of points nearly uniformly distributed over a sphere, using these points to define nearly equilateral triangles, using a solid angle formula [108] to compute $\int_{\Delta\Omega_n} d\vec{x}$ and $\int_{\Delta\Omega_n} \frac{\hat{n}\bullet\hat{R}}{R^2} d\vec{x}$, and assigning to each point, $\vec{x}_n$, the weight

$$\frac{1}{3}\sum_{m=1}^{M(i)} \int_{\Delta\Omega_m} d\vec{x} \ , \ \{\Delta\Omega_m : \vec{x}_i \text{ is a vertex of triangle } \Delta\Omega_m\} \qquad (5\text{-}15)$$

The point locations were determined as follows: The sphere was divided into latitudinal bands symetric about the equator with each band equidistant from its two neighbors. Points were placed on each band with a constant arc length between points. This arc length was choosen to be as close as possible to the arc length between bands. In summary,

$$\theta = \left(\frac{\pi}{N+1}\right) n \quad : \begin{matrix} N = \text{number of bands} \\ n \in [1, N] \text{ indexs bands} \end{matrix} \qquad (5\text{-}16a)$$

$$\varphi = \frac{2\pi}{L} l \quad : l \in [0, L-1] \qquad (5\text{-}16b)$$

$$L = \frac{2\pi \sin\theta}{\left(\frac{\pi}{N+1}\right)} \text{ rounded to nearest integer} \qquad (5\text{-}16c)$$

Pole points were also included.

The performance and convergence of this method was evaluated by integrating the various kernels of equations 5-4 combined with ω=0 solutions for

Φ and $\vec{A}$ under source conditions where the integrations could be performed analytically, i.e., $\vec{x}_j=(0,0,0)^{5-1}$, $\hat{j}=(1,0°,0°)$, and $\vec{x}_f=(R_c,0°,0°)$. The analytical integrations are tabulated below in section 8.1.1. When kernels were singular, the singular point was omitted from the sums and singularity subtraction [5, 16, 26], described in the following section, was used. The performance of the method changed irratically as the order of integration was increased (see table 5-1). It was concluded that it would be difficult to support convergence to solutions if this method were used.

TABLE 5-1 **Convergence of TR integrations**

$\vec{x}_f = (1, 0°, 0°)$
$\vec{x}_j = (1, 0°, 0°)$
$\vec{j} = (5, 0°, 0°)$

term	number of points →							
$\left\lvert \int \frac{\hat{R}\cdot\hat{n}}{R^2}\Phi - \int_{N(umerical)} \right\rvert$	214	562	288	460	156	106	368	674
	.003	.009	.012	.021	.034	.078	.22	1
$\left\lVert \int \frac{\hat{n}}{R}\Phi - \int_N \right\rVert$	214	562	156	460	106	288	368	674
	.012	.013	.019	.021	.023	.023	.32	1
$\sum_{k=1}^{3} \left\lvert \int \frac{\hat{n}_k}{R}A_k - \int_N \right\rvert$	562	460	214	156	288	106	368	674
	.016	.025	.047	.052	.057	.1	.19	1

relative magnitude of deviation with respect to worst integrator

5-1 All coordinates will be reported in spherical coordinates: (r, τ, φ) with τ and φ in degrees, τ=0 is the positive z-axis, and φ=0 is the positive x-axis.

6. Quick overview of numerical method used

The purpose of the next two sections is to present and justify the methodology used to estimate solutions of equations 5-4. The purpose of this section is to present a brief overview of the numerical methods used.

6.1 Method of cubature

The major determing factor in choosing a cubature method is the singularity of some of our kernels. Since these kernels are integrable, the first strategy is to introduce the following conversion (singularity subtraction) into equations 5-4 [5, 16, 26]:

$$\int_{S-\vec{x}_f} K(\vec{x},\vec{x}_f)\,f(\vec{x}) = \int_{S-\vec{x}_f} K(\vec{x},\vec{x}_f)\Big(f(\vec{x})-f(\vec{x}_f)\Big) + f(\vec{x}_f)\int_{S-\vec{x}_f} K(\vec{x},\vec{x}_f) \qquad (6\text{-}1)$$

The point is to lessen the severity of the singularities. The next strategy is to use sets of integration points that take advantage of the axial symmetry of the singularities and do not include points at the singularities [4, 6, 8]. The following choice was suggested by [11]:

$$\int_{\varphi=0}^{2\pi}\int_{\theta=0}^{\pi} f(\theta,\varphi)\sin\theta d\theta d\varphi = \frac{\pi}{m}\sum_{j=1}^{2m}\sum_{i=1}^{m} w_i f(\theta_i,\varphi_j) \qquad (6\text{-}2a)$$

$$w_i = \text{Gauss–Legendre weights where} \qquad (6\text{-}2b)$$

$$\cos\theta_i = \text{Gauss–Legendre nodes on } [-1,1] \text{ for an m node integrator} \qquad (6\text{-}2c)$$

$$\varphi_j = \frac{j\pi}{m} \qquad (6\text{-}2d)$$

This Gauss-Legendre method will be referred to as (GL).

The need to use these integration point locations for each $\vec{x}_f$ and the need to construct a closed linear system of equations requires choosing a set of points ($\vec{x}_f$) from which values of Φ and $\vec{A}$ at the integration points are found by inter-

polation. An interpolation based on splines specific for interpolation on a sphere was used [110, 111]:

$$f(\vec{x}_g; \vec{x}_{f_p}, m, \lambda) = \sum_{p}^{n_p} f(\vec{x}_{f_p}) \left[\sum_{\rho}^{n_p} \left[R(\vec{x}_g, \vec{x}_{f_p}; m) \mathbf{D}_{p,\rho} \right] - d_p \right] \tag{6-3a}$$

$$d_p \ : \vec{d}^{\,t(\text{ranspose})} = -\frac{\vec{u}^t \mathbf{A}^{-1}}{\vec{u}^t \mathbf{A}^{-1} \vec{u}} \tag{6-3b}$$

$$\vec{u} = \begin{bmatrix} 1 \\ \vdots \\ 1 \end{bmatrix} \qquad \mathbf{A} = \mathbf{R} + n_p \lambda \mathbf{I} \tag{6-3c}$$

$$\mathbf{R} \ : R_{ij} = R(\vec{x}_{f_i}, \vec{x}_{f_j}; m) = \frac{1}{2\pi} \left[\frac{1}{(2m-2)!} q(\hat{x}_{f_i} \bullet \hat{x}_{f_j}; 2m-2) - \frac{1}{(2m-1)!} \right] \tag{6-3d}$$

$$q(x; m) = \int_0^1 (1-h)^m (1-2hx+h^2)\, dh \qquad m \in [0, \infty) \tag{6-3e}$$

$\mathbf{I} \equiv$ identity matrix

n_p = number of interpolation points

m, λ are free parameters to be determined

$\vec{x}_g$ = location vector of an integration point

$$\mathbf{D} : D_{ij} \equiv A_{ij} + d_j \sum_{k}^{n_p} (A^{-1})_{ik} \tag{6-3f}$$

It will be referred to as the Wahba interpolator. Note that index g is for integration point and index p is for interpolation point. On choosing $\vec{x}_f$ locations, the decision was to use the same points used for TR methods; all points

tions, the decision was to use the same points used for TR methods; all points were used to obtain interpolation estimates of function values at the integration points. Parameters m and λ were choosen by finding parameter values that maximized interpolator accuracy in interpolating ω=0 solutions of equations 5-4:

$$\vec{A}(\vec{x})\,|_{\omega=0,\vec{x}_j=(0,0,0)} = \frac{\mu_0 \begin{bmatrix}\cos\theta_{FT}\\ \sin\theta_{FT}\end{bmatrix}}{20\pi R_c}(\vec{J} - 3\vec{J}\bullet\,\hat{x}\hat{x}) \qquad (6\text{-}4)$$

$$\Phi(\vec{x})\,|_{\omega=0} = \frac{\begin{bmatrix}\cos\theta_{FT}\\ \sin\theta_{FT}\end{bmatrix}}{4\pi\sigma_{in}R_c^2}\vec{J}\bullet\left(\frac{2\hat{d}}{d^2} + \frac{1}{d}\frac{\hat{x}+\hat{d}}{1+\hat{x}\bullet\,\hat{d}}\right) \qquad (6\text{-}5)$$

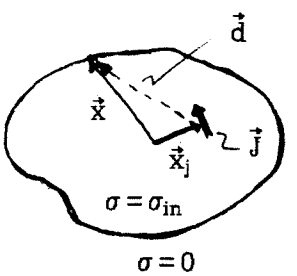

figure 6-1

For $\vec{A}$ it was also required that the source be centrally located; only for this source case could I integrate $\int_S \frac{\hat{n}}{R}\Phi$.

6.2 The discretized equations

Equations 5-4 are discretized as follows. Combining the integrator,

$$\int_{S-\vec{x}_f} f = \sum_{g}^{N_g} w_g f(\vec{x}_g) \tag{6-6}$$

with the interpolator,

$$f(\vec{x}_g) = \sum_{p}^{N_p} w_p f(\vec{x}_p) \tag{6-7}$$

and equation 6-1 gives

$$\int_{S-\vec{x}_f} Kf = \int_{S-\vec{x}_f} K(f - Sf_{p_f}) + Sf_{p_f} K_{\int} \tag{6-8a}$$

$$\approx \sum_{p \neq p_f}^{N_p} f_p \sum_{g_{p_f}}^{N_g} w_{p,g_{p_f}} K_{g_{p_f},p_f} w_{g_{p_f}} + f_{p_f} \left[SK_{\int} + \sum_{g_{p_f}}^{N_g} (w_{p,g_{p_f}} - S) K_{g_{p_f},p_f} w_{g_{p_f}} \right] \tag{6-8b}$$

$$S \equiv \begin{cases} 1 & \text{k singular} \\ 0 & \text{k bounded} \end{cases}$$

$$K_{\int} \equiv \int_{S-\vec{x}_f} K$$

Equation 6-8b is then applied to equations 5-4 to obtain a finite system of equations for the variables $\underset{im}{\Phi_{re}}|_{\vec{x}_f}$ and $\underset{im}{\vec{A}_{re}}|_{\vec{x}_f}$ This system is displayed in equations 6-9.

$$\frac{\mu_0}{4\pi}\left(\vec{J}_{\substack{re\\im}}\frac{1}{R_j}\right)_{\vec{x}_{p=p_f}} =$$

$$\vec{A}_{\substack{re\\im}}|_{\vec{x}_{p=p_f}} - \frac{\sqrt{\omega\mu_0\sigma_{in}}}{4\pi}\left(\frac{1}{R_c}+\frac{1}{4\ \Sigma l}\right)\begin{bmatrix}1 & -1\\ 1 & 1\end{bmatrix}\sum_p \Omega_u(\vec{x}_p,\vec{x}_{p=p_f})\vec{A}_{\substack{re\\im}}|_{\vec{x}_p}$$

$$+\frac{\mu_0}{4\pi}\sum_p \vec{\Omega}_v(\vec{x}_p,\vec{x}_{p=p_f})\left(\begin{bmatrix}\sigma_{in} & -(\sigma_{in}e_{im}+\varepsilon_{in}\omega)\\ \sigma_{in}e_{im}+\varepsilon_{in}\omega & \sigma_{in}\end{bmatrix}\Phi_{\substack{re\\im}}\right)|_{\vec{x}_p} \qquad (6\text{-}9a)$$

$$-\frac{1}{2\pi\sigma_{in}^2}\left(\frac{\hat{R}_j\bullet\hat{J}}{R_j^2}\begin{bmatrix}\sigma_{in} & \varepsilon_{in}\omega\\ -\varepsilon_{in}\omega & \sigma_{in}\end{bmatrix}\vec{J}_{\substack{re\\im}}\right)|_{\vec{x}_{p=p_f}} =$$

$$\frac{\varepsilon_{in}\omega}{\sigma_{in}}\begin{bmatrix}0 & -1\\ 1 & 0\end{bmatrix}\Phi_{\substack{re\\im}}|_{\vec{x}_{p=p_f}} - \frac{\sqrt{\omega\mu_0\sigma_{in}}}{4\pi}\left(\frac{1}{R_c}-\frac{1}{4\ \Sigma l}\right)\begin{bmatrix}1 & -1\\ 1 & 1\end{bmatrix}\sum_p \Omega_u(\vec{x}_p,\vec{x}_{p=p_f})\Phi_{\substack{re\\im}}|_{\vec{x}_p}$$

$$-\frac{\omega\mu_0}{4\ \Sigma l}\frac{1}{4\pi\sigma_{in}}\begin{bmatrix}\varepsilon_{in}\omega & -\sigma_{in}\\ \sigma_{in} & \varepsilon_{in}\omega\end{bmatrix}\sum_p \Omega_R(\vec{x}_p,\vec{x}_{p=p_f})\Phi_{\substack{re\\im}}|_{\vec{x}_p} - \frac{\omega}{2\pi}\sum_p \vec{\Omega}_v(\vec{x}_p,\vec{x}_{p=p_f})\bullet\left(\begin{bmatrix}e_{im} & 1\\ -1 & e_{im}\end{bmatrix}\vec{A}_{\substack{re\\im}}\right)|_{\vec{x}_p}$$

$$-\frac{1}{2\pi\sigma_{in}}\begin{bmatrix}\sigma_{in} & \varepsilon_{in}\omega\\ -\varepsilon_{in}\omega & \sigma_{in}\end{bmatrix}\sum_p \Omega_s(\vec{x}_p,\vec{x}_{p=p_f})\Phi_{\substack{re\\im}}|_{\vec{x}_p} \qquad (6\text{-}9b)$$

$$\vec{J}_{\substack{re\\im}} \equiv \left(\int_{-L/2}^{L/2}|J_{rld}|\right)\begin{bmatrix}\cos\theta_{FT}+e_{im}\sin\theta_{FT}\\ \sin\theta_{FT}-e_{im}\cos\theta_{FT}\end{bmatrix}$$

$$\Omega_u(\vec{x}_p,\vec{x}_{p=p_f}) \equiv \sum_{g_{p_f}} w_{p,g_{p_f}} w_{g_{p_f}}$$

$$\Omega_R(\vec{x}_p,\vec{x}_{p=p_f}) \equiv \sum_{g_{p_f}} w_{p,g_{p_f}} R|_{\vec{x}_{g_{p_f}},\vec{x}_{p=p_f}} w_{g_{p_f}}$$

$$\Omega_s(\vec{x}_p,\vec{x}_{p=p_f}) \equiv \begin{cases}\sum_{g_{p_f}} w_{p,g_{p_f}}\dfrac{\hat{R}\bullet\hat{n}}{R^2}|_{\vec{x}_{g_{p_f}},\vec{x}_{p=p_f}} w_{g_{p_f}} & :p\neq p_f\\ \sum_{g_{p_f}}(w_{p,g_{p_f}}-1)\dfrac{\hat{R}\bullet\hat{n}}{R^2}|_{\vec{x}_{g_{p_f}},\vec{x}_{p=p_f}} w_{g_{p_f}} & :p=p_f\end{cases}$$

$$\Omega_v(\vec{x}_p,\vec{x}_{p=p_f}) \equiv \begin{cases}\sum_{g_{p_f}} w_{p,g_{p_f}}\dfrac{\hat{n}}{R}|_{\vec{x}_{g_{p_f}},\vec{x}_{p=p_f}} w_{g_{p_f}} & :p\neq p_f\\ \dfrac{4\pi}{3}R_c\hat{x}_{p=p_f}+\sum_{g_{p_f}}(w_{p,g_{p_f}}-1)\dfrac{\hat{n}}{R}|_{\vec{x}_{g_{p_f}},\vec{x}_{p=p_f}} w_{g_{p_f}} & :p=p_f\end{cases}$$

6.3 Solving the system of equations

I chose Cimmino's process [24, 48] to solve equations 6-9. For the equation $\mathbf{A}\vec{x}=\vec{b}$, the algorithm I used was

$$\vec{x}_{new} = \vec{x}_{old} - \frac{2}{n+1}\mathbf{A}^t \mathrm{Diag}(\|\vec{A}_{i\bullet}\|^{-2})(\mathbf{A}\vec{x}_{old} - \vec{b}) \qquad (6\text{-}10)$$

where n is the order of the linear system and $\vec{A}_{i\bullet}$ is the i^{th} row of $\mathbf{A}$. Iteration was terminated when average residuals for both equation 6-9a and 6-9b were below values for residuals calculated using $\omega=0$ solutions in discretized equations appropriate for $\omega=0$. Before applying the algorithm, the system was scaled in such a way that in the scaled system, $\mathbf{A}'\vec{x}'=\vec{b}'$, the coefficients of $\mathbf{A}'$ and $\vec{b}'$ were optimally equalized with respect to order of magnitude. Since the order of magnitude of coefficients associated with Φ can differ significantly from coefficients of $\vec{A}$ in each of equations 6-9, a scaling involving four multiplicative factors was used:

$$\begin{bmatrix} Pre_0\mathbf{I}_{6N_p} & 0 \\ 0 & Pre_1\mathbf{I}_{2N_p} \end{bmatrix} \mathbf{A} \begin{bmatrix} Pst_0\mathbf{I}_{6N_p} & 0 \\ 0 & Pst_1\mathbf{I}_{2N_p} \end{bmatrix} \vec{x}' = \begin{bmatrix} Pre_0\mathbf{I}_{6N_p} & 0 \\ 0 & Pre_1\mathbf{I}_{2N_p} \end{bmatrix} \vec{b} \qquad (6\text{-}11)$$

where Pre_0, Pre_1, Pst_0, and Pst_1 are the factors, $\mathbf{I}_m$ is the identity matrix of order m, and

$$\vec{x} = \begin{bmatrix} Pst_0\mathbf{I}_{6N_p} & 0 \\ 0 & Pst_1\mathbf{I}_{2N_p} \end{bmatrix} \vec{x}' \qquad (6\text{-}12)$$

The four factors were determined by minimizing the function

$$\left[\log\frac{Pre_0Pst_0a_0}{Pre_0Pst_1a_1}\right]^2+\left[\log\frac{Pre_0Pst_0a_0}{Pre_1Pst_0a_2}\right]^2+\left[\log\frac{Pre_0Pst_0a_0}{Pre_1Pst_1a_3}\right]^2$$
$$+\left[\log\frac{Pre_0Pst_1a_1}{Pre_1Pst_0a_2}\right]^2+\left[\log\frac{Pre_0Pst_1a_1}{Pre_1Pst_1a_3}\right]^2$$
$$+\left[\log\frac{Pre_1Pst_0a_2}{Pre_1Pst_1a_3}\right]^2$$
$$+\left[\log\frac{Pre_0b_0}{Pre_1b_1}\right]^2 \qquad (6\text{-}13)$$

where a_0 is the average absolute value of coefficients for $\vec{A}$ in equation 6-9a, a_1 is the analogous quantity for Φ coefficients of 6-9a, a_2 for $\vec{A}$ coefficients in 6-9b, a_3 for Φ coefficients in 6-9b, b_0 is the average absolute value of source terms of 6-9a, and b_1 is the analogous quantity for source terms of 6-9b. When averages could involve diagonal elements of the system matrix, diagonal elements were included or excluded from averages depending on which choice would maximize diagonal dominance of the scaled system matrix. The first six terms are a measure of the difference between order of magnitudes of $\mathbf{A}'$ elements, the last term is the analogous measure for $\vec{b}'$. The solution is

$$\log\frac{Pre_0}{Pre_1}=\frac{1}{5}\log\frac{a_2^2a_3^2b_1}{a_0^2a_1^2b_0} \qquad (6\text{-}14a)$$

$$\log\frac{Pst_0}{Pst_1}=\frac{1}{2}\log\frac{a_1a_3}{a_0a_2} \qquad (6\text{-}14b)$$

This completes the description of numerical techniques used to find solutions of equations 5-4.

6.4 Final measures

The following measure was used to assessthe degree of dependence on frequency for each component of $\begin{bmatrix}\vec{A}_{re}^{\,im}\\ \Phi_{re}^{\,im}\end{bmatrix}$ denoted by f's

$$\sqrt{\frac{\sum_{p}^{N_p}(f-f_{0Hz})^2_{\vec{x}_p}}{\sum_{p}^{N_p} f_{0Hz}{}^2|_{\vec{x}_p}}} \tag{6-15}$$

where f is representative of solutions to equations 5-4 and f_{0Hz} is representative of solutions to the ω=0 equations. The numerical techniques used to estimate solutions of equations 5-4 provides an estimate of this measure. To assess the error in this estimator, the substitution

$$f_N = f + \varepsilon_f \tag{6-16}$$

is made in equation 6-15. With estimates of the magnitude of ε_f, $|\varepsilon_f|$, the interval estimate

$$\sum_{p}^{N_p}\left(\begin{cases} 0 & : |f_N - f_{0Hz}| \le |\varepsilon_f| \\ f_N - f_{0Hz} + |\varepsilon_f| & : |f_N - f_{0Hz}| > |\varepsilon_f|, f_N - f_{0Hz} < 0 \\ f_N - f_{0Hz} - |\varepsilon_f| & : |f_N - f_{0Hz}| > |\varepsilon_f|, f_N - f_{0Hz} > 0 \end{cases}\right)^2 |_{\vec{x}_p}$$

$$\le \sum_{p}^{N_p}(f-f_{0Hz})^2_{\vec{x}_p} \approx \sum_{p}^{N_p}(f_N - f_{0Hz})^2_{\vec{x}_p} \tag{6-17}$$

$$\sum_{p}^{N_p}\left(\begin{cases} f_N - f_{0Hz} - |\varepsilon_f| & : f_N - f_{0Hz} < 0 \\ f_N - f_{0Hz} + |\varepsilon_f| & : f_N - f_{0Hz} > 0 \end{cases}\right)^2 |_{\vec{x}_p}$$

can be written. Regarding estimation of the $|\varepsilon_{f_{\vec{x}_p}}|$, note that the ε_f are the result of errors in calculating integrals of equations 5-4 and errors in solving the linear system of equations, 6-9. This suggests a way to obtain estimates of

the ε_f; consider the following process applied to an equation analogous to equations 5-4:

$$f_{\vec{x}_f} + \int_{S-\vec{x}_f} K_1 f + K_2 g = h_{\vec{x}_f} \tag{6-18a}$$

$$\downarrow \quad \int_{\text{Actual}} Kf = \left[\int_{N(\text{umerical})} Kf \right] + \delta_{I(\text{ntegration error})}^{Kf} \tag{6-18b}$$

$$f_{\vec{x}_f} + \int_{N-\vec{x}_f} K_1 f + K_2 g = h_{\vec{x}_f} - \delta_I^{K_1 f}\big|_{\vec{x}_f} - \delta_I^{K_2 g}\big|_{\vec{x}_f} \tag{6-18c}$$

$$\downarrow \quad f = f_N + \varepsilon_f, \quad \vec{x}_f \text{ notation subsequently dropped} \tag{6-18d}$$

$$f_N + \varepsilon_f + \int_N K_1 f_N + K_1 \varepsilon_f + K_2 g_N + K_2 \varepsilon_g = h - \delta_I^{K_1 f} - \delta_I^{K_2 g} \tag{6-18e}$$

$$\downarrow \quad f_N + \int_N K_1 f_N + K_2 g_N = h + \varepsilon_{L(\text{inear equation error})}^{f} \tag{6-18f}$$

$$\varepsilon_f + \int_N K_1 \varepsilon_f + K_2 \varepsilon_g = -\varepsilon_L^f - \delta_I^{K_1 f} - \delta_I^{K_2 g} \tag{6-18g}$$

$$\downarrow$$

$$|\varepsilon_f| = \left| \varepsilon_L^f + \delta_I^{K_1 f} + \delta_I^{K_2 g} + \int_N K_1 \varepsilon_f + K_2 \varepsilon_g \right| \tag{6-18h}$$

$$\leq |\varepsilon_L^f| + |\delta_I^{K_1 f}| + |\delta_I^{K_2 g}| + \int_N |K_1 \varepsilon_f| + |K_2 \varepsilon_g| \tag{6-18i}$$

$$|\vec{a} \bullet \vec{b}| \leq \|\vec{a}\| \|\vec{b}\| \tag{6-18j}$$

$$\leq |\varepsilon_L^f| + |\delta_I^{K_1 f}| + |\delta_I^{K_2 g}| + \sqrt{\int_N |\varepsilon_f|^2} \sqrt{\int_N |K_1|^2} + \sqrt{\int_N |\varepsilon_g|^2} \sqrt{\int_N |K_2|^2} \tag{6-18k}$$

To obtain an equation solvable for the $|\varepsilon_f|$, by the mean value theorem, I make the approximation

$$\int_N |\varepsilon_f|^2 \approx \|\partial S\| \frac{1}{N_p} \sum_p^{N_p} |\varepsilon|^2_{\vec{x}_p} \equiv \|\partial S\| \langle \varepsilon_f^2 \rangle \tag{6-19}$$

where $\|\partial S\|$ is the surface area of the region of integration. Then, averaging equation 6-18g over the N_p points,

$\langle \varepsilon_f \rangle \leq$

$$\langle \varepsilon_L^f \rangle + \langle \delta_I^{K_1 f} \rangle + \langle \delta_I^{K_2 g} \rangle + \langle \varepsilon_f \rangle \sqrt{\|\partial S\|} \langle \sqrt{\int_N |K_1|^2} \rangle + \langle \varepsilon_g \rangle \sqrt{\|\partial S\|} \langle \sqrt{\int_N |K_2|^2} \rangle \tag{6-20}$$

Finally, an estimate of the δ_I must be found in order to obtain a set of equations solvable for $\langle \varepsilon_{\substack{\Phi_{re} \\ im}} \rangle$ and $\langle \vec{\varepsilon}_{\substack{\vec{A}_{re} \\ im}} \rangle$. I could only calculate integration error bounds using $\omega=0$ solutions. Consequently, using ε_I to denote these errors, I assume, for scalar integrations,

$$\frac{\langle (\delta_I^{K\Phi_{re}})^2 + (\delta_I^{K\Phi_{im}})^2 \rangle}{\langle \Phi_{re}^2 + \Phi_{im}^2 \rangle_{\omega \neq 0}} \approx \frac{\langle (\varepsilon_I^{K\Phi_{re}})^2 + (\varepsilon_I^{K\Phi_{im}})^2 \rangle}{\langle \Phi_{re}^2 + \Phi_{im}^2 \rangle_{\omega = 0}} \tag{6-21}$$

and for vector integrations,

$$\frac{\langle \|\vec{\delta}_I^{\vec{K}\Phi_{re}}\|^2 + \|\vec{\delta}_I^{\vec{K}\Phi_{im}}\|^2 \rangle}{\langle \Phi_{re}^2 + \Phi_{im}^2 \rangle_{\omega \neq 0}} \approx \frac{\langle \|\vec{\varepsilon}_I^{\vec{K}\Phi_{re}}\|^2 + \|\vec{\varepsilon}_I^{\vec{K}\Phi_{im}}\|^2 \rangle}{\langle \Phi_{re}^2 + \Phi_{im}^2 \rangle_{\omega = 0}} \tag{6-22}$$

Analogous assumptions are made for integrals involving $\vec{A}$ where the normalizing factor is taken to be $\langle \|\vec{A}_{re}\|^2 + \|\vec{A}_{im}\|^2 \rangle$. I go on from these assumptions to assert the following estimates: for scalar integrands,

$$\langle \delta_I^{K\Phi_{re}}{}_{im} \rangle = \sqrt{\frac{\langle (\varepsilon_I^{K\Phi_{re}})^2 + (\varepsilon_I^{K\Phi_{im}})^2 \rangle}{\langle \Phi_{re}^2 + \Phi_{im}^2 \rangle_{\omega=0}}} \sqrt{\langle \Phi_{re}^2 \rangle_{\omega \neq 0}}_{im} \tag{6-23a}$$

$$\langle \delta_I^{\vec{K}\cdot\vec{A}_{re}}{}_{im} \rangle = \sqrt{\frac{\langle (\varepsilon_I^{\vec{K}\cdot\vec{A}_{re}})^2 + (\varepsilon_I^{\vec{K}\cdot\vec{A}_{im}})^2 \rangle}{\langle \|\vec{A}_{re}\|^2 + \|\vec{A}_{im}\|^2 \rangle_{\omega=0}}} \sqrt{\langle \|\vec{A}_{re}\|^2 \rangle_{\omega \neq 0}}_{im} \tag{6-23b}$$

and for vector integrands, using the x coordinate for example,

$$\langle \delta_I^{K_x\Phi_{re}}{}_{im} \rangle = \sqrt{\frac{\langle \|\vec{\varepsilon}_I^{K\Phi_{re}}\|^2 + \|\vec{\varepsilon}_I^{K\Phi_{im}}\|^2 \rangle}{3\langle \Phi_{re}^2 + \Phi_{im}^2 \rangle_{\omega=0}}} \sqrt{\langle \Phi_{re}^2 \rangle_{\omega \neq 0}}_{im} \tag{6-24a}$$

$$\langle \delta_I^{KA_{x_{re}}}{}_{im} \rangle = \sqrt{\frac{\langle \|\vec{\varepsilon}_I^{K\vec{A}_{re}}\|^2 + \|\vec{\varepsilon}_I^{K\vec{A}_{im}}\|^2 \rangle}{\langle \|\vec{A}_{re}\|^2 + \|\vec{A}_{im}\|^2 \rangle_{\omega=0}}} \sqrt{\langle A_{x_{re}}^2 \rangle_{\omega \neq 0}}_{im} \tag{6-24b}$$

Applying the above to equations 5-4 give

$$\left(1-\frac{\sqrt{\omega\mu_0\sigma_{in}}}{4\pi}\left(\frac{1}{R_c}+\frac{1}{4\ \Sigma l}\right)\|\partial S\|\right)<\vec{\varepsilon}^{\ \vec{A}_{re}}_{\ im}>-\frac{\sqrt{\omega\mu_0\sigma_{in}}}{4\pi}\left(\frac{1}{R_c}+\frac{1}{4\ \Sigma l}\right)\|\partial S\|<\vec{\varepsilon}^{\ \vec{A}_{im}}_{\ re}>$$

$$-\left(\frac{\mu_0\sigma_{in}}{4\pi}\sqrt{\|\partial S\|}<\sqrt{\int_N|\frac{\vec{n_k}}{R}|^2}>\right)<\varepsilon^{\ \Phi_{re}}_{\ im}>-\left(\frac{\mu_0\varepsilon_{in}\omega}{4\pi}\sqrt{\|\partial S\|}<\sqrt{\int_N|\frac{\vec{n_k}}{R}|^2}>\right)<\varepsilon^{\ \Phi_{re}}_{\ im}>$$

$$-\frac{\mu_0\sigma_{in}}{4\pi}\sqrt{\|\partial S\|}<\sqrt{\int_N|\frac{\vec{n_k e_{im}}}{R}|^2}><\varepsilon^{\ \Phi_{re}}_{\ im}>$$

$$=<\vec{\varepsilon}_L^{\ \vec{A}_{re}}_{\ im}>$$

$$+\frac{\sqrt{\omega\mu_0\sigma_{in}}}{4\pi}\left(\frac{1}{R_c}+\frac{1}{4\ \Sigma l}\right)\sqrt{\frac{<\|\vec{\varepsilon}_I^{\ \vec{A}_{re}}\|^2+\|\vec{\varepsilon}_I^{\ \vec{A}_{im}}\|^2>}{<\|\vec{A}_{re}\|^2+\|\vec{A}_{im}\|^2>_{\omega=0}}}\frac{\left(\sqrt{<\|\vec{A}_{re}\|^2>_{\omega\neq0}\ <\vec{A}^2_{k_{re}}>_{\omega\neq0}}+\sqrt{<\|\vec{A}_{im}\|^2>_{\omega\neq0}\ <\vec{A}^2_{k_{im}}>_{\omega\neq0}}\right)}{\sqrt{<\|\vec{A}_{re}\|^2+\|\vec{A}_{im}\|^2>_{\omega\neq0}}}$$

$$+\frac{\mu_0}{4\pi}\sqrt{\frac{<\|\vec{\varepsilon}_I^{\ \frac{\hat{n}\Phi_{re}}{R}}\|^2+\|\vec{\varepsilon}_I^{\ \frac{\hat{n}\Phi_{im}}{R}}\|^2>}{3<\Phi^2_{re}+\Phi^2_{im}>_{\omega=0}}}\left(\sigma_{in}\sqrt{<\Phi^2_{\substack{re\\im}}>_{\omega\neq0}}+\varepsilon_{in}\omega\sqrt{<\Phi^2_{\substack{im\\re}}>_{\omega\neq0}}\right)$$

$$+\frac{\mu_0\sigma_{in}}{4\pi}\sqrt{\frac{<\|\vec{\varepsilon}_I^{\ \frac{\hat{n}e_{1m}\Phi_{re}}{R}}\|^2+\|\vec{\varepsilon}_I^{\ \frac{\hat{n}e_{1m}\Phi_{1m}}{R}}\|^2>}{3<\Phi^2_{re}+\Phi^2_{im}>_{\omega=0}}}\sqrt{<\Phi^2_{\substack{im\\re}}>_{\omega\neq0}}\qquad\text{(6-25a)}$$

$$
\left\{ 1 - \frac{\sqrt{\omega\mu_0\sigma_{in}}}{4\pi}\left|\frac{1}{R_c} - \frac{1}{4\ \Sigma l}\right|\|\partial S\| - \frac{\omega\mu_0}{4\ \Sigma l}\frac{\varepsilon_{in}\omega}{4\pi\sigma_{in}}\sqrt{\|\partial S\|}<\sqrt{\int_N |R^2|}> - \frac{1}{2\pi}\sqrt{\|\partial S\|}<\sqrt{\int_N (\frac{\vec{n}\bullet\vec{R}}{R^2})^2}> \right\} <\varepsilon_{im}^{\Phi_{re}}>
$$

$$
-\left\{ \frac{\sqrt{\omega\mu_0\sigma_{in}}}{4\pi}\left|\frac{1}{R_c} - \frac{1}{4\ \Sigma l}\right|\|\partial S\| + \frac{\omega\mu_0}{4\ \Sigma l}\frac{\varepsilon_{in}\omega}{4\pi\sigma_{in}}\sqrt{\|\partial S\|}<\sqrt{\int_N |R^2|}> + \frac{\varepsilon_{in}\omega}{2\pi\sigma_{in}}\sqrt{\|\partial S\|}<\sqrt{\int_N (\frac{\vec{n}\bullet\vec{R}}{R^2})^2}> \right\} <\varepsilon_{re}^{\Phi_{im}}>
$$

$$
-\frac{\omega}{2\pi}\sqrt{\|\partial S\|}\sum_k^3\left\{ <\sqrt{\int_N (\frac{n_k}{R})^2}><\varepsilon_{im}^{\vec{A}_{k_{re}}}> + <\sqrt{\int_N (\frac{n_k e_{lm}}{R})^2}><\varepsilon_{re}^{\vec{A}_{k_{im}}}> \right\}
$$

$$
= <\varepsilon_L^{\Phi_{re}}>_{im} + \frac{\sqrt{\omega\mu_0\sigma_{in}}}{4\pi}\left|\frac{1}{R_c} - \frac{1}{4\ \Sigma l}\right|\sqrt{\frac{<(\varepsilon_I^{\Phi_{re}})^2 + (\varepsilon_I^{\Phi_{im}})^2>}{<\Phi_{re}^2 + \Phi_{im}^2>_{\omega=0}}}\left(\sqrt{<\Phi_{re}^2>_{\omega\neq 0}} + \sqrt{<\Phi_{im}^2>_{\omega\neq 0}}\right)
$$

$$
+ \frac{\omega\mu_0}{4\ \Sigma l}\frac{1}{4\pi}\sqrt{\frac{<(\varepsilon_I^{R\Phi_{re}})^2 + (\varepsilon_I^{R\Phi_{im}})^2>}{<\Phi_{re}^2 + \Phi_{im}^2>_{\omega=0}}}\left(\frac{\varepsilon_{in}\omega}{\sigma_{in}}\sqrt{<\Phi_{re}^2>_{\omega\neq 0}}_{im} + \sqrt{<\Phi_{im}^2>_{\omega\neq 0}}_{re}\right)
$$

$$
+ \frac{1}{2\pi}\sqrt{\frac{<(\varepsilon_I^{\frac{\hat{n}\bullet\hat{R}\Phi_{re}}{R^2}})^2 + (\varepsilon_I^{\frac{\hat{n}\bullet\hat{R}\Phi_{im}}{R^2}})^2 + >}{<\Phi_{re}^2 + \Phi_{im}^2>_{\omega=0}}}\left(\sqrt{<\Phi_{re}^2>_{\omega\neq 0}}_{im} + \frac{\varepsilon_{in}\omega}{\sigma_{in}}\sqrt{<\Phi_{im}^2>_{\omega\neq 0}}_{re}\right)
$$

$$
+ \frac{\omega}{2\pi}\sqrt{\frac{<\|\vec{\varepsilon}_I^{\frac{\hat{n}\bullet\vec{A}_{re}}{R}}\|^2 + \|\vec{\varepsilon}_I^{\frac{\hat{n}\bullet\vec{A}_{im}}{R}}\|^2>}{<\|\vec{A}_{re}\|^2 + \|\vec{A}_{im}\|^2>_{\omega=0}}}\sqrt{<\|\vec{A}_{im}\|^2>_{re}}_{\omega\neq 0}
$$

$$
+ \frac{\omega}{2\pi}\sqrt{\frac{<\|\vec{\varepsilon}_I^{\frac{e_{lm}\hat{n}}{R}\bullet\vec{A}_{re}}\|^2 + \|\vec{\varepsilon}_I^{\frac{e_{lm}\hat{n}}{R}\bullet\vec{A}_{im}}\|^2>}{<\|\vec{A}_{re}\|^2 + \|\vec{A}_{im}\|^2>_{\omega=0}}}\sqrt{<\|\vec{A}_{re}\|^2>_{im}}_{\omega\neq 0} \qquad (6\text{-}25b)
$$

Solving this system of 8 equations could give maximum estimates for $|\varepsilon_f|$ of equation 6-17. However, I obtained first order estimates by, effectively, setting $\|\partial S\|=0$ in equations 6-25. The reason for this extreme measure is discussed in the next section. One final note, analytical formulas for the integrals $\int R\Phi_{0Hz}$, $\int \frac{\hat{n}}{R}\Phi_{0Hz}$, $\int \vec{A}_{0Hz}$, and $\int \frac{\hat{n}}{R}\bullet \vec{A}_{0Hz}$ could only be derived for special cases of source parameters and $\vec{x}_f$. Integrals involving e_{im} could not be done at all. Consequently, for integrations that could not be done analytically, the ε_I were based on values given by a high order numerical integrator. The numerical integration technique used to do this is described by the following equations:

$$\theta_i = \begin{cases} \frac{\pi}{\gamma}\int_{-1}^{\frac{2i}{N+1}-1} e^{\frac{-4}{(1-s^2)}}ds & N \text{ even}: \; i\in[1\to\frac{N}{2}] \\ \pi-\frac{\pi}{\gamma}\int_{-1}^{1-\frac{i}{N+1}} e^{\frac{-4}{(1-s^2)}}ds & N \text{ even}: \; i\in[\frac{N}{2}+1\to N] \\ \frac{\pi}{\gamma}\int_{-1}^{\frac{2i}{N+1}-1} e^{\frac{-4}{(1-s^2)}}ds & N \text{ odd}: \; i\in[1\to\frac{N+1}{2}-1] \\ \pi-\frac{\pi}{\gamma}\int_{-1}^{1-\frac{i}{N+1}} e^{\frac{-4}{(1-s^2)}}ds & N \text{ odd}: \; i\in[\frac{N+1}{2}\to N] \end{cases} \tag{6-26a}$$

$$\varphi_j = \frac{j\pi}{N} \text{ or } (j-\frac{1}{2})\frac{\pi}{N} \tag{6-26b}$$

$$w_i = \begin{cases} \frac{2}{N+1}\frac{\pi}{\gamma}\sin\theta_i \; e^{-4/\left[1-(\frac{2i}{N+1}-1)^2\right]} & N \text{ even}: \; i\in[1\to\frac{N}{2}] \\ \frac{2}{N+1}\frac{\pi}{\gamma}\sin\theta_i \; e^{-4/\left[1-(1-\frac{i}{N+1})^2\right]} & N \text{ even}: \; i\in[\frac{N}{2}+1\to N] \\ \frac{2}{N+1}\frac{\pi}{\gamma}\sin\theta_i \; e^{-4/\left[1-(\frac{2i}{N+1}-1)^2\right]} & N \text{ odd}: \; i\in[1\to\frac{N+1}{2}-1] \\ \frac{2}{N+1}\frac{\pi}{\gamma}\sin\theta_i \; e^{-4/\left[1-(1-\frac{i}{N+1})^2\right]} & N \text{ odd}: \; i\in[\frac{N+1}{2}\to N] \end{cases} \tag{6-26c}$$

$$\gamma \equiv \int_{-1}^{1} e^{\frac{-4}{(1+s^2)}}ds \tag{6-26d}$$

It was suggested by Iri Morguti and Takasawa [10] and has been extended to be appropriate for integration on the sphere by [12]. This method will be referred to as (IMT). This completes the description of numerical methods used.

7. Justification and further details

In this section, I discuss further justifications for methodological choices and describe details of implementation in depth. The sequence of topics follows the order used above.

7.1 Choosing integration nodes and weights

Here, I will compare the three methods, TR, GL, and IMT, of defining nodes and weights for numerical integration. The three methods are compared in table 7-1. There I have tabulated the deviations of numerical integrations from analytical values normalized by absolute integrals (integration of absolute values of the integrands). For $\vec{x}_f$ and source cases where analytical formulas are not avalible, high order IMT integration (1152 points) were used in place of analytical values.

TABLE 7-1 Deviations of numerical from actual integrations normalized by absolute integrations; $\vec{x}_f = (1, 0°, 0°)$.

integrand →		$\vec{x}_j = (0, 0°, 0°)$ $\hat{J} = (1, 45°, -135°)$			$\vec{x}_j = (.5, 72°, -132°)$ $\hat{J} = (1, 105°, 95°)$
number of integration points →		$\frac{\hat{n}}{R}(\Phi - \Phi\|_{\vec{x}_f})$	$\frac{n_k}{R}(A_k - A_k\|_{\vec{x}_f})$	$\frac{\hat{n}\cdot\hat{R}}{R^2}(\Phi - \Phi\|_{\vec{x}_f})$	$\frac{\hat{n}\cdot\hat{R}}{R^2}(\Phi - \Phi\|_{\vec{x}_f})$
TR	106	3.2(-3)	3.4(-3)	9.4(-4)	2.6(-6)
	156	3.2(-3)	1.8(-3)	8.7(-4)	1.5(-3)
	214	1.6(-3)	6.6(-1)	1.9(-3)	8.0(-2)
	288	1.2(-3)	1.2(-3)	2.8(-4)	3.0(-5)
IMT	8	1.3	9.4(-2)	5.5(-1)	3.3(-1)
	72	1.0(-2)	4.3(-2)	7.2(-4)	2.0(-2)
	200	1.8(-5)	2.2(-4)	4.1(-6)	7.2(-3)
	512	2.7(-8)	1.3(-9)	1.6(-8)	1.9(-4)
GL	8	2.2(-2)	7.8(-2)	9.5(-3)	5.6(-2)
	72	1.0(-3)	3.2(-3)	5.0(-4)	4.2(-4)
	200	2.3(-4)	7.3(-4)	1.2(-4)	1.0(-4)
	512	5.9(-5)	1.9(-4)	3.0(-5)	2.7(-5)

It can be observed that the convergence of the TR scheme is unreliable. We also see that, for the most part, it performs worse than the other two. It can be observed that the IMT method performs relatively poorly at low integrator orders but converges faster than the GL method for all integrands but $\frac{\hat{n}\bullet\hat{R}}{R^2}\Delta\Phi\,|_{\text{non-central source}}$. Table 7-2 shows that the IMT method does indeed converge faster than the GL method for this integrand. We see that both IMT and GL methods appear to converge uniformly.

TABLE 7-2 Comparison of GL and IMT integration of $\frac{\hat{n}\bullet\hat{R}}{R^2}(\Phi-\Phi|_{\vec{x}_1})$ with $\hat{J}=(1,50°,50°)$.

eccentricity of source along z-axis ⟶		0.0	0.4	0.8
integration order ↓				
GL	32	1.4(-3)	8.7(-3)	9.1(-3)
	72	4.7(-4)	2.4(-3)	6.4(-3)
	200	1.1(-4)	5.2(-4)	6.5(-3)
	512	2.8(-5)	1.3(-4)	2.1(-3)
	2048	3.7(-6)	1.7(-5)	2.2(-4)
IMT	32	2.0(-2)	2.4(-2)	7.7(-3)
	72	6.8(-4)	5.4(-3)	5.4(-3)
	200	3.8(-6)	1.6(-5)	1.7(-3)
	512	1.5(-8)	2.4(-7)	1.1(-4)
	1152	1.6(-10)	1.7(-10)	1.5(-6)

7.2 On interpolation

7.2.1 Choosing an interpolator

Before implementing the Wahba interpolator, a simpler scheme suggested by Kel'zon [65] was tried. For this scheme, interpolation point locations were constrained by the equations

$$\theta_i = \frac{2i+1}{2n+2}\pi \quad i\in[0,n] \tag{7-1a}$$

$$\varphi_j = \frac{2j}{m+1}\pi \quad j\in[0,m] \tag{7-1b}$$

$$m+1 = 2(n+1) \tag{7-1c}$$

Equation 7-1c is included because the distribution of spacial frequencies of the functions being interpolated cannot be legitimately anticipated. This constraint would result in the most even sampling over the surface given equations 7-1a,b. As a test of interpolator performance, the deviation between interpolated and actual ω=0 solutions for Φ and $\vec{A}$ at point locations specified by a 6 node (72 point) GL integrator were calculated for 5 different $\vec{x}_f$. It was assumed that these 72 integration points provided a representative sampling of interpolator behavior over the sphere. Calculations were done for only 5 $\vec{x}_f$ because results from doing the calculations for all interpolation points indicated that a handful of points were sufficient to indicate interpolator behavior. Computing time was the main deterrent to using more points. Table 7-3 displays these deviations for Φ averaged over GL points and the 5 $\vec{x}_f$ for several interpolator orders. Deviations were normalized by the average magnitude of Φ.

TABLE 7-3 Average deviation between Kel'zon interpolated Φ and actual values normalized by the average magnitude of Φ ; $\vec{x}_j = (.3, 0°, 0°)$.

source case	$\hat{J} = (1, 0°, 0°)$	$\hat{J} = (1, 90°, 0°)$
interpolation point distribution (n+1)/(m+1)		
10/20	.082	.078
12/24	.12	.15
14/28	.11	.15
20/40	.044	.044
25/50	.09	.12
30/60	.076	.11
40/80	.02	.02
Maximum deviations of a 156 point Wahba interpolator, $\vec{x}_j = (.5, 0°, 0°)$.	.0023	.0020

It can be observed that the method seems unreliable. However, reliable convergence has been achieved with $n+1 \geq 50$ for interpolating Φ corresponding to a radial source. For this function, $m+1$ is irrelevant since Φ depends only on θ so $n+1=50$ can be considered a lower bound of the domain within which the method is reliably convergent. In conclusion, to interpolate unknown functions within the domain of reliable interpolator convergence, Kel'zon interpolation would require impractically high order interpolators.

Table 7-3 also contains comparable data from a Wahba interpolator. Obviously, this method is much more efficient. In fact, Kel'zon interpolation of Φ for radial sources at an eccentricity of 0.3 does not achieve the same level of accuracy even at $n+1=200$. This was the main justification for using Wahba interpolation. The domain for reliable convergence of Wahba interpolation was not found because of computational costs involved. However, the sparse data that was generated does indicate convergence. Table 7-4 displays, for Wahba interpolation, the average magnitude of deviations between actual and interpolated values for Φ and $\vec{A}$ normalized by the average of their actual magnitudes.

TABLE 7-4 **Average magnitude of the deviation between Wahba interpolated values and actual values normalized by the average magnitude of the funtion being interpolated; m=3.**

source case →	$\hat{J} = (1, 0°, 0°)$			$\hat{J} = (1, 90°, 0°)$			
order of interpolator →	156	106	64	156	106	64	
function ↓							source location ↓
Φ	.0014	.0033	.0099	.00099	.0023	.010	$\vec{x}_j = (.5, 0°, 0°)$
$\vec{A}$	.0011	.0013	.0063	.0011	.0012	.0058	$\vec{x}_j = (0, 0°, 0°)$

To clarify the nature of the average, recall that to each interpolation point is assigned a set of integration points (in the case of a GL integrator, this is done by rotation of integrator point locations defined by 6-2b,d) at which function values are to be estimated. The average is over all integration points and interpolation points. Convergence is also indicated by graphs 7-2 and 7-3 in section 7.2.3 which display the average unnormalized deviation for Φ with $\vec{x}_j=(.3, 0°, 0°)$ and $\hat{J}=(1, 50°, 50°)$ at an interpolation point near the positive pole. Further explaination of these graphs can be found in section 7.2.3; for our purpose here, simply note that the curves for interpolators based on higher point densities are shifted below those corresponding to lower point densities.

7.2.2 Point distribution for Wahba interpolator

Equations 6-3 indicate that Wahba interpolation does not require the use of all interpolation points to determine function values at integration points. Choosing to use all interpolation points was based on the view that forcing the characteristics of the interpolating function to depend on all known data would result in higher accuracy interpolations. It turns out that this is true only if $\mathbf{A}^{-1}$ could be computed for all m of q(x;m) and λ combinations. In practice, the success rate in finding $\mathbf{A}^{-1}$ decreased as interpolator order increased and/or as m increased. In addition, interpolator accuracy was observed to increase with increasing m. This means using fewer interpolation points may become advantageous at high m values. However, using small subsets of interpolation points for each integration point introduces many complexities in implementation.

Given that all interpolation points are used for each integration point, how should the interpolation points be distributed? Both Kel'zon point distributions and the semi-uniform density points were tried. It was observed that $\mathbf{A}^{-1}$

was much harder to find for Kel'zon points than for the semi-uniform points, i.e., when Kel'zon points were used, fewer m and λ combinations resulted in successful inversions. In addition, when inversions were successful, the resulting interpolators based on Kel'zon points were usually not as accurate as interpolators based on the semi-uniform points. It is clear that maximizing interpolation point distribution uniformity is optimal: since interpolation accuracy increases with sampling density and we do not know the distribution of spacial frequencies for functions being interpolated, it follows that it would be judicious to use uniform point distributions.

7.2.3 Choosing λ and m of q(x,m)

The task of choosing smoothing order, m, and λ involves finding an extremum of the surface defined by the point (m, λ) and a performance measure of the associated interpolator. The performance measure used was the same as that for examing Kel'zon interpolators. Observing interpolator performance for several choices of source and $\vec{x}_I$ suggested that each point in this domain defined a performance surface approximately parallel to that for other combinations of source and $\vec{x}_I$. Consequently, for computational expedience, I chose the source to be characterized by $\vec{x}_j$=(.3,0°,0°) and $\hat{J}$=(1,50°,50°). I assumed this source would be representative of all possible cases reasoning that because of spherical symmetry, only radial and tangential sources on the positive z-axis need be considered. $\vec{x}_I$ was chosen to be a point near the positive pole point; interpolator performance was poorest at points close to the positive pole.

I systematized the examination of points (m, λ) by chosing m from the set [1 -> 4] and used the function

$$\%_{sls} = 1 - \frac{\sum_{p}^{N_p} |R_{pp}|}{\sum_{p}^{N_p} |R_{pp}| + N_p^2 \lambda} \tag{7-2}$$

to help specify a reasonable range of λ to consider. This function (percent **s**moothing **l**east **s**quares) can be loosely considered a measure of the degree (percentage) to which the interpolation depends on the smoothness of the interpolating function and 1-$\%_{sls}$ can be loosely considered the degree to which the interpolation depends on minimizing the least squares deviation between the interpolating function and actual function values at interpolation points [33]. Specifically, Wahba's interpolator minimizes

$$\underbrace{\frac{1}{N_p}\sum_{p}^{N_p}(\tilde{f}(\vec{x}_p) - f(\vec{x}_p))^2}_{\text{least squares part}} + \lambda \underbrace{\begin{cases} \int_S (\Delta^{m/2}\tilde{f})^2 & \text{m even} \\ \int_S \left(\frac{(\Delta^{(m-1)/2}\tilde{f})_\varphi^2}{\sin^2\theta} + (\Delta^{(m-1)/2}\tilde{f})_\theta^2 \right) & \text{m odd} \end{cases}}_{\text{smoothing part}} \tag{7-3}$$

where $\tilde{f}$ is the interpolating function and Δ is the Laplace-Betrami operator, and $()_\alpha$ denotes differentiation with respect to α. Thus, with a little algebra, it can be seen that $\%_{sls}$=0 implies λ=0 and as $\%_{sls}$ approaches unity, λ approaches infinity.

Results of the grid search can be observed in graphs 7-1 to 7-3. Smoothing order, m, greater than 3 could not be sufficiently explored because for most of the $\%_{sls}$, **A** could not be inverted; for those where inversion was successful, interpolator performance was miserable. I am confident that maxima found for interpolator accuracy are global maxima; $\%_{sls}$ in the range [0→0.9] were examined. Here is a summary of general trends observed as smoothing order was increased, two of which have been mentioned previously:

1. Fewer successful **A** inversions could be obtained.
2. The $\%_{sls}$ interval within which reasonable interpolators could be found shrunk.
3. Interpolator performance maxima became larger.

I would like to note that trends 1 and 2 are independent: trend 1 was observed with $\%_{sls}$ within the interval where reasonable interpolators were found.

graph 7-1 Wahba interpolator performance;
m=1, 106 point.

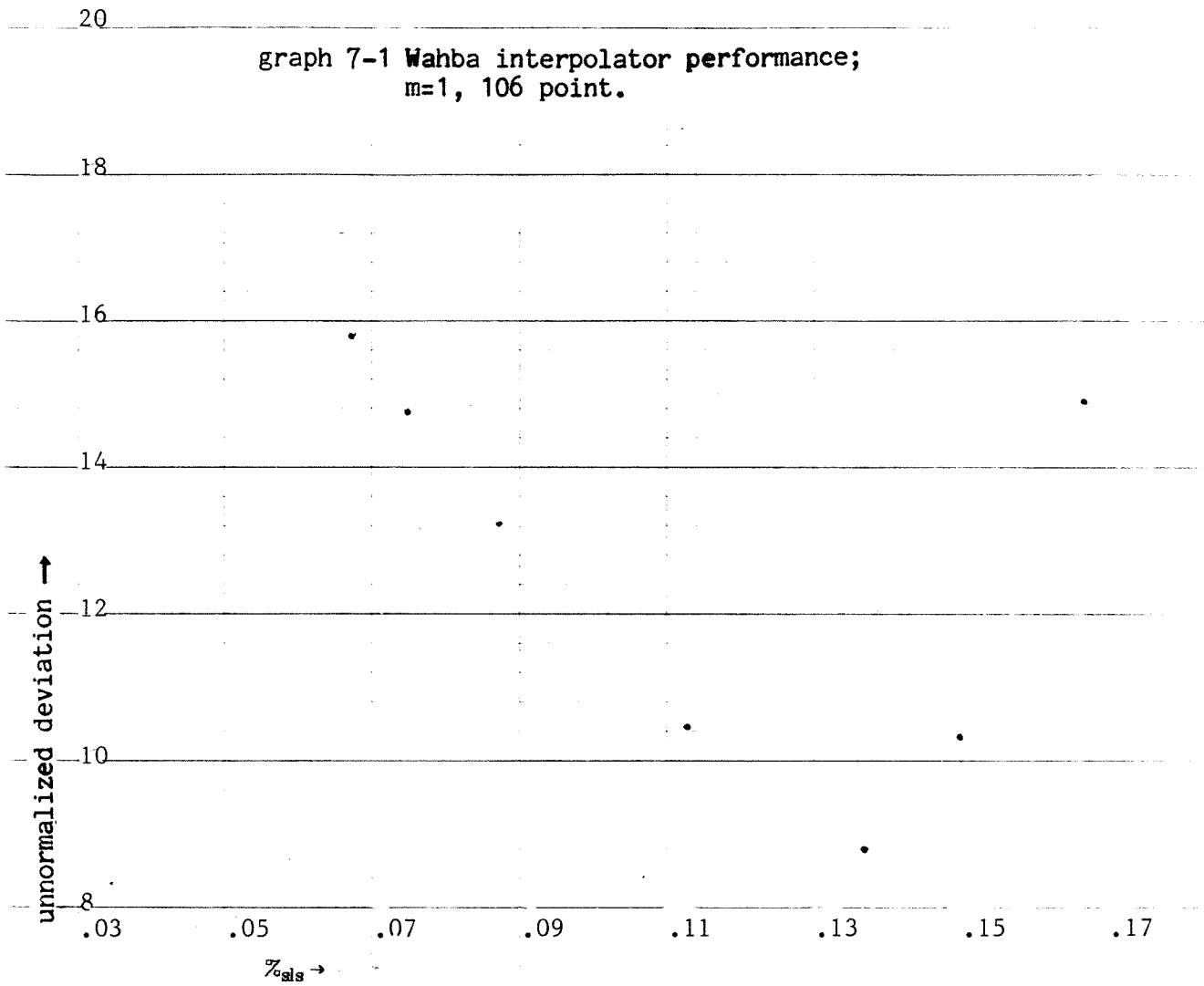

graph 7-2 Wahba interpolator performance;
m=2.

• 106 point
× 156 point

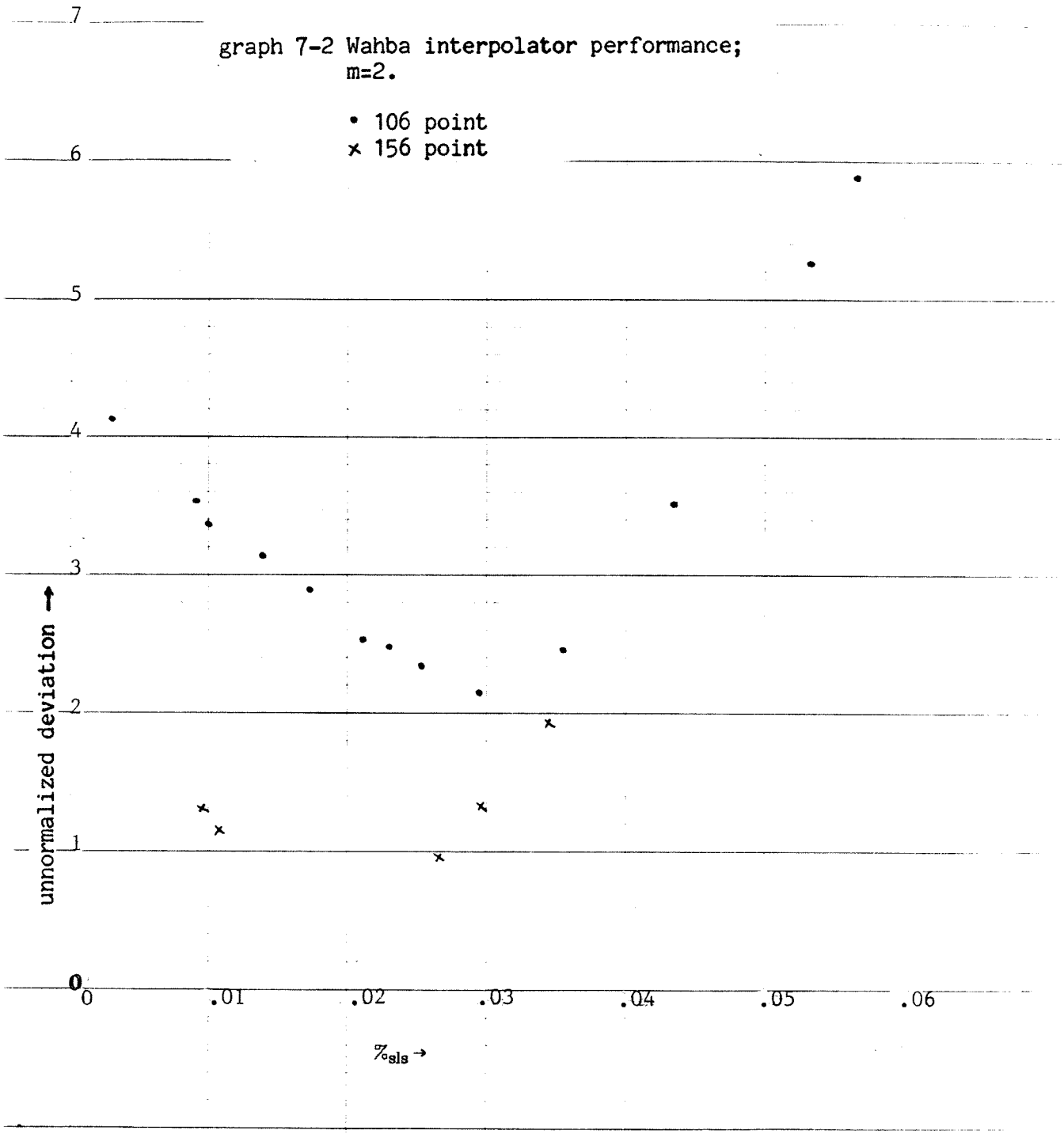

graph 7-3 Wahba interpolator performance; m=3.

• 106 point
× 156 point

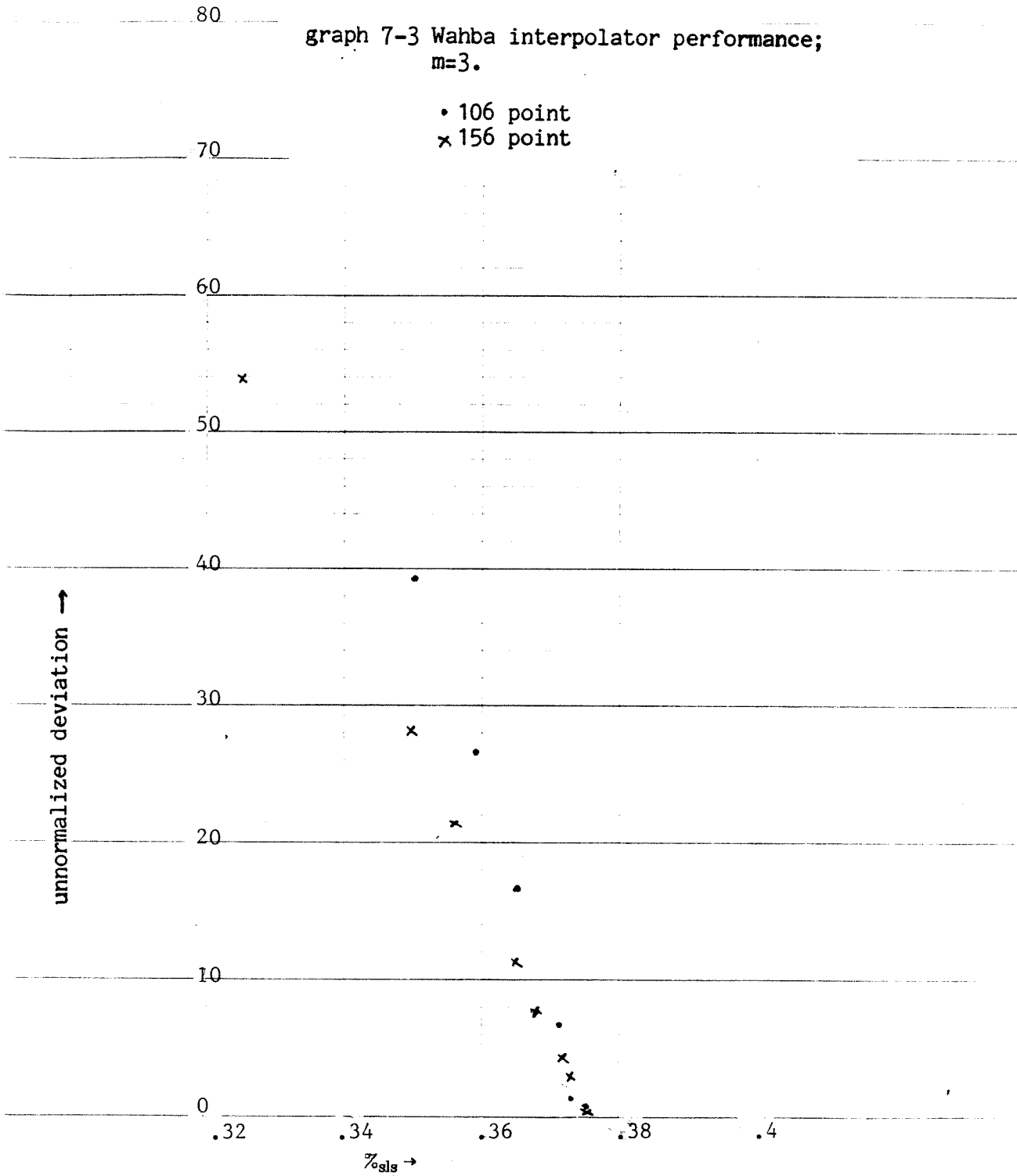

7.3 On the linear equation solver

7.3.1 Choosing Cimmino's process

Standard techniques to solve linear systems could not be used because of the possible singularity of the system matrix. To show that solutions to equations 5-4 may not be unique, note that arbitrary functions can be added to $\vec{A}$ and Φ without changing the solutions found for $\vec{E}$ and $\vec{B}$ so long as

$$\nabla \times {}^{\omega}\vec{A}_{arb(itrary)} = 0 \qquad (7\text{-}4a)$$

$$\nabla \cdot {}^{\omega}\vec{A}_{arb} = -\mu\tilde{\sigma}^{\omega}\Phi_{arb} \qquad (7\text{-}4b)$$

$$i\omega^{\omega}\vec{A}_{arb} = -\nabla^{\omega}\Phi_{arb} \qquad (7\text{-}4c)$$

Equation 7-4a is satisfied by 7-4c. Combining 7-4b with 7-4c, I obtain

$$\nabla^{2\omega}\Phi_{arb} - i\omega\mu\tilde{\sigma}^{\omega}\Phi_{arb} = 0 \qquad (7\text{-}5)$$

which has at least one non-trivial solution,

$${}^{\omega}\Phi_{arb} = \begin{cases} C\dfrac{e^{kr}}{r} & r \notin [R_c - \delta l_{max},\ R_c + \delta l_{max}] \\ ? & r \in [R_c - \delta l_{max},\ R_c + \delta l_{max}] \end{cases} \qquad (7\text{-}6a)$$

$$k^2 \equiv i\omega\mu\tilde{\sigma} \qquad (7\text{-}6b)$$

$$C = \text{some arbitrary constant} \qquad (7\text{-}6c)$$

$$r = \text{distance from the origin} \qquad (7\text{-}6d)$$

Thus, we know that solutions to the system of differential equations 2-11 are non-unique. I had stated in section 2.4 that this means solutions to the

integral equations obtained from 2-11 are non-unique. However, are solutions to simplified forms non-unique? To investigate this, let us find solutions to homogeneous equations 5-4 of the form

$$\Phi|_{S(urface)} = P_\Phi + iQ_\Phi \tag{7-7a}$$

$$\vec{A}|_S = (P_{\vec{A}} + iQ_{\vec{A}})\hat{n} \tag{7-7b}$$

for real constants P_Φ, Q_Φ, $P_{\vec{A}}$, and $Q_{\vec{A}}$ where $\hat{n}$ is the outward normal to S. With these forms and equations 5-4, a non-trivial solution to the homogeneous equations can be found if the following matrix is non-singular:

$$\begin{bmatrix}-1 & 0\\ 0 & -1\end{bmatrix} + R_c^2\sqrt{\omega\mu_0\sigma_{in}}\left(\frac{1}{R_c} - \frac{1}{4\ \Sigma l}\right)\begin{bmatrix}1 & -1\\ 1 & 1\end{bmatrix} + \frac{\omega\mu_0 R_c^3}{3\sigma_{in}\ \Sigma l}\begin{bmatrix}\varepsilon_{in}\omega & -\sigma_{in}\\ \sigma_{in} & \varepsilon_{in}\omega\end{bmatrix}$$
$$+ \frac{1}{\sigma_{in}}\begin{bmatrix}\sigma_{in} & -\varepsilon_{in}\omega\\ \varepsilon_{in}\omega & \sigma_{in}\end{bmatrix} - \frac{\mu_0\omega}{6\pi}\begin{bmatrix}\sigma_{in}(e_1+e_2)+\varepsilon_{in}\omega & \sigma_{in}-e_1(\sigma_{in}e_2+\varepsilon_{in}\omega)\\ e_1(\sigma_{in}e_2+\varepsilon_{in}\omega)-\sigma_{in} & \sigma_{in}(e_1+e_2)+\varepsilon_{in}\omega\end{bmatrix} \tag{7-8}$$

$$e_1 \equiv \int_S \frac{e_{im}}{R}$$

$$e_2 \equiv \left\| \int_S \frac{\hat{n}}{R} e_{im} \right\|$$

Non-singularity can be shown for the special case represented by equations 4-20 where the matrix above reduces to

$$R_c^2\sqrt{\mu_0\omega\sigma_{in}}\left(\frac{1}{4\ \Sigma l} - \frac{1}{R_c}\right)\begin{bmatrix}-1 & 1\\ -1 & -1\end{bmatrix} + \frac{\omega\mu_0 R_c^3}{3\ \Sigma l}\begin{bmatrix}0 & -1\\ 1 & 0\end{bmatrix}$$
$$\equiv \begin{bmatrix}-a & a-b\\ b-a & -a\end{bmatrix} \text{ inverse is } \begin{bmatrix}\frac{1-a}{a^2} & \frac{1}{a(b-a)}\\ \frac{1}{a(a-b)} & \frac{-1}{(b-a)^2}\end{bmatrix} \tag{7-9}$$

Thus, non-singularity is shown if it can be shown that $b-a\neq 0$. For the head system, this is approximately equivalent to examining

$$\frac{\sqrt{\sigma_{in}}}{R_c} \stackrel{?}{\neq} \frac{4}{3}\sqrt{\mu_0\omega} \tag{7-10}$$

For parameters of interest here,

$$.95 \lesssim \frac{\sqrt{\sigma_{in}}}{R_c} \lesssim 25 \tag{7-11}$$

$$\frac{4}{3}\sqrt{\mu_0\omega} = .95 \quad : \omega = 2\pi 6.4\text{x}10^4 \tag{7-12}$$

So, unless we only wish to examine solutions in the vicinity of $6.4\text{x}10^4$Hz, solutions of equations 4-20 will be, in general, non-unique.

There are several techniques to deal with singular systems. Wielandt deflation techniques [24, 74, 75], the methods used by biopotential people [20, 87], require finding a basis for the homogeneous integral equations. I have just revealed one of the basis vectors for equations 4-20; however, I am not sure whether or not there are others. Atkinson's technique [7] to convert singular Fredholm equations of the second kind to an equation with unique solutions could not be used for the same reason. A technique by [99], a method suggested for biopotential research, turns out to be a primitive version of Atkinson's technique. Generalized inverse techniques [63, 106] seemed much more difficult to implement than Cimmino's process. In conclusion, it seemed judicious to use Cimmino's process since it is guaranteed to converge to one of the possible solutions [24].

7.3.2 A minor detail in Cimmino's algorithm

The factor $\frac{2}{n+1}$ was changed from $\frac{2}{n}$ reported in texts describing the method. In order to understand the motivation behind this, one needs to know how Cimmino's process predicts the intersection of the planes corresponding to each equation of the linear system to be solved. The process finds the center of mass for a set of points defined by reflecting an initial point through each plane. The denominator n is appropriate if the initial point is excluded from this set; using n+1 includes it. This change is shown to improve convergence in the example below:

$$\begin{bmatrix} 5 & -1 & 3 \\ 2 & 0 & 1 \\ 3 & 2 & 1 \end{bmatrix} \vec{x} = \begin{bmatrix} 1 \\ -5 \\ 2 \end{bmatrix} \text{ with solution } \vec{x} = \begin{bmatrix} -39 \\ 23 \\ 73 \end{bmatrix} \qquad \text{(7-13a)}$$

$$\vec{x}_0 = \begin{bmatrix} 2 \\ -1 \\ 100 \end{bmatrix}$$

With n as the denominator, one iteration of Cimmino's process gives

$$\vec{x}_1 = \begin{bmatrix} -75.14 \\ -7.46 \\ -61.57 \end{bmatrix} \quad \|\vec{x}_1 - \vec{x}\| = 48.62 \qquad \text{(7-13b)}$$

With n+1 as the denominator, one iteration of Cimmino's process gives

$$\vec{x}_1 = \begin{bmatrix} -55.8 \\ -5.84 \\ -71.17 \end{bmatrix} \quad \|\vec{x}_1 - \vec{x}\| = 33.46 \qquad \text{(7-13c)}$$

7.3.3 Determining termination of iteration

This was a difficult problem because it was observed that, starting from exact solutions for the case ω=0 (equation 6-5 which also determines $\vec{A}|_{\omega=0}$) and seeking to find solutions to the ω=0 equations, Cimmino's process still proceeded to change the solution vector. Yet, indeed, the magnitude of the residual, $\|\mathbf{A}\vec{x}-\vec{b}\|$ (where **A** is a system matrix, $\vec{x}$ is a proposed solution, and $\vec{b}$ is the constraint vector), was decreasing steadily. This behavior illustrates that exact solutions are not necessarily solutions to the dicreetized equations. Another factor that may be at the root of this behavior is the possible non-uniqueness of solutions. Cimmino's process may be converging to a solution that has a better fit to the discretized equations. This is a serious problem since the goal of this investigation must be achieved by finding, for a given set of parameters other than ω, the minimum distance between the ω=0 solution space and the $\omega\neq0$ solution space. I have made the assumption that finding the minimum distance between the $\omega\neq0$ solution space and the point in ω=0 solution space represented by equation 6-5 would be a good estimate of the global minimum. Proceeding from this assumption, I need to substantiate the assertion that the criterion used for halting iteration results in finding the $\omega\neq0$ solution that is closest to the ω=0 solution expressed by equation 6-5.

I will begin my effort to substantiate the criterion used by saying that, for all parameter cases studied, convergence rate was similar to that for seeking solutions to ω=0 equations starting from ω=0 solutions: a linear reduction in the magnitude of the residual vector was observed. This observation indicates the difficulty of basing halt criterion on some measure of convergence rate. This is a reason for choosing a criterion based on the value of the residual vector. Toward evaluating the particular criterion I used, consider the five solutions that are involved:

1. the solution to the discretized $\omega=0$ equations, $\vec{X}_{d(iscreet)}|_{\omega=0}$,
2. the solution to the continuous $\omega=0$ equations evaluated at the $\vec{x}_f$, $\vec{X}_{c(ontinuous)}|_{\omega=0}$,
3. the solution to the dicreetized $\omega\neq0$ equations that Cimmino's process will converge to given a huge number of iterations, $\vec{X}_d|_{\omega\neq0}$,
4. the solution to the continuous $\omega\neq0$ equations closest to $\vec{X}_c|_{\omega=0}$ evaluated at the $\vec{x}_f$, i.e.,

$$\vec{X}_c|_{\omega\neq0} = \underset{\zeta}{MIN}(\|\vec{X}_c|_{\omega=0} - \vec{X}_\zeta\|): \vec{X}_\zeta \in \text{solution space for } \omega\neq0 \text{ solutions}, \tag{7-14}$$

and

5. the solution that is found under the convergence criterion used, $\vec{X}_{a(ctualized)}|_{\omega\neq0}$.

I will use the $\vec{X}$ to denote either $\vec{A}_{\substack{re\\im}}$ or $\vec{\Phi}_{\substack{re\\im}}$, not the whole solution vector. I will denote residuals corresponding to these solutions by $\Delta\vec{b}$ where $\Delta\vec{b}_d\equiv0$. The correspondence between residuals for $\vec{A}$ and Φ equations and solutions for $\vec{A}$ and Φ can be made since I solved equations 4-20. Using this notation, the criterion I used assumes that

$$\text{if } \|\Delta\vec{b}_a|_{\omega\neq0}\| \approx \|\Delta\vec{b}_c|_{\omega=0}\| \text{ then } \vec{X}_a|_{\omega\neq0} \approx \vec{X}_c|_{\omega\neq0} \tag{7-15}$$

Here are two lines of reasoning that suggest the validity of equation 7-15.

1. Suppose the relationship between $\vec{X}_c|_{\omega=0}$ and $\vec{X}_d|_{\omega=0}$ is the same as that between $\vec{X}_c|_{\omega\neq0}$ and $\vec{X}_d|_{\omega\neq0}$ in the sense that $\Delta\vec{b}_c|_{\omega\neq0} \approx \Delta\vec{b}_c|_{\omega=0}$. Then the criterion would be based on the assumption that

$$\vec{X}_a|_{\omega\neq 0} \approx \vec{X}_c|_{\omega\neq 0} \text{ when } \Delta\vec{b}_a|_{\omega\neq 0} \approx \Delta\vec{b}_c|_{\omega\neq 0}. \qquad (7\text{-}16)$$

Some sort of support for the supposition comes from noting that the contribution to residuals of $\vec{A}$ equations by integration errors, based on integrating $\omega=0$ solutions, is dominated by the integral $\int \frac{\hat{n}}{R}\Phi$ for frequencies up to about 5kHz (see table 4-3). For $\vec{A}|_{\omega=0}$ equations, this is the only integration. So, if it is assumed that, for the $\omega\neq 0$ case, this integration also dominates contributions to residuals by integration errors, we can venture the guess that contributions to residuals by integration errors for the case $\omega\neq 0$ approximate those for the case $\omega=0$. This supports the supposition because non-zero $\Delta\vec{b}_c$ arises only because non-zero integration errors exist. For Φ equations, the same reasoning cannot be applied: with $\int \frac{\hat{n}\bullet\hat{R}}{R^2}\Phi$ being the only integration in $\Phi|_{\omega=0}$ equations, it can be observed from table 4-3 that error in this integration would be dominant only up to about 10Hz. Reguardless, using this line of reasoning, equation 7-16 can finally be substantiated by claiming that Cimmino's process is initiated at a point close enough to $\vec{X}_c|_{\omega\neq 0}$ such that $\Delta\vec{b}(\vec{X})$ is a single valued function of $\vec{X}$. This claim is exactly that required by the second line of reasoning to justify equation 7-15.

2. If it can be assumed that $\vec{X}_c|_{\omega\neq 0}$ and $\vec{X}_d|_{\omega\neq 0}$ are very close to the respective solution for the case $\omega=0$, equation 7-15 can be justified. The point is made by noting that Cimmino's process is initiated at $\vec{X}_c|_{\omega=0}$ and claiming that if $\vec{X}_c|_{\omega=0}$ is in close proximity to $\vec{X}_c|_{\omega\neq 0}$, $\Delta\vec{b}$ would be a single valued function of $\vec{X}$. To support these claims, I refer to table 7-5 and tables 8-7. It will be seen that $\vec{X}_a|_{\omega\neq 0}$ are very close to $\vec{X}_c|_{\omega=0}$ for all parameter cases studied; a measure of the deviation between the two solutions is shown in tables 8-7.

Table 7-5 shows residuals for Φ and $\vec{A}$ equations averaged over magnitudes of real, imaginary, and spacial components and normalized by a similar average taken over elements of the constraint vector (the source terms) corresponding to each equation type. The cases reported are those for which the difference between residuals for $\vec{X}_c|_{\omega=0}$ in $\omega\neq 0$ equations and residuals for $\vec{X}_c|_{\omega=0}$ in $\omega=0$ equations are usually the largest compared to other choices for parameters. Medium types will be explained in detail in section 8. The point here is to note that residuals for $\vec{X}_c|_{\omega=0}$ in $\omega\neq 0$ equations hardly differ from those for $\vec{X}_c|_{\omega=0}$ in $\omega=0$ equations.

TABLE 7-5 Normalized residuals for $\omega=0$ solutions in 10^4Hz equations compared to mormalized residuals for $\omega=0$ solutions in $\omega=0$ equations.

$\hat{J} = (1, 0°, 0°)$

$\theta_{FT} = 0$

source eccentrcity →		0.0		0.4		0.8	
medium type	equation type →	Φ	$\vec{A}$	Φ	$\vec{A}$	Φ	$\vec{A}$
cerebral spinal fluid	0Hz	1.999	2.889(-4)	1.999	.2010	2.001	.4041
	10^4Hz	2.025	3.499(-4)	2.024	.2011	2.013	.4050
skull		1.951	2.889(-4)	1.951	.2010	1.953	.4041
		1.972	2.898(-4)	1.972	.2010	1.976	.4041
small brain		1.936	2.889(-4)	1.936	.2010	1.938	.4041
		1.965	2.937(-4)	1.965	.2010	1.969	.4041
medium brain		1.936	2.889(-4)	1.936	.2010	1.938	.4041
		1.942	3.084(-4)	1.952	.2010	1.968	.4044
large brain		1.936	2.889(-4)	1.936	.2010	1.938	.4041
		1.992	3.343(-4)	1.994	.2011	1.993	.4049

Note that equations 4-20 and 4-21 remain valid up to 10^4Hz if a 10% criterion is used in equation 4-17. In summary, I have revealed the difficulties in selecting a criterion with which to halt Cimmino's process. I believe that, given the behavior of Cimmino's process in the application pursued here, the best of the possible criteria was selected.

Before moving on, I would like to mention that the discussion above makes it clear that, if convergence is achieved, using residuals in error estimates would be inappropriate. At convergence, we have $\Delta\vec{b}_a|_{\omega\neq 0} \approx \Delta\vec{b}_c|_{\omega=0}$. With the claim that $\Delta\vec{b}_a|_{\omega\neq 0} \approx \Delta\vec{b}_c|_{\omega\neq 0}$, it is obvious that the residual has little to do with the uncertainty in $\vec{X}_a|_{\omega\neq 0}$ with respect to $\vec{X}_c|_{\omega\neq 0}$.

7.4 On scaling

7.4.1 The need for scaling

It turns out that, for some parameter cases, the top 6n rows of the system represented by equations 6-9 can differ from the bottom 2n rows by six orders of magnitude. A 4x4 example, based on a 10Hz system matrix, compares scaled and unscaled implementations of Cimmino's process.

$$\begin{bmatrix} 5 & -.3 & .9 & -7(-9) \\ -8 & 6 & -.1 & -5(-9) \\ -1 & -.2 & 4 & -4(-9) \\ 60 & -40 & 50 & 1 \end{bmatrix} \vec{x} = \begin{bmatrix} 7(-7) \\ -6(-7) \\ 2(-7) \\ 1 \end{bmatrix} \text{ solution is } \vec{x} = \begin{bmatrix} 1.258(-7) \\ -8.166(-8) \\ 4.38(-8) \\ 1 \end{bmatrix} \quad \text{(7-17a)}$$

Iterative history when no scaling is used:

$$\begin{bmatrix} 0 \\ 0 \\ 0 \\ 1 \end{bmatrix}, \begin{bmatrix} 6.817(-8) \\ -4.971(-8) \\ 2.487(-8) \\ 1 \end{bmatrix}, \begin{bmatrix} 7.443(-8) \\ -5.333(-8) \\ 1.544(-8) \\ 1 \end{bmatrix}, \begin{bmatrix} 7.726(-8) \\ -5.434(-8) \\ 1.132(-8) \\ 1 \end{bmatrix}, \begin{bmatrix} 7.901(-8) \\ -5.459(-8) \\ 9.099(-9) \\ 1 \end{bmatrix} \quad \text{(7-17b)}$$

Comparable iterative history when the scaling

$$\mathbf{Pre} = \begin{bmatrix} 10^4 & & & \\ & 10^4 & & \\ & & 10^4 & \\ & & & 10^4 \end{bmatrix} \quad \mathbf{Pst} = \begin{bmatrix} 1 & & & \\ & 1 & & \\ & & 1 & \\ & & & 10^5 \end{bmatrix} \qquad (7\text{-}17c)$$

is used:

$$\begin{bmatrix} 0 \\ 0 \\ 0 \\ 1 \end{bmatrix}, \begin{bmatrix} 8.940(-8) \\ -6.387(-8) \\ 4.256(-8) \\ 1 \end{bmatrix}, \begin{bmatrix} 1.137(-7) \\ -7.834(-8) \\ 4.730(-8) \\ 1 \end{bmatrix}, \begin{bmatrix} 1.212(-7) \\ -8.140(-8) \\ 4.626(-8) \\ 1 \end{bmatrix}, \begin{bmatrix} 1.238(-7) \\ -8.191(-8) \\ 4.509(-8) \\ 1 \end{bmatrix} \qquad (7\text{-}17d)$$

It is obvious that without scaling, convergence is slower or Cimmino's process is divergent.

7.4.2 The choice of scaling

From the findings above, it was concluded that an effective scaling would be one which minimized the difference, in order of magnitude, between all non-zero elements of the system matrix. Scaling so defined was compared with a scaling that minimized the difference in order of magnitude between all non-zero elements of the system matrix separately from effecting the same for the constraint vector. The two methods were compared by comparing rates of residual reduction for several parameter cases. The chosen method was only slightly better.

I compared two methods of excluding or including diagonal elements of the system matrix in averages from which scaling was calculated: the scheme which resulted in maximizing the diagonal dominance of the scaled system matrix and the complement of this scheme. It was thought that there could be

a difference in performance between the two schemes since diagonal dominance is a sufficient condition for convergence of Gauss-Seidel iteration. By observing the rate at which Cimmino's process reduced the residual, scaling that maximized diagonal dominance performed better for parameter cases where residuals of $\omega=0$ solutions in $\omega\neq 0$ equations were larger than residuals for $\omega=0$ solutions in $\omega=0$ equations. In contrast, when numerical methods could not resolve the difference between $\omega=0$ and $\omega\neq 0$ solutions, i.e., residuals of $\omega=0$ solutions in $\omega\neq 0$ equations were less than residuals for $\omega=0$ solutions in $\omega=0$ equations, scaling that minimized diagonal dominance performed better.

7.5 On the measure for frequency dependence

Note that this measure does not allow assessing the significance of magnetic induction. The following shows that it is not possible to make such an assessment given the methods of solving Maxwell's equations used here. In order to assess the degree of electromagnetic coupling, optimally, we would like to compare the magnitude of the rotational component of $\vec{E}$ with the magnitude of the irrotational component. Considering equation 2-8b and writing

$$\vec{A} = \nabla a_{ir(rotational)} + \nabla\times\vec{a}_{ro(tational)} \qquad (7\text{-}18)$$

we see that this would mean comparing $\|\nabla\Phi + i\omega\nabla a_{ir}\|$ to $\omega\|\nabla\times\vec{a}_{ro}\|$. Making this comparison would mean solving, from equation 2-10a,

$$\nabla^2 a_{ir} = -\mu\tilde{\sigma}\Phi \qquad (7\text{-}19)$$

Unfortunately, this cannot be done unless we solve for Φ throughout space, exactly the problem with using Coulomb's gauge. A further problem is the need to calculate $\nabla\Phi$. A look at the $\omega=0$ equation for Φ suffices to reveal the

problem. Taking the gradient of equation 2-26b with respect to $\vec{x}_f$, setting I=1, and using equation 3-14b evaluated at ω=0 gives

$$4\pi\bar{\sigma}\nabla_{\vec{x}_f}\Phi^{re}_{im}|_{\vec{x}_f} = -4\pi\Phi^{re}_{im}|_{\vec{x}_f}\nabla_{\vec{x}_f}\bar{\sigma} - \frac{\begin{bmatrix}\cos\theta_{FT}\\ \sin\theta_{FT}\end{bmatrix}}{R_j^3}(3\hat{R}_j\bullet\vec{J}\hat{R}_j-\vec{J}) + \int_{S-\vec{x}_f}\sigma_{in}\frac{(3\hat{n}\bullet\hat{R}\hat{R}-\hat{n})}{R^3}\Phi^{re}_{im} \tag{7-20}$$

where $\nabla_{\vec{x}_f}$ is used to denote the gradient operator that takes derivatives with respect to $\vec{x}_f$ and I have written $\vec{J}$ for $\hat{J}\int_{-L/2}^{L/2}|J_{rld}|$. For a central source and $\vec{x}_f=(R_c,0°,0°)$,

$$4\pi\bar{\sigma}\nabla_{\vec{x}_f}\Phi^{re}_{im}|_{\vec{x}_f} = \frac{-3\begin{bmatrix}\cos\theta_{FT}\\ \sin\theta_{FT}\end{bmatrix}}{\sigma_{in}R_c^2}\hat{n}_{\vec{x}_f}\bullet\vec{J}\nabla_{\vec{x}_f}\bar{\sigma} - \frac{\begin{bmatrix}\cos\theta_{FT}\\ \sin\theta_{FT}\end{bmatrix}}{R_c^3}(2J_z\hat{z}-J_x\hat{x}-J_y\hat{y})$$
$$+\frac{\begin{bmatrix}\cos\theta_{FT}\\ \sin\theta_{FT}\end{bmatrix}}{R_c^3}\left(\frac{5}{4}J_z\hat{z}-\frac{3}{4}\sqrt{\frac{2}{1-\cos\theta}}|_{\theta=0}J_z\hat{z}+2J_x\hat{x}+2J_y\hat{y}\right) \tag{7-21a}$$
$$= -\pi\Phi|_{\vec{x}_f}\left(4\nabla_{\vec{x}_f}\bar{\sigma}+\frac{\sigma_{in}}{R_c}\hat{n}_{\vec{x}_f}\left(1+\sqrt{\frac{2}{1-\cos\theta}}|_{\theta=0}\right)\right)+\frac{3\begin{bmatrix}\cos\theta_{FT}\\ \sin\theta_{FT}\end{bmatrix}}{R_c^3}(J_x\hat{x}+J_y\hat{y}) \tag{7-21b}$$

Note that one term is singular. For the ω=0 case, we know this singular term must cancel $\nabla_{\vec{x}_f}\bar{\sigma}$. This is because $\nabla_{\vec{x}_f}\Phi$ cannot have a component normal to the conductor surface by conservation of charge since in the vicinity of the surface, there is only conduction current and we have $\vec{E} = -\nabla\Phi$. On the other hand, theoretical developments of section 2 allowed us to define a finite $\nabla_{\vec{x}_f}\bar{\sigma}$ at

the conductor surface. It can be concluded that the term $\nabla_{\vec{x}_f}\int_{S-\vec{x}_f}\frac{\hat{n}\bullet\hat{R}}{R^2}\Phi$ must not be handled properly by simply integrating $\int_{S-\vec{x}_f}\Phi\nabla_{\vec{x}_f}\frac{\hat{n}\bullet\hat{R}}{R^2}$ but, for ω=0 solutions, other constraints allow the correct specification of this integral. For the general case, the obvious route to take is to expand the surface back to the volumn $\partial_{\delta l_{in}}V_{in}\cup\partial_{\delta l_{out}}V_{out}$ in the vicinity of $\vec{x}_f$. Integrating over a small cylinder about $\vec{x}_f$ proves the attempt futile. The size of the cylinder depends on $\vec{J}$, $\delta l_{in}+\delta l_{out}$, and Φ. This dependence is indicated by terms involving components of $\vec{J}$ and the expanded form for $\nabla_{\vec{x}_f}\int\frac{\hat{n}\bullet\hat{R}}{R^2}\Phi$; both terms make a contribution to the $\hat{z}$ component (the $\hat{n}_{\vec{x}_f}$ component). In conclusion, it is unclear how integrals in the gradient of equation 5-4b should be calculated for $\omega\neq0$ solutions.

7.6 Error computations

7.6.1 Published error estimates

A search for computable error bounds applicable to the numerical methods used here was unsuccessful. The best candidate was found in [3]. Writing Fredholm's integral equation of the second kind as

$$(\mathbf{I}-\mathbf{K})\vec{f} = \vec{J} \tag{7-22}$$

the error estimate is

$$\begin{aligned}\|\vec{f}_{N(umerical)} - \vec{f}_{A(ctual)}\| &\equiv \|(\mathbf{I}-\mathbf{K}_N)^{-1}\vec{J} - (\mathbf{I}-\mathbf{K}_A)^{-1}\vec{J}\| \\ &\leq \|(\mathbf{I}-\mathbf{K}_N)^{-1}\| \left(\frac{\|\mathbf{K}_N\vec{J}-\mathbf{K}_A\vec{J}\| + \|(\mathbf{K}_N-\mathbf{K}_A)\mathbf{K}_A\|\,\|(\mathbf{I}-\mathbf{K}_N)\vec{J}\|}{1-\|(\mathbf{I}-\mathbf{K}_N)^{-1}\|\,\|(\mathbf{K}_N-\mathbf{K}_A)\mathbf{K}_A\|} \right.\end{aligned} \tag{7-23}$$

where $\mathbf{K}_A$ is a compact operator. The bounds are for one dimensional Fredholm equations over the interval [0→1]. These bounds can be extended to the dimensionality and region of integration we require, Ω of equation 5-3. Required conditions on the integral operator $\mathbf{K}_A$ have been shown to be satisfied by one dimensional analogs of our kernels [6, 8]. Unfortunately, to evaluate the bounds, the first iterated kernel must be computed in a form sufficient to estimate

$$\underset{x\in\Omega}{MAX} \int_{\Omega} \left| \sum_{n=1}^{N_p} w_n K(x,t_n)K(t_n,y) - \int_{\Omega} K(x,t)K(t,y)dt \right| dy \tag{7-24}$$

where N_p is the order of the numerical integration, w_n are the integration weights, and t_n index the corresponding integration point locations. We have

seen that this involves very difficult integrations. In addition, an equation with unique solutions must be constructed.

Other published error bounds offered less with respect to applicability or computability. Several authors have given error bounds for numerical integration of singular integrands [4, 11, 40, 62, 71, 72, 73]. Most bounds presented depended on the ability to evaluate certain properties of the integrand such as the size of higher order derivatives; this makes them useless for our purposes. Others were not meant to be computed and served only to compare the accuracy of the method with other methods or to show convergence. There have been error bounds derived for numerical methods used to solve Fredholm integral equations similar to those of interest here [3, 6, 8, 59, 64, 72, 107] Some of these were for numerical methods differing in principle from those used here, e.g., projection methods. Others were not meant to be calculated and served to compare the methods with others or show convergence.

7.6.2 On error estimates used here

7.6.2.1 A possible alternative From an examination of equation 6-18d, it appears that we can simply solve this equation to obtain estimates for the ε_f. I will point out some problems with using this method to show that the method used is indeed preferable. Of course, fundamentally, we cannot solve for the exact values of the ε_f since integration errors are not known; but, if estimates of this error are used, will solving the resulting equation produce first order estimates of the ε_f? These estimates would be meaningful only if we could be assured that estimates of integration error were accurate not only in order of magnitude but also in sign. Possible non-uniqueness of the equation requires further assumptions. The component of found solutions that is a solution to the homogeneous equation must be removed since we are only interested in

the solution component that strictly depends on the constraint vector and we are not assured that contributions from solutions to the homogeneous equations will combine with the solution component of interest in such a way as to give conservative error estimates. Removal is achievable if it can be assumed that the homogeneous component existing upon using Cimmino's process on the inhomogeneous equation is equal to the solution found by applying Cimmino's process to the corresponding homogeneous equation. In view of these necessary assumptions, it seemed that the approach used was prudent.

7.6.2.2 On assumptions underlying equations 6-25 The crucial assumptions underlying equations 6-25 are expressed by equations 6-19, and equations 6-21 to 6-24. For equation 6-19, note that to the extent

$$\int_{\text{Actual}} |\varepsilon_f|^2 \approx \int_{\text{Numerical}} |\varepsilon_f|^2 \tag{7-25}$$

we also have

$$\frac{1}{\|\partial S\|} \int |\varepsilon_f|^2 \approx \langle \varepsilon_f^2 \rangle \tag{7-26}$$

Thus, it appears that equation 6-19 is reasonable. For equations 6-21 and 6-22, I will say that I cannot think of a more reasonable way to estimate absolute magnitudes of integration errors: a distinction between real and imaginary parts for Φ and $\vec{A}$ and the spacial components of $\vec{A}$ is not made since the relationship between these constituents may change from that for ω=0 solutions. For equations 6-23 and 6-24, I reasoned that the magnitude of the integration error must be proportional to the magnitude of the integrand; the equations shown seemed a reasonable way to express this dependence. This choice is consistent in the following sense: if equations 6-23 and 6-24 are squared (both sides of the equality squared), imaginary and real equations are summed,

equations are summed over spacial components, and $|\delta_I| \approx <\delta_I>$ is assumed, identities analogous to equations 6-21 and 6-22 result. In equation 6-24a, the same integration error is assumed for all spacial components; averages over all $\vec{x}_f$ should be the same for each spacial component since $\vec{x}_f$ are approximately uniformly distributed over the sphere.

7.6.2.3 Motivations behind simple error estimator used I conclude this section on error estimates with a discussion of the reasons behind assuming an identity matrix in place of the system matrix of equation 6-25. It can be observed from equation 6-20 that if

$$\sqrt{\|\delta S\|} < \sqrt{\int_N |K_1|^2} > \geq 1 \qquad (7\text{-}27)$$

equality in equation 6-20 can never be achieved. This means that if equation 7-27 were the case, analogously, in equations 6-25, there would be no positive definite solutions to the system. It turns out that indeed, this was always the case for at least one constituent of equations 6-25. Writing equations 6-25 in the analogous form

$$\mathbf{I}\vec{\varepsilon} = \vec{\delta} + \mathbf{K}\vec{\varepsilon} \qquad (7\text{-}28)$$

I reasoned that since it was impossible to achieve equality with positive definite $\vec{\varepsilon}$, a legitimate maximum estimate of error would be obtained by finding the following maximum.

$$\underset{\vec{\gamma}}{\mathrm{MAX}}(\mathbf{I} - \vec{\gamma}\mathbf{K})^{-1}\vec{\delta} \quad : \vec{\gamma} \in \text{unit hypercube} \qquad (7\text{-}29)$$

The hope was that a maximum would be found in a small locus about $\vec{\gamma}^{\text{transpose}} = (1, 1, \ldots, 1)$. Unfortunately, I found that $(\mathbf{I} - \vec{\gamma}\mathbf{K})^{-1}\vec{\delta}$ was positive definite for only a very small locus about the origin ($\gamma_i < .15 \; \forall i$) and in addition, a

singularity existed in this locus. In desperation, I tried **K** with all diagonal entries set to zero with no success. It seemed no reasonable error estimate could be obtained using this method.

Taking the hint from the exploration of error estimates as a function of $\vec{\gamma}$, taking $\vec{\gamma}$=0 seemed the best that could be done. This error estimate would be conservative if we were assured that errors superposed constructively; otherwise, perhaps it is an estimate of average error.

8. Results

In this section, I discuss how convergence of the discretized model to the continuous model is to be shown. Convergence results are then presented. The section is concluded with a presentation of estimates for the degree of frequency dependence with error estimates.

8.1 Showing convergence

I propose that convergence of equations 6-9 to solutions of equations 5-4 is strongly supported if it is found that upon increasing interpolated integrator order,

1. interpolated integrators applied to $\omega=0$ solutions are observed to be uniformly convergent,
2. each successive linear system is not ill conditioned, and
3. the derivative of the numerical solutions with respect to interpolated integrator order tends to zero.

8.1.1 Requirement 1

Table 8-1 tabulates integrals for which analytical formulas or semi-analytical formulas are available. The one dimensional integrations that could not be done analytically were estimated using Gauss-Legendre integration. Table 8-2 displays the performance of several interpolated integrators for the case $\vec{x}_f=(R_c, 0°, 0°)$, $\hat{J}=(1, 0°, 0°)$, $\vec{x}_j=(0, 0, 0)$. Only for this case could I calculate integration errors normalized by absolute integrals using only analytical or semi-analytical formula. For terms involving the kernel R, the kernel was interpolated because computations for interpolated integration weights, a very expensive computation, had been completed before terms involving the kernel R were included in the equations.

TABLE 8-1a Integrations of $\omega=0$ solutions over a sphere of radius R_c.

$$\int \Phi = 0$$

$$\int R\Phi = \frac{\begin{bmatrix}\cos\theta_{FT}\\ \sin\theta_{FT}\end{bmatrix}}{4\pi\sigma_{in}}\left(\frac{-24R_c}{15}\right)\hat{n}_{\vec{x}_f}\cdot\vec{J}_r \qquad : \vec{x}_j = (0, 0°, 0°)$$

$$\int \frac{\hat{n}\cdot\hat{R}}{R^2}(\Phi-\Phi_{\vec{x}_f}) = \frac{\begin{bmatrix}\cos\theta_{FT}\\ \sin\theta_{FT}\end{bmatrix}}{4\pi\sigma_{in}}\left(\frac{-4\pi}{R_c^2}\right)\frac{\hat{R}_j\cdot\vec{J}_r}{R_j^2}$$

$$\int \frac{\hat{n}}{R}\Phi = \frac{\begin{bmatrix}\cos\theta_{FT}\\ \sin\theta_{FT}\end{bmatrix}}{4\pi\sigma_{in}}\frac{4\pi R_c}{5}(4\vec{J}_r+3\vec{J}_r\cdot\hat{n}_{\vec{x}_f}\hat{n}_{\vec{x}_f}) \qquad : \vec{x}_j = (0, 0°, 0°)$$

$$\int \vec{A} = \begin{bmatrix}0\\0\\0\end{bmatrix} \qquad : \vec{x}_j = (0, 0°, 0°)$$

$$\int \frac{n_k A_k}{R} = \frac{\mu_0\begin{bmatrix}\cos\theta_{FT}\\ \sin\theta_{FT}\end{bmatrix}}{4\pi}\left(\frac{-16\pi}{175}\right)\vec{J}_r\cdot\hat{n}_{\vec{x}_f}\begin{bmatrix}1\\1\\14/3\end{bmatrix} \qquad : \begin{array}{c}\vec{x}_j = (0, 0°, 0°),\\ \vec{x}_f = (1, 0°, 0°), (1, 180°, 0°),\\ k\in[x, y, z]\end{array}$$

$$\int \frac{\hat{n}\cdot\vec{A}}{R} = \frac{\mu_0\begin{bmatrix}\cos\theta_{FT}\\ \sin\theta_{FT}\end{bmatrix}}{4\pi}\left(\frac{-8\pi}{15}\right)\hat{n}_{\vec{x}_f}\vec{J}_r \qquad : \vec{x}_j = (0, 0°, 0°)$$

TABLE 8-1b Absolute integrations of $\omega=0$ solutions over a sphere of radius R_c.

$$\int |\Phi| = \frac{\begin{bmatrix} |\cos\theta_{FT}| \\ |\sin\theta_{FT}| \end{bmatrix}}{4\pi\sigma_{in}} J_r 6\pi$$

$$\int |R\Phi| = \frac{\begin{bmatrix} |\cos\theta_{FT}| \\ |\sin\theta_{FT}| \end{bmatrix}}{4\pi\sigma_{in}} \frac{8R_c}{5}(1+\sqrt{2}) \qquad : \vec{x}_j = (0, 0°, 0°)$$

$$\int \left| \frac{\hat{n}\cdot\hat{R}}{R^2}(\Phi - \Phi_{\vec{x}_f}) \right| = \frac{\begin{bmatrix} |\cos\theta_{FT}| \\ |\sin\theta_{FT}| \end{bmatrix}}{4\pi\sigma_{in}} \frac{4\pi J_r}{R_c^2} \qquad : \begin{array}{c} \vec{x}_j = (0, 0°, 0°), \\ \vec{x}_f = (1, 0°, 0°), (1, 180°, 0°) \end{array}$$

$$\int \left| \frac{n_k \Phi}{R} \right| = \frac{\begin{bmatrix} |\cos\theta_{FT}| \\ |\sin\theta_{FT}| \end{bmatrix}}{4\pi\sigma_{in}} \frac{12 J_r}{R_c} \left[\begin{array}{c} \left\{ \mp \left(\int_0^{\frac{\pi}{2}} \sqrt{1+\cos\nu}\cos 2\nu \, d\nu - \int_{\frac{\pi}{2}}^{\pi} \sqrt{1+\cos\nu}\cos 2\nu \, d\nu \right) \right\} \\ \left\{ \mp \left(\int_0^{\frac{\pi}{2}} \sqrt{1+\cos\nu}\cos 2\nu \, d\nu - \int_{\frac{\pi}{2}}^{\pi} \sqrt{1+\cos\nu}\cos 2\nu \, d\nu \right) \right\} \\ \frac{7\pi}{15} \end{array} \right]$$

upper sign, $\hat{x}_f = (1, 0°, 0°)$
lower sign, $\hat{x}_f = (1, 180°, 0°)$

$$\approx \int \left| \frac{\hat{n}\cdot\hat{R}}{R^2}(\Phi - \Phi_{\vec{x}_f}) \right| = \frac{\begin{bmatrix} |\cos\theta_{FT}| \\ |\sin\theta_{FT}| \end{bmatrix}}{4\pi\sigma_{in}} \frac{12 J_r}{R_c} \begin{bmatrix} 0.6437902832994915 \\ 0.6437902832994915 \\ \frac{7\pi}{15} \end{bmatrix}$$

$$: \begin{array}{c} \vec{x}_j = (0, 0°, 0°), \\ \vec{J}_r = (J_r, 0°, 0°), \\ \vec{x}_f = (1, 0°, 0°), (1, 180°, 0°) \end{array}$$

TABLE 8-1b continued.

$$\int |\vec{A}| = \frac{\mu_0 \begin{bmatrix} |\cos\theta_{FT}| \\ |\sin\theta_{FT}| \end{bmatrix}}{4\pi} \frac{R_c 8 J_r}{5} \begin{bmatrix} 1 \\ 1 \\ \frac{2\pi}{3\sqrt{3}} \end{bmatrix} \quad : \vec{x}_j = (0, 0°, 0°)$$

$$\int \left| \frac{n_k A_k}{R} \right| = \frac{\mu_0 \begin{bmatrix} |\cos\theta_{FT}| \\ |\sin\theta_{FT}| \end{bmatrix}}{4\pi} \frac{8\pi J_r}{525} \left| \sqrt{2} \begin{bmatrix} 3(\frac{11}{\sqrt{2}}-2) \\ 3(\frac{11}{\sqrt{2}}-2) \\ 2\sqrt{1+\frac{1}{\sqrt{3}}}(23-\frac{13}{\sqrt{3}})+2\sqrt{1-\frac{1}{\sqrt{3}}}(23+\frac{13}{\sqrt{3}}) \\ -37-\frac{23}{\sqrt{2}} \end{bmatrix} \right|$$

$$: \begin{array}{c} \vec{x}_j = (0, 0°, 0°), \\ \vec{J}_r = (J_r, 0°, 0°), \\ \vec{x}_f = (1, 0°, 0°), (1, 180°, 0°) \end{array}$$

$$\int \left| \frac{\hat{n} \bullet \vec{A}}{R} \right| = \frac{\mu_0 \begin{bmatrix} |\cos\theta_{FT}| \\ |\sin\theta_{FT}| \end{bmatrix}}{4\pi} \frac{8\pi}{15\sqrt{2}} (4-\sqrt{2}) \quad : \begin{array}{c} \vec{x}_j = (0, 0°, 0°), \\ \vec{J}_r = (J_r, 0°, 0°), \\ \vec{x}_f = (1, 0°, 0°), (1, 180°, 0°) \end{array}$$

TABLE 8-2 Deviation of interpolated integrators from analytical integrations normalized by the absolute integration.

For vector integrands, the largest deviation taken over all spacial components is reported.

For R kernel, the kernel was interpolated, other kernels were not.

$\vec{x}_j = (0, 0°, 0°)$ $\vec{J}_r = (J_r, 0°, 0°)$ $\hat{x}_f = (1, 0°, 0°)$

Part A Variation with integrator order.
Interpolator is 106 point Wahba with q=2.

number of GL points →	32	72	200	512
integrand ↓				
Φ	$<10^{-14}$	$<10^{-14}$	$<10^{-14}$	$<10^{-14}$
$R\Phi$	6.28(-3)	1.30(-3)	4.17(-3)	8.30(-4)
$\frac{\hat{n}\cdot\hat{R}}{R^2}(\Phi-\Phi_{\vec{x}_f})$	1.94(-3)	4.11(-4)	1.67(-4)	5.08(-5)
$\frac{\hat{n}}{R}\Phi$	3.13(-3)	5.40(-4)	2.77(-4)	1.16(-4)
$\vec{A}$	8.27(-4)	3.83(-4)	1.02(-3)	1.85(-4)
$\frac{n_k A_k}{R}$	1.28(-2)	3.64(-3)	1.06(-3)	3.50(-4)
$\frac{\hat{n}\cdot\vec{A}}{R}$	1.05(-3)	6.54(-4)	2.54(-4)	2.85(-4)

Part B Variation with interpolator order.
Integrator is 288 point GL.

number of Wahba q=3 points →	64	106	156
integrand ↓			
Φ	$<10^{-14}$	$<10^{-14}$	$<10^{-14}$
$R\Phi$	1.74(-3)	7.29(-4)	2.76(-4)
$\frac{\hat{n}\cdot\hat{R}}{R^2}(\Phi-\Phi_{\vec{x}_f})$	2.22(-4)	5.23(-5)	2.96(-5)
$\frac{\hat{n}}{R}\Phi$	4.31(-4)	5.91(-5)	1.32(-5)
$\vec{A}$	2.03(-4)	1.66(-5)	1.19(-4)
$\frac{n_k A_k}{R}$	1.36(-3)	5.69(-4)	6.73(-4)
$\frac{\hat{n}\cdot\vec{A}}{R}$	9.80(-4)	1.06(-4)	2.61(-4)

We would like to know whether or not we can assume that convergence would be similar for untested circumstances. For cases where $\vec{x}_f \neq (R_c, 0°, 0°)$, $\vec{x}_f \neq (R_c, 180°, 0°)$, and/or $\vec{x}_j \neq (0, 0, 0)$, the convergence of interpolated integration can be tested with respect to high order GL or IMT integrators. Considering the observation that the IMT method converges faster than the GL method, doing this would indicate convergence since Atkinsen has proven convergence of the GL method for continuously differentiable functions on the domain of integration. Specifically, using the terminology of equation 6-2a, he showed that

$$\left| \int_{\text{Actual}} - \text{m}^{\text{th}}\,\text{order} \int_{\text{Numerical}} \right| \leq C(2m-1)^{-k} \qquad (8\text{-}1)$$

where f() is k times continuously differentiable on the unit sphere for some constant C. The usefulness of using high order numerical integration to subsitute for analytical formula is supported by noting, from data of table 7-2, that high order integrators are quite accurate compared to lower integration orders. This procedure was used to generate the data of table 8-3 which reports interpolated integrator performance averaged over all interpolation points.

TABLE 8-3 Normalized interpolated integrator errors averaged over all interpolation points.

Comments of table 8-2 apply. Interpolated integrators are also exactly the same.

$\vec{x}_j = (0, 0°, 0°)$ $\vec{J}_r = (J_r, 0°, 0°)$

Part A Variation with integrator order.

number of GL points →	32	72	200	512
integrand ↙				
Φ	$<10^{-14}$	$<10^{-14}$	$<10^{-14}$	$<10^{-14}$
$R\Phi$	2.65(-3)	4.89(-4)	3.85(-4)	5.48(-4)
$\frac{\hat{n}\cdot\hat{R}}{R^2}(\Phi-\Phi_{\vec{x}_j})$	1.08(-3)	2.80(-4)	1.18(-4)	5.65(-6)
$\frac{\hat{n}}{R}\Phi$	4.79(-3)	1.70(-3)	6.33(-4)	2.09(-4)
$\vec{A}$	1.59(-3)	1.44(-3)	1.12(-3)	1.85(-4)
$\frac{n_k A_k}{R}$	1.28(-2)	3.69(-3)	1.16(-3)	3.50(-4)
$\frac{\hat{n}\cdot\vec{A}}{R}$	2.83(-4)	3.15(-4)	2.03(-4)	4.41(-5)

Part B Variation with interpolator order.

number of Wahba q=3 points →	64	106	156
integrand ↙			
Φ	2.96(-6)	$<10^{-14}$	2.52(-6)
$R\Phi$	1.22(-3)	5.49(-4)	2.85(-4)
$\frac{\hat{n}\cdot\hat{R}}{R^2}(\Phi-\Phi_{\vec{x}_j})$	1.82(-4)	4.17(-5)	1.99(-5)
$\frac{\hat{n}}{R}\Phi$	4.62(-4)	2.40(-4)	3.33(-4)
$\vec{A}$	2.03(-4)	5.27(-5)	1.19(-4)
$\frac{n_k A_k}{R}$	1.64(-3)	5.69(-4)	6.78(-4)
$\frac{\hat{n}\cdot\vec{A}}{R}$	7.94(-4)	1.79(-5)	1.46(-4)

Before exploring cases where the source is not centrally located, I would like to discuss convergence results presented thus far. Several cases of table 8-2a, exhibit divergence of the interpolated integrators at the highest order integrator. This observation might be explained by noting that when using a fixed interpolator order, at high enough integrator orders, enough interpolation errors could accumulate to cause interpolated integrator divergence. However, an examination of table 8-3a indicates that for the integrator orders used, this may only happen for the RΦ integrand; note the divergence at integration order 512. How can the sporadic occurrence of poor interpolated integrator performance in table 8-2a be explained given that we have observed smooth convergence of integrators and interpolators? Poor performance observed in tables 8-2b and 8-3b may be a clue. It can be seen that for several integrands, given interpolator order 156, performance is poorer than when using an interpolator order of 106. Yet, we have seen that interpolator accuracy increases with interpolator order. I can think of two effects that may be responsible for this divergence:

- Perhaps opportune cancellation of integrator and interpolator errors occurring at interpolator order 106 do not occur when function values at integration points are estimated more accurately.
- With the understanding that relative positions of integrator points remain fixed but their positions relative to interpolation points changes for integrating at each interpolation point, it could be that for some combination of integration and interpolation points, interpolations, for some integrands, are exceptionally poor or exceptionally good on the average.

A comparison of table 8-4 with table 7-1 indicates that there may be some validity to these two hypotheses. It can be observed that interpolated integrators

actually perform better than straight integrators for low order integrations. This can only happen as a result of opportune cancellation of errors. These cancellations certainly depend on the relative position between interpolation and integration points.

TABLE 8-4 Normalized interpolated integrator errors for the circumstances of table 6-1.

	integrands	$\frac{\hat{n}}{R}(\Phi-\Phi_{\vec{x}_f})$	$\frac{n_k}{R}(A_k-A_k\|_{\vec{x}_f})$	$\frac{\hat{n}\cdot\hat{R}}{R^2}(\Phi-\Phi_{\vec{x}_f})$	$\frac{\hat{n}\cdot\hat{R}}{R^2}(\Phi-\Phi_{\vec{x}_f})$
	source	$\vec{x}_j=(0,0°,0°)$ $\vec{J}_r=(J_r,45°,-135°)$			$\vec{x}_j=(.5,72°,-132°)$
	q=3 Wahba interpolator order				$\vec{J}_r=(J_r,105°,95°)$
288 point GL	64	4.0(-4)	1.1(-3)	1.9(-4)	3.5(-4)
	106	1.6(-4)	4.1(-4)	4.6(-5)	5.9(-5)
	156	2.2(-4)	4.9(-4)	2.6(-5)	6.5(-6)
	GL order				
106 point q=2 Wahba	8	2.9(-3)	1.1(-2)	1.7(-3)	2.5(-3)
	72	1.0(-3)	2.6(-3)	3.6(-4)	2.9(-3)
	200	4.1(-4)	8.9(-4)	1.5(-4)	1.2(-4)
	512	1.3(-4)	2.5(-4)	4.5(-5)	6.1(-5)

In conclusion, tables 8-2 and 8-3 show that interpolated integrators do not exhibit uniform convergence for all integrands; however, data presented does support convergence. Comparison of tables 8-4 and 7-1 shows that, though uniform convergence is not achieved, interpolated integration should still be

the method of choice with respect to TR integrators.

In order to examine integrator performance for non-centrally located sources, a tremendous amount of computation is required since no analytical formula is available for $\vec{A}$. I have done the computations for one set of interpolation points for the purpose of estimating errors ε_I of equations 6-21 to 6-25. Results are shown in table 8-5. Though performance measures for several integrands were not based on analytical formula, the reasoning which follows supports the assertion that performance estimates are reasonable. Considering data of tables 8-2 to 8-4, it is observed that the performance of all integrands differ from that of $\frac{\hat{n}\bullet\hat{R}}{R^2}(\Phi-\Phi_{\vec{x}_i})$ by at most an order of magnitude. It can be observed that this is exactly the case for data of table 8-5. The point is made by noting that $\frac{\hat{n}\bullet\hat{R}}{R^2}(\Phi-\Phi_{\vec{x}_i})$ is an integrand for which analytical solutions are known for all source cases.

TABLE 8-5 Performance profile of interpolated integrator finally used. Integration performance is averaged over all interpolation points, comments of table 8-2 apply.

Interpolator is 156 point Wahba with q=3.
Integrator is 288 point GL.

$\hat{x}_j \rightarrow$	$(0, 0°, 0°)$		$(0.4, 0°, 0°)$		$(0.8, 0°, 0°)$	
$\vec{J}_r \rightarrow$	r	t	r	t	r	t
integrand ↓	r(adial) $\equiv (J_r, 0°, 0°)$		t(angential) $\equiv (J_r, 90°, 0°)$			
Φ	2.52(-6)	1.30(-6)	2.63(-5)	1.53(-5)	4.97(-3)	7.09(-4)
$R\Phi$	2.85(-4)	2.87(-4)	3.12(-4)	2.98(-4)	6.67(-3)	6.67(-3)
$\frac{\hat{n}\cdot\hat{R}}{R^2}(\Phi-\Phi_{\vec{x}_r})$	1.99(-5)	1.86(-5)	4.68(-5)	3.14(-5)	6.73(-3)	9.25(-4)
$\frac{\hat{n}}{R}\Phi$	3.33(-4)	3.44(-4)	8.13(-4)	8.68(-4)	3.19(-2)	1.88(-2)
$\vec{A}$	1.19(-4)	1.36(-4)	9.42(-5)	8.75(-5)	2.00(-3)	8.24(-4)
$\frac{n_k A_k}{R}$	6.78(-4)	6.94(-4)	9.48(-4)	7.69(-4)	4.56(-3)	6.07(-3)
$\frac{\hat{n}\cdot\vec{A}}{R}$	1.46(-4)	1.49(-4)	1.50(-4)	1.54(-4)	7.41(-3)	5.10(-4)

8.1.2 Requirements 2 and 3

The fulfillment of these two requirements was supported by first, increasing integrator order with interpolator order fixed and calculating the average magnitude of the difference between successive solutions and second, increasing interpolator order with integrator order fixed and calculating the average magnitude of the difference between successive solutions at the pole points. Only these two points were common to all interpolators. Table 8-6 displays these differences normalized by the number of points by which the interpolated integrator was increased and the largest of the values resulting from the first normalization. Thus, values reported estimate the magnitude of the first derivative of solutions with repect to interpolated integrator order normalized by the largest value. Note that I have reported values for increasing integrator order with the average taken only over the 2 pole points. The purpose of this is to indicate that such an average does indeed exhibit requirement 3 giving support to trends observed in the sparse data generated by increasing interpolator order. I conclude that fulfillment of requirement 3 has been observed.

TABLE 8-6 Normalized estimates of derivatives of calculated solutions with respect to interpolated integrator order.

function →	interpolated integrator order →	Φ_{re}	Φ_{im}	$\vec{A}_{re}$ x	$\vec{A}_{re}$ y	$\vec{A}_{re}$ z	$\vec{A}_{im}$ x	$\vec{A}_{im}$ y	$\vec{A}_{im}$ z
106 point Wahba with q=2, derivative estimates averaged over all 106 points	32/72 †	1	1	1	1	1	1	1	1
	72/200	.09	.18	.081	.093	.05	.086	.091	.049
	200/512	.012	.018	.0081	.0087	.0019	.0079	.0081	.015
derivative estimates averaged over the two pole points	32/72	1	1	-	-	1	-	-	1
	72/200	.31	- ‡	-	-	.040	-	-	.043
	200/512	.13	-	-	-	.014	-	-	.016
288 point GL average taken over the two pole points	64/106	-	-	1	-	1	1	-	1
	106/156	-	-	.0083	-	.23	.0084	-	.23

† x/y = changing from order x to order y.

‡ the difference between successive solutions was below the resolution of the computer rendering the calculation meaningless.

Would these results say anything about the condition of the successive linear systems? Perceiving the increase of interpolated integrator order as adding a small perturbation to the system matrix corresponding to a lower order interpolated integrator, consider

$$\mathbf{A}_m\vec{x}_m = \vec{b} \tag{8-2a}$$

$$\mathbf{A}_{m+1}\vec{x}_{m+1} = \mathbf{A}_m\vec{x}_{m+1} + \delta_A\vec{x}_{m+1} \tag{8-2b}$$

$$\mathbf{A}_m\vec{x}_{m+1} = \vec{b} - \delta_A\vec{x}_{m+1} \tag{8-2c}$$

where m denotes the order of the lower order interpolated integrator and m+1 that of the higher order interpolated integrator. Then, we see that increasing interpolated integrator order can be perceived as introducing slight perturbations in the constraint vector $\vec{b}$. From this we can say that the results specified above do indicate that successive linear systems are not ill conditioned. There is a bit of a problem with applying this reasoning when increasing the interpolated integrator order results in changing the set of points over which the linear system is constructed; i.e., when interpolator order is increased. This problem can be circumvented by assuming there is a subset of the new set of points that are close or equal to points utilized by the lower order interpolated integrator. Then, there is a submatrix of $\mathbf{A}_{m+1}$ to which we can apply the reasoning above. In conclusion, fulfillment of requirement 2 is supported by data of table 8-6.

8.2 Final measure results

Tables 8-7, located at the end of this section, show a measure similar to equation 6-15 but protected against the possibility of a real, imaginary, or spacial component being identically 0 at all $\vec{x}_f$; i.e.,

$$\sqrt{\frac{\sum_{p}^{N_p}\left\{(\Phi_{re}|_{\omega\neq 0}-\Phi_{re}|_{\omega=0})^2+(\Phi_{im}|_{\omega\neq 0}-\Phi_{im}|_{\omega=0})^2\right\}|_{\vec{x}_p}}{\sum_{p}^{N_p}\left\{(\Phi_{re}|_{\omega=0})^2+(\Phi_{im}|_{\omega=0})^2\right\}|_{\vec{x}_p}}} \qquad (8\text{-}3a)$$

is used for Φ (**S**calar **p**otential) and

$$\sqrt{\frac{\sum_{p}^{N_p}\left\{\sum_{k}^{3}\left[(A_{k_{re}}|_{\omega\neq 0}-A_{k_{re}}|_{\omega=0})^2+(A_{k_{im}}|_{\omega\neq 0}-A_{k_{im}}|_{\omega=0})^2\right]\right\}|_{\vec{x}_p}}{\sum_{p}^{N_p}\left\{\|\vec{A}_{re}|_{\omega=0}\|^2+\|\vec{A}_{im}|_{\omega=0}\|^2\right\}|_{\vec{x}_p}}} \qquad (8\text{-}3b)$$

is used for $\vec{A}$ (**V**ector **p**otential). I also report these measures predicted by two unbounded conductor models with respect to the unbounded conductor model that is frequency independent. For equations 4-21, the corresponding unbounded conductor model is

$$\vec{A}_{\vec{x}_f}=\vec{J}\frac{\mu_0}{4\pi}\frac{1}{R_j}\begin{bmatrix}\cos\theta_{FT}+e_{im}\sin\theta_{FT}\\ \sin\theta_{FT}-e_{im}\cos\theta_{FT}\end{bmatrix} \qquad (8\text{-}4a)$$

$$\Phi_{\vec{x}_f}=-\frac{1}{2\pi\sigma_{in}^2}\frac{\hat{R}_j\bullet\vec{J}}{R_j^2}\begin{bmatrix}\sigma_{in} & \varepsilon_{in}\omega\\ -\varepsilon_{in}\omega & \sigma_{in}\end{bmatrix}\begin{bmatrix}\cos\theta_{FT}+e_{im}\sin\theta_{FT}\\ \sin\theta_{FT}-e_{im}\cos\theta_{FT}\end{bmatrix} \qquad (8\text{-}4b)$$

For equations 4-20, the model is that above with $e_{im}\equiv 0$. Measures 8-3 for unbounded conductors are, for Φ,

$$\sqrt{\frac{\int_S\left(\frac{\hat{R}_j\bullet\vec{J}}{R_j^2}\right)^2\left[(\varepsilon_{in}\omega)^2+e_{im}^2(\sigma_{in}^2+(\varepsilon_{in}\omega)^2)-2\varepsilon_{in}\omega\sigma_{in}e_{im}\right]}{\int_S\sigma^2\left(\frac{\hat{R}_j\bullet\vec{J}}{R_j^2}\right)^2}} \qquad (8\text{-}5a)$$

and for $\vec{A}$,

$$\sqrt{\frac{\int_S \frac{e_{im}^2}{R_j^2}}{\int_S \frac{1}{R_j^2}}} \qquad (8\text{-}5b)$$

These were calculated with a high order IMT integrator.

Figure 8-1 provides a guide to reading the tables. Error intervals were calculated with omission of ε_L terms from equations 6-25 as suggested by the discussion in section 7.3.3. Parameters R_c, σ, ε, and Σl were chosen appropriate for modeling a small brain (SML, table 8-7a), a brain of typical size (MED, table 8-7b), a large brain (LRG, table 8-7c), a typical brain sized cavity filled with cerebral spinal fluid (CSF, table 8-7d), and a typical brain sized conductor consisting of bone (SKL, table 8-7e).

The choices of θ_{FT} were sufficient to investigate the entire possible range $[0, 2\pi]$ since $\theta_{FT}\in[\pi, 2\pi)$ simply introduces an overall (-) sign in $\theta_{FT}\in[0, \pi)$ equations and, for $\theta_{FT}\in[\frac{\pi}{2}, \pi)$, consider the following: ω=0 solutions suggest

$$\vec{A}_{re}\big|_{\theta_{FT}+\frac{\pi}{2}} = -\vec{A}_{im}\big|_{\theta_{FT}} \qquad (8\text{-}6a)$$

$$\vec{A}_{im}\big|_{\theta_{FT}+\frac{\pi}{2}} = \vec{A}_{re}\big|_{\theta_{FT}} \qquad (8\text{-}6b)$$

$$\Phi_{re}\big|_{\theta_{FT}+\frac{\pi}{2}} = -\Phi_{im}\big|_{\theta_{FT}} \qquad (8\text{-}6c)$$

$$\Phi_{im}\big|_{\theta_{FT}+\frac{\pi}{2}} = \Phi_{re}\big|_{\theta_{FT}} \qquad (8\text{-}6d)$$

Inserting these guesses into equations 5-4 appropriate for equations 4-20 evaluated at $\theta_{FT}+\frac{\pi}{2}$ give, using representative notation for source terms and kernels,

$$\begin{bmatrix}-1 & 0\\ 0 & 1\end{bmatrix}\vec{A}_{\substack{re\\im}}\Big|_{\theta_{FT},\vec{x}_t} = \vec{j}\begin{bmatrix}-\sin\theta_{FT}\\ \cos\theta_{FT}\end{bmatrix}$$
$$+\int K_{\vec{A}_1}\begin{bmatrix}1 & -1\\ 1 & 1\end{bmatrix}\begin{bmatrix}-1 & 0\\ 0 & 1\end{bmatrix}\vec{A}_{\substack{re\\im}}\Big|_{\theta_{FT},\vec{x}} - \vec{K}_{\vec{A}_2}\begin{bmatrix}1 & 0\\ 0 & 1\end{bmatrix}\begin{bmatrix}-1 & 0\\ 0 & 1\end{bmatrix}\Phi_{\substack{re\\im}}\Big|_{\theta_{FT},\vec{x}} \qquad (8\text{-}7a)$$

$$\begin{bmatrix}-1 & 0\\ 0 & 1\end{bmatrix}\Phi_{\substack{re\\im}}\Big|_{\theta_{FT},\vec{x}_t} = j\begin{bmatrix}\sigma_{in} & \varepsilon_{in}\omega\\ -\varepsilon_{in}\omega & \sigma_{in}\end{bmatrix}\begin{bmatrix}-\sin\theta_{FT}\\ \cos\theta_{FT}\end{bmatrix}\cdot$$
$$+\int\left(K_{\Phi_1}\begin{bmatrix}1 & -1\\ 1 & 1\end{bmatrix} + K_{\Phi_2}\begin{bmatrix}0 & -1\\ 1 & 0\end{bmatrix} + K_{\Phi_3}\begin{bmatrix}1 & 0\\ 0 & 1\end{bmatrix}\right)\begin{bmatrix}-1 & 0\\ 0 & 1\end{bmatrix}\Phi_{\substack{re\\im}}\Big|_{\theta_{FT},\vec{x}} \qquad (8\text{-}7b)$$

showing that, indeed, equations 8-6 are solutions to the $\theta_{FT}+\frac{\pi}{2}$ equations. Thus only $\theta_{FT}\in[0, \frac{\pi}{2})$ need be considered.

Figure 8-1, below, is a guide to reading tables 8-7.

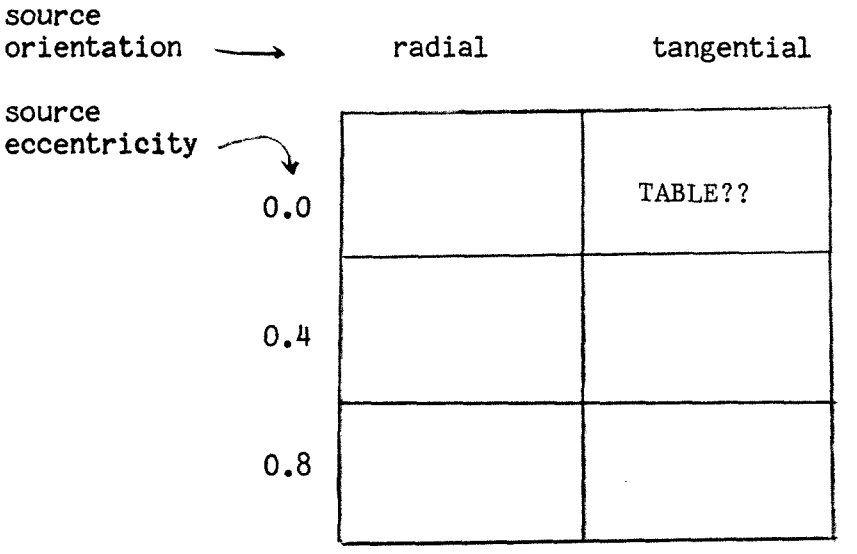

Within each block, the format is

R_c σ_{in} $\varepsilon_{in}\omega$ Σl $\frac{\omega}{2\pi}$

$\hat{x}_j$ $\vec{J}_r$

$\Phi_{\text{measure, unbounded (equation 8-5a)}} \mid e_{im}\neq 0$ $\vec{A}_{\text{measure, unbounded (equation 8-5b)}} \mid e_{im}\neq 0$

$\Phi_{\text{measure, unbounded (equation 8-5a)}} \mid e_{im}=0$ $\vec{A}_{\text{measure, unbounded (equation 8-5b)}} \mid e_{im}=0$

θ_{FT}

$\Phi_{\text{measure, bounded (equation 8-3a)}}$:	lower bound	estimate	upper bound
$\vec{A}_{\text{measure, bounded (equation 8-3b)}}$:	lower bound	estimate	upper bound

θ_{FT}

.

.

.

etc.

figure 8-1

TABLE 8-7a$_0$

```
0.04 0.17 0.00044 0.00015 50
0 0 0  5 0 0
Sp 0.002820   Vp 0.000232
Sp 0.002588   Vp 0.000000
0
        lwrest    errest    upr errest
Sp      0.001421  0.001646  0.001882
Vp      0.001925  0.002419  0.003009
22
        lwrest    errest    upr errest
Sp      0.000000  0.000000  0.000266
Vp      0.000000  0.000000  0.000762
45
        lwrest    errest    upr errest
Sp      0.000000  0.000000  0.000266
Vp      0.000000  0.000000  0.000762
68
        lwrest    errest    upr errest
Sp      0.000000  0.000002  0.000267
Vp      0.000709  0.001176  0.001808
```

```
0.04 0.17 0.00044 0.00015 50
0.4 0 0  5 0 0
Sp 0.002772   Vp 0.000225
Sp 0.002588   Vp 0.000000
0
        lwrest    errest    upr errest
Sp      0.001740  0.001895  0.002065
Vp      0.001759  0.002167  0.002720
22
        lwrest    errest    upr errest
Sp      0.000000  0.000000  0.000232
Vp      0.000000  0.000000  0.000915
45
        lwrest    errest    upr errest
Sp      0.000000  0.000000  0.000232
Vp      0.000000  0.000000  0.000915
68
        lwrest    errest    upr errest
Sp      0.000000  0.000003  0.000233
Vp      0.000699  0.001082  0.001715
```

```
0.04 0.17 0.00044 0.00015 50
0.4 0 0  5 90 0
Sp 0.002790   Vp 0.000225
Sp 0.002588   Vp 0.000000
0
        lwrest    errest    upr errest
Sp      0.001663  0.001837  0.002023
Vp      0.000782  0.001149  0.001732
22
        lwrest    errest    upr errest
Sp      0.000000  0.000000  0.000240
Vp      0.000000  0.000000  0.000864
45
        lwrest    errest    upr errest
Sp      0.000000  0.000000  0.000240
Vp      0.000000  0.000000  0.000864
68
        lwrest    errest    upr errest
Sp      0.000000  0.000002  0.000241
Vp      0.000000  0.000008  0.000867
```

```
0.04 0.17 0.00044 0.00015 50
0.8 0 0  5 0 0
Sp 0.002669   Vp 0.000200
Sp 0.002588   Vp 0.000000
0
        lwrest    errest    upr errest
Sp      0.002552  0.002842  0.003830
Vp      0.000000  0.000011  0.038207
22
        lwrest    errest    upr errest
Sp      0.000000  0.000000  0.001887
Vp      0.000000  0.000000  0.038414
45
        lwrest    errest    upr errest
Sp      0.000000  0.000000  0.001887
Vp      0.000000  0.000000  0.038414
68
        lwrest    errest    upr errest
Sp      0.000000  0.000004  0.001888
Vp      0.000000  0.000006  0.038310
```

```
0.04 0.17 0.00044 0.00015 50
0.8 0 0  5 90 0
Sp 0.002695   Vp 0.000200
Sp 0.002588   Vp 0.000000
0
        lwrest    errest    upr errest
Sp      0.001994  0.002593  0.003825
Vp      0.000001  0.000012  0.019448
22
        lwrest    errest    upr errest
Sp      0.000000  0.000000  0.001931
Vp      0.000000  0.000001  0.019539
45
        lwrest    errest    upr errest
Sp      0.000000  0.000000  0.001931
Vp      0.000000  0.000001  0.019539
68
        lwrest    errest    upr errest
Sp      0.000000  0.000003  0.001932
Vp      0.000000  0.000006  0.019493
```

0.04 0.17 0.0011 0.00015 500
0 0 0 5 0 0
Sp 0.007205 Vp 0.000735
Sp 0.006471 Vp 0.000000
0

	lwrest	errest	upr errest
Sp	0.004676	0.004935	0.005198
Vp	0.004190	0.004700	0.005265

22

	lwrest	errest	upr errest
Sp	0.000000	0.000000	0.000301
Vp	0.000000	0.000001	0.000764

45

	lwrest	errest	upr errest
Sp	0.000000	0.000000	0.000301
Vp	0.000000	0.000000	0.000764

68

	lwrest	errest	upr errest
Sp	0.001392	0.001646	0.001914
Vp	0.001845	0.002341	0.002934

TABLE 8-7a$_1$

0.04 0.17 0.0011 0.00015 500
0.4 0 0 5 0 0
Sp 0.007052 Vp 0.000714
Sp 0.006471 Vp 0.000000
0

	lwrest	errest	upr errest
Sp	0.005495	0.005679	0.005870
Vp	0.003933	0.004349	0.004847

22

	lwrest	errest	upr errest
Sp	0.000000	0.000000	0.000268
Vp	0.000000	0.000001	0.000916

45

	lwrest	errest	upr errest
Sp	0.000000	0.000000	0.000268
Vp	0.000000	0.000001	0.000916

68

	lwrest	errest	upr errest
Sp	0.001717	0.001895	0.002092
Vp	0.001760	0.002169	0.002723

0.04 0.17 0.0011 0.00015 500
0.4 0 0 5 90 0
Sp 0.007109 Vp 0.000714
Sp 0.006471 Vp 0.000000
0

	lwrest	errest	upr errest
Sp	0.005302	0.005505	0.005714
Vp	0.001917	0.002303	0.002814

22

	lwrest	errest	upr errest
Sp	0.000000	0.000000	0.000276
Vp	0.000000	0.000001	0.000865

45

	lwrest	errest	upr errest
Sp	0.000000	0.000000	0.000276
Vp	0.000000	0.000001	0.000865

68

	lwrest	errest	upr errest
Sp	0.001638	0.001837	0.002052
Vp	0.000783	0.001150	0.001734

0.04 0.17 0.0011 0.00015 500
0.8 0 0 5 0 0
Sp 0.006728 Vp 0.000632
Sp 0.006471 Vp 0.000000
0

	lwrest	errest	upr errest
Sp	0.005299	0.005680	0.006681
Vp	0.000000	0.001526	0.038709

22

	lwrest	errest	upr errest
Sp	0.000000	0.000000	0.002269
Vp	0.000000	0.000001	0.038429

45

	lwrest	errest	upr errest
Sp	0.000000	0.000000	0.002269
Vp	0.000000	0.000001	0.038429

68

	lwrest	errest	upr errest
Sp	0.002506	0.002843	0.004104
Vp	0.000000	0.000012	0.038221

0.04 0.17 0.0011 0.00015 500
0.8 0 0 5 90 0
Sp 0.006810 Vp 0.000632
Sp 0.006471 Vp 0.000000
0

	lwrest	errest	upr errest
Sp	0.006889	0.007769	0.009108
Vp	0.000048	0.001862	0.020116

22

	lwrest	errest	upr errest
Sp	0.000000	0.000000	0.002522
Vp	0.000000	0.000002	0.019547

45

	lwrest	errest	upr errest
Sp	0.000000	0.000000	0.002522
Vp	0.000000	0.000002	0.019547

68

	lwrest	errest	upr errest
Sp	0.001851	0.002593	0.004305
Vp	0.000000	0.000011	0.019455

```
0.04 0.17 0.0018 0.00015 1000
0 0 0  5 0 0
Sp 0.011629   Vp 0.001041
Sp 0.010588   Vp 0.000000
0
       lwrest    errest    upr errest
Sp     0.009581  0.009857  0.010136
Vp     0.007440  0.007956  0.008506
22
       lwrest    errest    upr errest
Sp     0.000000  0.000000  0.000322
Vp     0.000000  0.000001  0.000765
45
       lwrest    errest    upr errest
Sp     0.000000  0.000000  0.000322
Vp     0.000000  0.000001  0.000765
68
       lwrest    errest    upr errest
Sp     0.003016  0.003291  0.003574
Vp     0.002952  0.003457  0.004034
```

TABLE 8-7a$_2$

```
0.04 0.17 0.0018 0.00015 1000
0.4 0 0  5 0 0
Sp 0.011412   Vp 0.001011
Sp 0.010588   Vp 0.000000
0
       lwrest    errest    upr errest
Sp     0.011141  0.011341  0.011545
Vp     0.008311  0.008727  0.009192
22
       lwrest    errest    upr errest
Sp     0.000000  0.000000  0.000290
Vp     0.000000  0.000001  0.000917
45
       lwrest    errest    upr errest
Sp     0.000000  0.000000  0.000290
Vp     0.000000  0.000001  0.000917
68
       lwrest    errest    upr errest
Sp     0.003590  0.003788  0.003997
Vp     0.002844  0.003258  0.003778
```

```
0.04 0.17 0.0018 0.00015 1000
0.4 0 0  5 90 0
Sp 0.011493   Vp 0.001011
Sp 0.010588   Vp 0.000000
0
       lwrest    errest    upr errest
Sp     0.008946  0.009166  0.009389
Vp     0.004216  0.004608  0.005071
22
       lwrest    errest    upr errest
Sp     0.000000  0.000000  0.000298
Vp     0.000000  0.000001  0.000866
45
       lwrest    errest    upr errest
Sp     0.000000  0.000000  0.000298
Vp     0.000000  0.000001  0.000866
68
       lwrest    errest    upr errest
Sp     0.003454  0.003672  0.003899
Vp     0.001912  0.002300  0.002813
```

```
0.04 0.17 0.0018 0.00015 1000
0.8 0 0  5 0 0
Sp 0.010953   Vp 0.000895
Sp 0.010588   Vp 0.000000
0
       lwrest    errest    upr errest
Sp     0.010860  0.011344  0.012277
Vp     0.000554  0.004578  0.039853
22
       lwrest    errest    upr errest
Sp     0.000000  0.000000  0.002501
Vp     0.000000  0.000002  0.038438
45
       lwrest    errest    upr errest
Sp     0.000000  0.000000  0.002501
Vp     0.000000  0.000002  0.038438
68
       lwrest    errest    upr errest
Sp     0.002479  0.002843  0.004278
Vp     0.000000  0.000012  0.038230
```

```
0.04 0.17 0.0018 0.00015 1000
0.8 0 0  5 90 0
Sp 0.011069   Vp 0.000895
Sp 0.010588   Vp 0.000000
0
       lwrest    errest    upr errest
Sp     0.011887  0.012929  0.014358
Vp     0.001021  0.003725  0.020929
22
       lwrest    errest    upr errest
Sp     0.000000  0.000000  0.002880
Vp     0.000000  0.000003  0.019552
45
       lwrest    errest    upr errest
Sp     0.000000  0.000000  0.002880
Vp     0.000000  0.000003  0.019552
68
       lwrest    errest    upr errest
Sp     0.004247  0.005182  0.006895
Vp     0.000000  0.000017  0.019413
```

TABLE 8-7a$_3$

```
0.04 0.17 0.0056 0.00015 10000
0 0 0  5 0 0
Sp 0.036262   Vp 0.003321
Sp 0.032941   Vp 0.000000
0
        lwrest    errest    upr errest
Sp      0.027371  0.027774  0.028179
Vp      0.016066  0.016562  0.017076
22
        lwrest    errest    upr errest
Sp      0.000000  0.000000  0.000477
Vp      0.000000  0.000005  0.000774
45
        lwrest    errest    upr errest
Sp      0.000000  0.000000  0.000477
Vp      0.000000  0.000003  0.000773
68
        lwrest    errest    upr errest
Sp      0.011074  0.011483  0.011896
Vp      0.007366  0.007881  0.008431
```

```
0.04 0.17 0.0056 0.00015 10000
0.4 0 0  5 0 0
Sp 0.035570   Vp 0.003226
Sp 0.032941   Vp 0.000000
0
        lwrest    errest    upr errest
Sp      0.031617  0.031924  0.032234
Vp      0.023955  0.024371  0.024811
22
        lwrest    errest    upr errest
Sp      0.000000  0.000000  0.000452
Vp      0.000000  0.000003  0.000924
45
        lwrest    errest    upr errest
Sp      0.000000  0.000000  0.000452
Vp      0.000000  0.000003  0.000924
68
        lwrest    errest    upr errest
Sp      0.012900  0.013210  0.013528
Vp      0.008340  0.008761  0.009231
```

```
0.04 0.17 0.0056 0.00015 10000
0.4 0 0  5 90 0
Sp 0.035829   Vp 0.003226
Sp 0.032941   Vp 0.000000
0
        lwrest    errest    upr errest
Sp      0.030618  0.030950  0.031285
Vp      0.026121  0.026520  0.026936
22
        lwrest    errest    upr errest
Sp      0.000000  0.000000  0.000458
Vp      0.000000  0.000003  0.000871
45
        lwrest    errest    upr errest
Sp      0.000000  0.000000  0.000458
Vp      0.000000  0.000003  0.000871
68
        lwrest    errest    upr errest
Sp      0.012468  0.012805  0.013148
Vp      0.005383  0.005778  0.006234
```

```
0.04 0.17 0.0056 0.00015 10000
0.8 0 0  5 0 0
Sp 0.034106   Vp 0.002855
Sp 0.032941   Vp 0.000000
0
        lwrest    errest    upr errest
Sp      0.038455  0.039394  0.040716
Vp      0.014963  0.023185  0.050453
22
        lwrest    errest    upr errest
Sp      0.000000  0.000000  0.004225
Vp      0.000000  0.000005  0.038505
45
        lwrest    errest    upr errest
Sp      0.000000  0.000000  0.004225
Vp      0.000000  0.000005  0.038505
68
        lwrest    errest    upr errest
Sp      0.013421  0.014163  0.015837
Vp      0.001331  0.006121  0.040571
```

```
0.04 0.17 0.0056 0.00015 10000
0.8 0 0  5 90 0
Sp 0.034476   Vp 0.002855
Sp 0.032941   Vp 0.000000
0
        lwrest    errest    upr errest
Sp      0.036446  0.038479  0.041005
Vp      0.020553  0.026038  0.037427
22
        lwrest    errest    upr errest
Sp      0.000000  0.000000  0.005531
Vp      0.000000  0.000009  0.019589
45
        lwrest    errest    upr errest
Sp      0.000000  0.000000  0.005531
Vp      0.000000  0.000009  0.019588
68
        lwrest    errest    upr errest
Sp      0.013592  0.015486  0.018450
Vp      0.002411  0.005594  0.021952
```

TABLE 8-7b$_0$

```
0.08 0.17 0.00044 0.00015 50
0 0 0  5 0 0
Sp 0.003052   Vp 0.000464
Sp 0.002588   Vp 0.000000
0
       lwrest    errest    upr errest
Sp     0.001381  0.001646  0.001926
Vp     0.001817  0.002312  0.002907
22
       lwrest    errest    upr errest
Sp     0.000000  0.000000  0.000315
Vp     0.000000  0.000001  0.000765
45
       lwrest    errest    upr errest
Sp     0.000000  0.000000  0.000315
Vp     0.000000  0.000000  0.000764
68
       lwrest    errest    upr errest
Sp     0.000000  0.000002  0.000316
Vp     0.000662  0.001127  0.001764
```

```
0.08 0.17 0.00044 0.00015 50
0.4 0 0  5 0 0
Sp 0.002956   Vp 0.000451
Sp 0.002588   Vp 0.000000
0
       lwrest    errest    upr errest
Sp     0.001708  0.001895  0.002103
Vp     0.001760  0.002169  0.002724
22
       lwrest    errest    upr errest
Sp     0.000000  0.000000  0.000283
Vp     0.000000  0.000001  0.000917
45
       lwrest    errest    upr errest
Sp     0.000000  0.000000  0.000283
Vp     0.000000  0.000001  0.000917
68
       lwrest    errest    upr errest
Sp     0.000000  0.000003  0.000285
Vp     0.000699  0.001084  0.001719
```

```
0.08 0.17 0.00044 0.00015 50
0.4 0 0  5 90 0
Sp 0.002992   Vp 0.000451
Sp 0.002588   Vp 0.000000
0
       lwrest    errest    upr errest
Sp     0.001628  0.001837  0.002063
Vp     0.000783  0.001151  0.001735
22
       lwrest    errest    upr errest
Sp     0.000000  0.000000  0.000290
Vp     0.000000  0.000001  0.000865
45
       lwrest    errest    upr errest
Sp     0.000000  0.000000  0.000290
Vp     0.000000  0.000001  0.000865
68
       lwrest    errest    upr errest
Sp     0.000000  0.000003  0.000292
Vp     0.000000  0.000008  0.000868
```

```
0.08 0.17 0.00044 0.00015 50
0.8 0 0  5 0 0
Sp 0.002752   Vp 0.000399
Sp 0.002588   Vp 0.000000
0.
       lwrest    errest    upr errest
Sp     0.002488  0.002843  0.004218
Vp     0.000000  0.000012  0.038227
22
       lwrest    errest    upr errest
Sp     0.000000  0.000000  0.002422
Vp     0.000000  0.000002  0.038435
45
       lwrest    errest    upr errest
Sp     0.000000  0.000000  0.002422
Vp     0.000000  0.000002  0.038435
68
       lwrest    errest    upr errest
Sp     0.000000  0.000009  0.002428
Vp     0.000000  0.000007  0.038331
```

```
0.08 0.17 0.00044 0.00015 50
0.8 0 0  5 90 0
Sp 0.002803   Vp 0.000399
Sp 0.002588   Vp 0.000000
0
       lwrest    errest    upr errest
Sp     0.001796  0.002593  0.004504
Vp     0.000002  0.000011  0.019457
22
       lwrest    errest    upr errest
Sp     0.000000  0.000000  0.002758
Vp     0.000000  0.000003  0.019550
45
       lwrest    errest    upr errest
Sp     0.000000  0.000000  0.002758
Vp     0.000000  0.000003  0.019550
68
       lwrest    errest    upr errest
Sp     0.000000  0.000003  0.002760
Vp     0.000000  0.000006  0.019503
```

TABLE 8-7b$_1$

0.08 0.17 0.0011 0.00015 500
0 0 0 5 0 0
Sp 0.007939 Vp 0.001468
Sp 0.006471 Vp 0.000000
0

	lwrest	errest	upr errest
Sp	0.004540	0.004929	0.005328
Vp	0.003604	0.004096	0.004656

22

	lwrest	errest	upr errest
Sp	0.000000	0.000000	0.000455
Vp	0.000000	0.000004	0.000773

45

	lwrest	errest	upr errest
Sp	0.000000	0.000000	0.000455
Vp	0.000000	0.000003	0.000772

68

	lwrest	errest	upr errest
Sp	0.001267	0.001643	0.002051
Vp	0.001562	0.002047	0.002648

0.08 0.17 0.0011 0.00015 500
0.4 0 0 5 0 0
Sp 0.007637 Vp 0.001426
Sp 0.006471 Vp 0.000000
0

	lwrest	errest	upr errest
Sp	0.005381	0.005673	0.005980
Vp	0.003937	0.004357	0.004860

22

	lwrest	errest	upr errest
Sp	0.000000	0.000000	0.000429
Vp	0.000000	0.000003	0.000923

45

	lwrest	errest	upr errest
Sp	0.000000	0.000000	0.000429
Vp	0.000000	0.000003	0.000923

68

	lwrest	errest	upr errest
Sp	0.001618	0.001892	0.002213
Vp	0.001761	0.002174	0.002734

0.08 0.17 0.0011 0.00015 500
0.4 0 0 5 90 0
Sp 0.007749 Vp 0.001426
Sp 0.006471 Vp 0.000000
0

	lwrest	errest	upr errest
Sp	0.005180	0.005498	0.005830
Vp	0.001920	0.002308	0.002823

22

	lwrest	errest	upr errest
Sp	0.000000	0.000000	0.000435
Vp	0.000000	0.000003	0.000870

45

	lwrest	errest	upr errest
Sp	0.000000	0.000000	0.000435
Vp	0.000000	0.000003	0.000870

68

	lwrest	errest	upr errest
Sp	0.001527	0.001833	0.002178
Vp	0.000784	0.001154	0.001741

0.08 0.17 0.0011 0.00015 500
0.8 0 0 5 0 0
Sp 0.006990 Vp 0.001263
Sp 0.006471 Vp 0.000000
0

	lwrest	errest	upr errest
Sp	0.005082	0.005678	0.007760
Vp	0.000002	0.001531	0.038775

22

	lwrest	errest	upr errest
Sp	0.000000	0.000000	0.003967
Vp	0.000000	0.000004	0.038494

45

	lwrest	errest	upr errest
Sp	0.000000	0.000000	0.003967
Vp	0.000000	0.000004	0.038494

68

	lwrest	errest	upr errest
Sp	0.000000	0.000027	0.003986
Vp	0.000000	0.000008	0.038389

0.08 0.17 0.0011 0.00015 500
0.8 0 0 5 90 0
Sp 0.007152 Vp 0.001263
Sp 0.006471 Vp 0.000000
0

	lwrest	errest	upr errest
Sp	0.003671	0.005175	0.008672
Vp	0.000009	0.000017	0.019439

22

	lwrest	errest	upr errest
Sp	0.000000	0.000000	0.005142
Vp	0.000000	0.000008	0.019583

45

	lwrest	errest	upr errest
Sp	0.000000	0.000000	0.005142
Vp	0.000000	0.000008	0.019582

68

	lwrest	errest	upr errest
Sp	0.001319	0.002588	0.006645
Vp	0.000000	0.000013	0.019487

TABLE 8-7b$_2$

```
0.08 0.17 0.0018 0.00015 1000
0 0 0  5 0 0
Sp 0.012667   Vp 0.002079
Sp 0.010588   Vp 0.000000
0
       lwrest    errest    upr errest
Sp     0.006100  0.006561  0.007033
Vp     0.004385  0.004845  0.005370
22
       lwrest    errest    upr errest
Sp     0.000000  0.000000  0.000540
Vp     0.000000  0.000007  0.000778
45
       lwrest    errest    upr errest
Sp     0.000000  0.000000  0.000540
Vp     0.000000  0.000005  0.000777
68
       lwrest    errest    upr errest
Sp     0.002825  0.003282  0.003760
Vp     0.002413  0.002926  0.003523
```

```
0.08 0.17 0.0018 0.00015 1000
0.4 0 0  5 0 0
Sp 0.012239   Vp 0.002020
Sp 0.010588   Vp 0.000000
0
       lwrest    errest    upr errest
Sp     0.009082  0.009435  0.009801
Vp     0.006131  0.006555  0.007039
22
       lwrest    errest    upr errest
Sp     0.000000  0.000000  0.000517
Vp     0.000000  0.000004  0.000926
45
       lwrest    errest    upr errest
Sp     0.000000  0.000000  0.000517
Vp     0.000000  0.000004  0.000926
68
       lwrest    errest    upr errest
Sp     0.003435  0.003777  0.004155
Vp     0.002845  0.003266  0.003793
```

```
0.08 0.17 0.0018 0.00015 1000
0.4 0 0  5 90 0
Sp 0.012399   Vp 0.002020
Sp 0.010588   Vp 0.000000
0
       lwrest    errest    upr errest
Sp     0.006936  0.007318  0.007715
Vp     0.003068  0.003462  0.003949
22
       lwrest    errest    upr errest
Sp     0.000000  0.000000  0.000523
Vp     0.000000  0.000004  0.000873
45
       lwrest    errest    upr errest
Sp     0.000000  0.000000  0.000523
Vp     0.000000  0.000004  0.000873
68
       lwrest    errest    upr errest
Sp     0.001466  0.001829  0.002248
Vp     0.000783  0.001155  0.001744
```

```
0.08 0.17 0.0018 0.00015 1000
0.8 0 0  5 0 0
Sp 0.011323   Vp 0.001788
Sp 0.010588   Vp 0.000000
0
       lwrest    errest    upr errest
Sp     0.010534  0.011329  0.013498
Vp     0.000548  0.004588  0.039954
22
       lwrest    errest    upr errest
Sp     0.000000  0.000000  0.004906
Vp     0.000000  0.000005  0.038530
45
       lwrest    errest    upr errest
Sp     0.000000  0.000000  0.004906
Vp     0.000000  0.000005  0.038530
68
       lwrest    errest    upr errest
Sp     0.002232  0.002837  0.006282
Vp     0.000000  0.000014  0.038320
```

```
0.08 0.17 0.0018 0.00015 1000
0.8 0 0  5 90 0
Sp 0.011553   Vp 0.001788
Sp 0.010588   Vp 0.000000
0
       lwrest    errest    upr errest
Sp     0.008239  0.010325  0.014343
Vp     0.001013  0.003729  0.021029
22
       lwrest    errest    upr errest
Sp     0.000000  0.000000  0.006588
Vp     0.000000  0.000011  0.019603
45
       lwrest    errest    upr errest
Sp     0.000000  0.000000  0.006588
Vp     0.000000  0.000011  0.019602
68
       lwrest    errest    upr errest
Sp     0.001090  0.002583  0.008007
Vp     0.000000  0.000015  0.019506
```

TABLE 8-7b$_3$

```
0.08 0.17 0.0056 0.00015 10000
0 0 0  5 0 0
Sp 0.039562   Vp 0.006620
Sp 0.032941   Vp 0.000000
0
       lwrest    errest    upr errest
Sp     0.003840  0.004808  0.005847
Vp     0.005506  0.005657  0.005903
22
       lwrest    errest    upr errest
Sp     0.000000  0.000000  0.001167
Vp     0.000000  0.000022  0.000812
45
       lwrest    errest    upr errest
Sp     0.000000  0.000000  0.001167
Vp     0.000000  0.000015  0.000808
68
       lwrest    errest    upr errest
Sp     0.000697  0.001584  0.002660
Vp     0.002511  0.002805  0.003247
```

```
0.08 0.17 0.0056 0.00015 10000
0.4 0 0  5 0 0
Sp 0.038201   Vp 0.006430
Sp 0.032941   Vp 0.000000
0
       lwrest    errest    upr errest
Sp     0.017684  0.018469  0.019290
Vp     0.014837  0.015284  0.015763
22
       lwrest    errest    upr errest
Sp     0.000000  0.000000  0.001172
Vp     0.000000  0.000007  0.000951
45
       lwrest    errest    upr errest
Sp     0.000000  0.000000  0.001172
Vp     0.000000  0.000007  0.000951
68
       lwrest    errest    upr errest
Sp     0.002973  0.003680  0.004570
Vp     0.002797  0.003235  0.003785
```

```
0.08 0.17 0.0056 0.00015 10000
0.4 0 0  5 90 0
Sp 0.038708   Vp 0.006430
Sp 0.032941   Vp 0.000000
0
       lwrest    errest    upr errest
Sp     0.013473  0.014322  0.015208
Vp     0.008762  0.009175  0.009632
22
       lwrest    errest    upr errest
Sp     0.000000  0.000000  0.001171
Vp     0.000000  0.000008  0.000891
45
       lwrest    errest    upr errest
Sp     0.000000  0.000000  0.001171
Vp     0.000000  0.000008  0.000891
68
       lwrest    errest    upr errest
Sp     0.001028  0.001766  0.002753
Vp     0.000758  0.001139  0.001746
```

```
0.08 0.17 0.0056 0.00015 10000
0.8 0 0  5 0 0
Sp 0.035286   Vp 0.005688
Sp 0.032941   Vp 0.000000
0
       lwrest    errest    upr errest
Sp     0.044971  0.046961  0.051077
Vp     0.024105  0.033819  0.058883
22
       lwrest    errest    upr errest
Sp     0.000000  0.000000  0.011920
Vp     0.000000  0.000015  0.038795
45
       lwrest    errest    upr errest
Sp     0.000000  0.000000  0.011920
Vp     0.000000  0.000015  0.038794
68
       lwrest    errest    upr errest
Sp     0.006807  0.008339  0.016082
Vp     0.000000  0.003023  0.039619
```

```
0.08 0.17 0.0056 0.00015 10000
0.8 0 0  5 90 0
Sp 0.036018   Vp 0.005688
Sp 0.032941   Vp 0.000000
0
       lwrest    errest    upr errest
Sp     0.024733  0.030221  0.040289
Vp     0.014985  0.020309  0.032770
22
       lwrest    errest    upr errest
Sp     0.000000  0.000000  0.017317
Vp     0.000000  0.000032  0.019747
45
       lwrest    errest    upr errest
Sp     0.000000  0.000000  0.017317
Vp     0.000000  0.000032  0.019744
68
       lwrest    errest    upr errest
Sp     0.001574  0.005028  0.019875
Vp     0.000000  0.000048  0.019603
```

TABLE 8-7c_0

0.12 0.17 0.00044 0.00015 50
0 0 0 5 0 0
Sp 0.003284 Vp 0.000696
Sp 0.002588 Vp 0.000000
0

	lwrest	errest	upr errest
Sp	0.001315	0.001645	0.001999
Vp	0.001661	0.002148	0.002745

22

	lwrest	errest	upr errest
Sp	0.000000	0.000000	0.000396
Vp	0.000000	0.000003	0.000770

45

	lwrest	errest	upr errest
Sp	0.000000	0.000000	0.000396
Vp	0.000000	0.000002	0.000769

68

	lwrest	errest	upr errest
Sp	0.000000	0.000003	0.000398
Vp	0.000597	0.001051	0.001692

0.12 0.17 0.00044 0.00015 50
0.4 0 0 5 0 0
Sp 0.003142 Vp 0.000676
Sp 0.002588 Vp 0.000000
0

	lwrest	errest	upr errest
Sp	0.001655	0.001893	0.002167
Vp	0.001761	0.002172	0.002730

22

	lwrest	errest	upr errest
Sp	0.000000	0.000000	0.000368
Vp	0.000000	0.000002	0.000920

45

	lwrest	errest	upr errest
Sp	0.000000	0.000000	0.000368
Vp	0.000000	0.000002	0.000920

68

	lwrest	errest	upr errest
Sp	0.000000	0.000005	0.000371
Vp	0.000699	0.001086	0.001723

0.12 0.17 0.00044 0.00015 50
0.4 0 0 5 90 0
Sp 0.003194 Vp 0.000676
Sp 0.002588 Vp 0.000000
0

	lwrest	errest	upr errest
Sp	0.001570	0.001835	0.002130
Vp	0.000784	0.001153	0.001739

22

	lwrest	errest	upr errest
Sp	0.000000	0.000000	0.000374
Vp	0.000000	0.000002	0.000868

45

	lwrest	errest	upr errest
Sp	0.000000	0.000000	0.000374
Vp	0.000000	0.000002	0.000868

68

	lwrest	errest	upr errest
Sp	0.000000	0.000003	0.000376
Vp	0.000000	0.000007	0.000870

0.12 0.17 0.00044 0.00015 50
0.8 0 0 5 0 0
Sp 0.002835 Vp 0.000598
Sp 0.002588 Vp 0.000000
0

	lwrest	errest	upr errest
Sp	0.002387	0.002842	0.004924
Vp	0.000001	0.001523	0.038854

22

	lwrest	errest	upr errest
Sp	0.000000	0.000000	0.003317
Vp	0.000000	0.000003	0.038469

45

	lwrest	errest	upr errest
Sp	0.000000	0.000000	0.003317
Vp	0.000000	0.000003	0.038469

68

	lwrest	errest	upr errest
Sp	0.000000	0.000018	0.003330
Vp	0.000000	0.000008	0.038364

0.12 0.17 0.00044 0.00015 50
0.8 0 0 5 90 0
Sp 0.002912 Vp 0.000598
Sp 0.002588 Vp 0.000000
0

	lwrest	errest	upr errest
Sp	0.001503	0.002591	0.005724
Vp	0.000005	0.000012	0.019473

22

	lwrest	errest	upr errest
Sp	0.000000	0.000000	0.004141
Vp	0.000000	0.000006	0.019569

45

	lwrest	errest	upr errest
Sp	0.000000	0.000000	0.004141
Vp	0.000000	0.000006	0.019569

68

	lwrest	errest	upr errest
Sp	0.000000	0.000004	0.004143
Vp	0.000000	0.000007	0.019521

TABLE 8-7c$_1$

```
0.12 0.17 0.0011 0.00015 500
0 0 0  5 0 0
Sp 0.008671   Vp 0.002201
Sp 0.006471   Vp 0.000000
0
       lwrest    errest    upr errest
Sp     0.001056  0.001629  0.002276
Vp     0.001689  0.001955  0.002427
22
       lwrest    errest    upr errest
Sp     0.000000  0.000000  0.000712
Vp     0.000000  0.000013  0.000788
45
       lwrest    errest    upr errest
Sp     0.000000  0.000000  0.000712
Vp     0.000000  0.000008  0.000786
68
       lwrest    errest    upr errest
Sp     0.000000  0.000013  0.000724
Vp     0.000519  0.000962  0.001622
```

```
0.12 0.17 0.0011 0.00015 500
0.4 0 0  5 0 0
Sp 0.008225   Vp 0.002138
Sp 0.006471   Vp 0.000000
0
       lwrest    errest    upr errest
Sp     0.003308  0.003759  0.004275
Vp     0.002839  0.003265  0.003798
22
       lwrest    errest    upr errest
Sp     0.000000  0.000000  0.000697
Vp     0.000000  0.000004  0.000933
45
       lwrest    errest    upr errest
Sp     0.000000  0.000000  0.000697
Vp     0.000000  0.000004  0.000933
68
       lwrest    errest    upr errest
Sp     0.000000  0.000019  0.000712
Vp     0.000693  0.001088  0.001737
```

```
0.12 0.17 0.0011 0.00015 500
0.4 0 0  5 90 0
Sp 0.008389   Vp 0.002138
Sp 0.006471   Vp 0.000000
0
       lwrest    errest    upr errest
Sp     0.001343  0.001817  0.002388
Vp     0.000780  0.001154  0.001748
22
       lwrest    errest    upr errest
Sp     0.000000  0.000000  0.000701
Vp     0.000000  0.000004  0.000877
45
       lwrest    errest    upr errest
Sp     0.000000  0.000000  0.000701
Vp     0.000000  0.000004  0.000877
68
       lwrest    errest    upr errest
Sp     0.000000  0.000014  0.000711
Vp     0.000000  0.000009  0.000879
```

```
0.12 0.17 0.0011 0.00015 500
0.8 0 0  5 0 0
Sp 0.007257   Vp 0.001892
Sp 0.006471   Vp 0.000000
0.
       lwrest    errest    upr errest
Sp     0.004734  0.005651  0.009905
Vp     0.000009  0.003046  0.039533
22
       lwrest    errest    upr errest
Sp     0.000000  0.000000  0.006810
Vp     0.000000  0.000007  0.038601
45
       lwrest    errest    upr errest
Sp     0.000000  0.000000  0.006810
Vp     0.000000  0.000007  0.038601
68
       lwrest    errest    upr errest
Sp     0.000000  0.000059  0.006854
Vp     0.000000  0.000009  0.038496
```

```
0.12 0.17 0.0011 0.00015 500
0.8 0 0  5 90 0
Sp 0.007497   Vp 0.001892
Sp 0.006471   Vp 0.000000
0
       lwrest    errest    upr errest
Sp     0.002742  0.005141  0.012535
Vp     0.000019  0.000025  0.019496
22
       lwrest    errest    upr errest
Sp     0.000000  0.000000  0.009522
Vp     0.000000  0.000016  0.019642
45
       lwrest    errest    upr errest
Sp     0.000000  0.000000  0.009522
Vp     0.000000  0.000016  0.019640
68
       lwrest    errest    upr errest
Sp     0.000000  0.000017  0.009531
Vp     0.000000  0.000018  0.019592
```

TABLE 8-7c$_2$

```
0.12 0.17 0.0018 0.00015 1000
0 0 0  5 0 0
Sp 0.013704   Vp 0.003116
Sp 0.010588   Vp 0.000000
0
        lwrest    errest    upr errest
Sp      0.000016  0.000024  0.000919
Vp      0.000993  0.001097  0.001551
22
        lwrest    errest    upr errest
Sp      0.000000  0.000000  0.000904
Vp      0.000000  0.000018  0.000799
45
        lwrest    errest    upr errest
Sp      0.000000  0.000000  0.000904
Vp      0.000000  0.000012  0.000796
68
        lwrest    errest    upr errest
Sp      0.000000  0.000024  0.000925
Vp      0.000750  0.001097  0.001703
```

```
0.12 0.17 0.0018 0.00015 1000
0.4 0 0  5 0 0
Sp 0.013069   Vp 0.003027
Sp 0.010588   Vp 0.000000
0
        lwrest    errest    upr errest
Sp      0.005018  0.005602  0.006258
Vp      0.003916  0.004349  0.004869
22
        lwrest    errest    upr errest
Sp      0.000000  0.000000  0.000897
Vp      0.000000  0.000004  0.000940
45
        lwrest    errest    upr errest
Sp      0.000000  0.000000  0.000897
Vp      0.000000  0.000004  0.000940
68
        lwrest    errest    upr errest
Sp      0.000000  0.000031  0.000923
Vp      0.000685  0.001084  0.001741
```

```
0.12 0.17 0.0018 0.00015 1000
0.4 0 0  5 90 0
Sp 0.013304   Vp 0.003027
Sp 0.010588   Vp 0.000000
0
        lwrest    errest    upr errest
Sp      0.002985  0.003614  0.004327
Vp      0.001902  0.002299  0.002826
22
        lwrest    errest    upr errest
Sp      0.000000  0.000000  0.000899
Vp      0.000000  0.000004  0.000882
45
        lwrest    errest    upr errest
Sp      0.000000  0.000000  0.000899
Vp      0.000000  0.000004  0.000882
68
        lwrest    errest    upr errest
Sp      0.000000  0.000025  0.000919
Vp      0.000000  0.000010  0.000884
```

```
0.12 0.17 0.0018 0.00015 1000
0.8 0 0  5 0 0
Sp 0.011698   Vp 0.002679
Sp 0.010588   Vp 0.000000
0 .
        lwrest    errest    upr errest
Sp      0.012709  0.014037  0.018429
Vp      0.002117  0.007622  0.041540
22
        lwrest    errest    upr errest
Sp      0.000000  0.000000  0.008937
Vp      0.000000  0.000009  0.038682
45
        lwrest    errest    upr errest
Sp      0.000000  0.000000  0.008937
Vp      0.000000  0.000009  0.038681
68
        lwrest    errest    upr errest
Sp      0.000000  0.000086  0.009003
Vp      0.000000  0.000008  0.038576
```

```
0.12 0.17 0.0018 0.00015 1000
0.8 0 0  5 90 0
Sp 0.012040   Vp 0.002679
Sp 0.010588   Vp 0.000000
0
        lwrest    errest    upr errest
Sp      0.006673  0.010214  0.019323
Vp      0.000996  0.003717  0.021109
22
        lwrest    errest    upr errest
Sp      0.000000  0.000000  0.012790
Vp      0.000000  0.000022  0.019686
45
        lwrest    errest    upr errest
Sp      0.000000  0.000000  0.012790
Vp      0.000000  0.000022  0.019683
68
        lwrest    errest    upr errest
Sp      0.000000  0.000032  0.012806
Vp      0.000000  0.000025  0.019634
```

TABLE 8-7c_3

```
0.12 0.17 0.0056 0.00015 10000
0 0 0  5 0 0
Sp 0.042840   Vp 0.009898
Sp 0.032941   Vp 0.000000
0
      lwrest    errest    upr errest
Sp    0.054286  0.056178  0.058091
Vp    0.052074  0.052365  0.052667
22
      lwrest    errest    upr errest
Sp    0.021832  0.023770  0.025761
Vp    0.023809  0.024332  0.024870
45
      lwrest    errest    upr errest
Sp    0.000000  0.000000  0.002319
Vp    0.000000  0.000021  0.000853
68
      lwrest    errest    upr errest
Sp    0.000000  0.000000  0.002319
Vp    0.000000  0.000015  0.000848
```

```
0.12 0.17 0.0056 0.00015 10000
0.4 0 0  5 0 0
Sp 0.040830   Vp 0.009612
Sp 0.032941   Vp 0.000000
0
      lwrest    errest    upr errest
Sp    0.064537  0.066059  0.067621
Vp    0.093308  0.093777  0.094253
22
      lwrest    errest    upr errest
Sp    0.022343  0.023885  0.025543
Vp    0.021774  0.022261  0.022773
45
      lwrest    errest    upr errest
Sp    0.000000  0.000000  0.002375
Vp    0.000000  0.000067  0.001025
68
      lwrest    errest    upr errest
Sp    0.000000  0.000000  0.002375
Vp    0.000000  0.000067  0.001025
```

```
0.12 0.17 0.0056 0.00015 10000
0.4 0 0  5 90 0
Sp 0.041576   Vp 0.009612
Sp 0.032941   Vp 0.000000
0
      lwrest    errest    upr errest
Sp    0.052617  0.054281  0.055983
Vp    0.071359  0.071791  0.072229
22
      lwrest    errest    upr errest
Sp    0.021440  0.023129  0.024911
Vp    0.016336  0.016779  0.017249
45
      lwrest    errest    upr errest
Sp    0.000000  0.000000  0.002364
Vp    0.000000  0.000072  0.000953
68
      lwrest    errest    upr errest
Sp    0.000000  0.000000  0.002364
Vp    0.000000  0.000072  0.000953
```

```
0.12 0.17 0.0056 0.00015 10000
0.8 0 0  5 0 0
Sp 0.036478   Vp 0.008498
Sp 0.032941   Vp 0.000000
0
      lwrest    errest    upr errest
Sp    0.160508  0.164469  0.170706
Vp    0.156775  0.169119  0.185217
22
      lwrest    errest    upr errest
Sp    0.000000  0.000000  0.024909
Vp    0.000000  0.000099  0.039306
45
      lwrest    errest    upr errest
Sp    0.000000  0.000000  0.024909
Vp    0.000000  0.000099  0.039306
68
      lwrest    errest    upr errest
Sp    0.000000  0.000000  0.024909
Vp    0.000000  0.000099  0.039306
```

```
0.12 0.17 0.0056 0.00015 10000
0.8 0 0  5 90 0
Sp 0.037566   Vp 0.008498
Sp 0.032941   Vp 0.000000
0
      lwrest    errest    upr errest
Sp    0.057661  0.069173  0.089466
Vp    0.071616  0.078585  0.087877
22
      lwrest    errest    upr errest
Sp    0.007529  0.016194  0.045751
Vp    0.003267  0.006890  0.023219
45
      lwrest    errest    upr errest
Sp    0.000000  0.000000  0.037092
Vp    0.000000  0.000133  0.020021
68
      lwrest    errest    upr errest
Sp    0.000000  0.000000  0.037092
Vp    0.000000  0.000133  0.020019
```

TABLE 8-7d_0

```
0.08 1.5 4.4e-06 0.00015 50
0 0 0  5 0 0
Sp 0.001378   Vp 0.001375
Sp 0.000003   Vp 0.000000
0
        lwrest    errest    upr errest
Sp      0.000001  0.000002  0.000444
Vp      0.001400  0.001878  0.002484
22
        lwrest    errest    upr errest
Sp      0.000000  0.000002  0.000444
Vp      0.001400  0.001878  0.002484
45
        lwrest    errest    upr errest
Sp      0.000000  0.000000  0.000442
Vp      0.000000  0.000003  0.000771
68
        lwrest    errest    upr errest
Sp      0.000000  0.000000  0.000442
Vp      0.000000  0.000001  0.000770
```

```
0.08 1.5 4.4e-06 0.00015 50
0.4 0 0  5 0 0
Sp 0.001141   Vp 0.001336
Sp 0.000003   Vp 0.000000
0
        lwrest    errest    upr errest
Sp      0.000004  0.000006  0.000420
Vp      0.000699  0.001087  0.001726
22
        lwrest    errest    upr errest
Sp      0.000000  0.000006  0.000421
Vp      0.000699  0.001087  0.001726
45
        lwrest    errest    upr errest
Sp      0.000000  0.000000  0.000416
Vp      0.000000  0.000003  0.000922
68
        lwrest    errest    upr errest
Sp      0.000000  0.000000  0.000416
Vp      0.000000  0.000003  0.000922
```

```
0.08 1.5 4.4e-06 0.00015 50
0.4 0 0  5 90 0
Sp 0.001218   Vp 0.001336
Sp 0.000003   Vp 0.000000
0
        lwrest    errest    upr errest
Sp      0.000001  0.000002  0.000424
Vp      0.000003  0.000007  0.000871
22
        lwrest    errest    upr errest
Sp      0.000000  0.000002  0.000424
Vp      0.000000  0.000007  0.000871
45
        lwrest    errest    upr errest
Sp      0.000000  0.000000  0.000422
Vp      0.000000  0.000003  0.000870
68
        lwrest    errest    upr errest
Sp      0.000000  0.000000  0.000422
Vp      0.000000  0.000003  0.000870
```

```
0.08 1.5 4.4e-06 0.00015 50
0.8 0 0  5 0 0
Sp 0.000591   Vp 0.001182
Sp 0.000003   Vp 0.000000
0
        lwrest    errest    upr errest
Sp      0.000017  0.000024  0.003841
Vp      0.000001  0.000008  0.038384
22
        lwrest    errest    upr errest
Sp      0.000000  0.000000  0.003824
Vp      0.000000  0.000004  0.038489
45
        lwrest    errest    upr errest
Sp      0.000000  0.000000  0.003824
Vp      0.000000  0.000004  0.038489
68
        lwrest    errest    upr errest
Sp      0.000000  0.000000  0.003824
Vp      0.000000  0.000004  0.038489
```

```
0.08 1.5 4.4e-06 0.00015 50
0.8 0 0  5 90 0
Sp 0.000698   Vp 0.001182
Sp 0.000003   Vp 0.000000
0
        lwrest    errest    upr errest
Sp      0.000001  0.000003  0.004928
Vp      0.000006  0.000009  0.019531
22
        lwrest    errest    upr errest
Sp      0.000000  0.000003  0.004928
Vp      0.000000  0.000009  0.019532
45
        lwrest    errest    upr errest
Sp      0.000000  0.000000  0.004926
Vp      0.000000  0.000008  0.019580
68
        lwrest    errest    upr errest
Sp      0.000000  0.000000  0.004926
Vp      0.000000  0.000008  0.019579
```

TABLE 8-7d$_1$

```
0.08 1.5 4.4e-05 0.00015 500
0 0 0  5 0 0
Sp 0.004364   Vp 0.004334
Sp 0.000029   Vp 0.000000
0
       lwrest    errest    upr errest
Sp     0.000004  0.000016  0.000872
Vp     0.001779  0.001946  0.002339
22
       lwrest    errest    upr errest
Sp     0.000000  0.000016  0.000873
Vp     0.001613  0.001946  0.002465
45
       lwrest    errest    upr errest
Sp     0.000000  0.000000  0.000859
Vp     0.000000  0.000012  0.000794
68
       lwrest    errest    upr errest
Sp     0.000000  0.000000  0.000859
Vp     0.000000  0.000006  0.000789
```

```
0.08 1.5 4.4e-05 0.00015 500
0.4 0 0  5 0 0
Sp 0.003616   Vp 0.004211
Sp 0.000029   Vp 0.000000
0
       lwrest    errest    upr errest
Sp     0.000013  0.000025  0.000869
Vp     0.000688  0.001085  0.001740
22
       lwrest    errest    upr errest
Sp     0.000000  0.000025  0.000871
Vp     0.000687  0.001085  0.001740
45
       lwrest    errest    upr errest
Sp     0.000000  0.000000  0.000849
Vp     0.000000  0.000004  0.000938
68
       lwrest    errest    upr errest
Sp     0.000000  0.000000  0.000849
Vp     0.000000  0.000004  0.000938
```

```
0.08 1.5 4.4e-05 0.00015 500
0.4 0 0  5 90 0
Sp 0.003861   Vp 0.004211
Sp 0.000029   Vp 0.000000
0
       lwrest    errest    upr errest
Sp     0.000003  0.000018  0.000865
Vp     0.000009  0.000010  0.000881
22
       lwrest    errest    upr errest
Sp     0.000000  0.000018  0.000865
Vp     0.000000  0.000010  0.000883
45
       lwrest    errest    upr errest
Sp     0.000000  0.000000  0.000852
Vp     0.000000  0.000004  0.000881
68
       lwrest    errest    upr errest
Sp     0.000000  0.000000  0.000852
Vp     0.000000  0.000004  0.000881
```

```
0.08 1.5 4.4e-05 0.00015 500
0.8 0 0  5 0 0
Sp 0.001881   Vp 0.003726
Sp 0.000029   Vp 0.000000
0
       lwrest    errest    upr errest
Sp     0.000052  0.000080  0.008459
Vp     0.000002  0.000009  0.038558
22
       lwrest    errest    upr errest
Sp     0.000000  0.000000  0.008400
Vp     0.000000  0.000008  0.038664
45
       lwrest    errest    upr errest
Sp     0.000000  0.000000  0.008400
Vp     0.000000  0.000008  0.038664
68
       lwrest    errest    upr errest
Sp     0.000000  0.000000  0.008400
Vp     0.000000  0.000008  0.038663
```

```
0.08 1.5 4.4e-05 0.00015 500
0.8 0 0  5 90 0
Sp 0.002221   Vp 0.003726
Sp 0.000029   Vp 0.000000
0
       lwrest    errest    upr errest
Sp     0.000003  0.000025  0.012009
Vp     0.000018  0.000023  0.019625
22
       lwrest    errest    upr errest
Sp     0.000000  0.000025  0.012009
Vp     0.000000  0.000023  0.019630
45
       lwrest    errest    upr errest
Sp     0.000000  0.000000  0.011997
Vp     0.000000  0.000021  0.019673
68
       lwrest    errest    upr errest
Sp     0.000000  0.000000  0.011997
Vp     0.000000  0.000021  0.019673
```

TABLE 8-7d_2

```
0.08 1.5 8.8e-05 0.00015 1000
0 0 0  5 0 0
Sp 0.006177   Vp 0.006119
Sp 0.000059   Vp 0.000000
0
       lwrest    errest    upr errest
Sp     0.000730  0.001585  0.002608
Vp     0.004494  0.004659  0.004939
22
       lwrest    errest    upr errest
Sp     0.000000  0.000032  0.001138
Vp     0.000940  0.001302  0.001893
45
       lwrest    errest    upr errest
Sp     0.000000  0.000000  0.001111
Vp     0.000000  0.000015  0.000806
68
       lwrest    errest    upr errest
Sp     0.000000  0.000000  0.001111
Vp     0.000000  0.000009  0.000800
```

```
0.08 1.5 8.8e-05 0.00015 1000
0.4 0 0  5 0 0
Sp 0.005121   Vp 0.005943
Sp 0.000059   Vp 0.000000
0
       lwrest    errest    upr errest
Sp     0.001268  0.001826  0.002716
Vp     0.001726  0.002157  0.002741
22
       lwrest    errest    upr errest
Sp     0.000000  0.000043  0.001149
Vp     0.000673  0.001075  0.001741
45
       lwrest    errest    upr errest
Sp     0.000000  0.000000  0.001112
Vp     0.000000  0.000006  0.000949
68
       lwrest    errest    upr errest
Sp     0.000000  0.000000  0.001112
Vp     0.000000  0.000006  0.000948
```

```
0.08 1.5 8.8e-05 0.00015 1000
0.4 0 0  5 90 0
Sp 0.005468   Vp 0.005943
Sp 0.000059   Vp 0.000000
0
       lwrest    errest    upr errest
Sp     0.001060  0.001768  0.002702
Vp     0.000762  0.001142  0.001747
22
       lwrest    errest    upr errest
Sp     0.000000  0.000035  0.001139
Vp     0.000000  0.000014  0.000892
45
       lwrest    errest    upr errest
Sp     0.000000  0.000000  0.001112
Vp     0.000000  0.000007  0.000889
68
       lwrest    errest    upr errest
Sp     0.000000  0.000000  0.001112
Vp     0.000000  0.000007  0.000889
```

```
0.08 1.5 8.8e-05 0.00015 1000
0.8 0 0  5 0 0
Sp 0.002670   Vp 0.005257
Sp 0.000059   Vp 0.000000
0
       lwrest    errest    upr errest
Sp     0.000073  0.000119  0.011264
Vp     0.000003  0.000009  0.038664
22
       lwrest    errest    upr errest
Sp     0.000000  0.000000  0.011175
Vp     0.000000  0.000013  0.038771
45
       lwrest    errest    upr errest
Sp     0.000000  0.000000  0.011175
Vp     0.000000  0.000013  0.038770
68
       lwrest    errest    upr errest
Sp     0.000000  0.000000  0.011175
Vp     0.000000  0.000013  0.038770
```

```
0.08 1.5 8.8e-05 0.00015 1000
0.8 0 0  5 90 0
Sp 0.003153   Vp 0.005257
Sp 0.000059   Vp 0.000000
0
       lwrest    errest    upr errest
Sp     0.000004  0.000050  0.016306
Vp     0.000025  0.000034  0.019683
22
       lwrest    errest    upr errest
Sp     0.000000  0.000050  0.016306
Vp     0.000000  0.000034  0.019690
45
       lwrest    errest    upr errest
Sp     0.000000  0.000000  0.016283
Vp     0.000000  0.000030  0.019731
68
       lwrest    errest    upr errest
Sp     0.000000  0.000000  0.016283
Vp     0.000000  0.000030  0.019730
```

TABLE 8-7d_3

```
0.08 1.5 0.00088 0.00015 10000
0 0 0  5 0 0
Sp 0.019684   Vp 0.019097
Sp 0.000587   Vp 0.000000
0
        lwrest    errest    upr errest
Sp      0.022022  0.024500  0.027062
Vp      0.019741  0.020105  0.020495
22
        lwrest    errest    upr errest
Sp      0.008346  0.010781  0.013419
Vp      0.009018  0.009584  0.010187
45
        lwrest    errest    upr errest
Sp      0.000000  0.000000  0.002972
Vp      0.000000  0.000026  0.000881
68
        lwrest    errest    upr errest
Sp      0.000000  0.000000  0.002972
Vp      0.000000  0.000015  0.000873
```

```
0.08 1.5 0.00088 0.00015 10000
0.4 0 0  5 0 0
Sp 0.016378   Vp 0.018537
Sp 0.000587   Vp 0.000000
0
        lwrest    errest    upr errest
Sp      0.027803  0.029766  0.031883
Vp      0.040580  0.041081  0.041597
22
        lwrest    errest    upr errest
Sp      0.009000  0.010837  0.013092
Vp      0.010160  0.010665  0.011215
45
        lwrest    errest    upr errest
Sp      0.000000  0.000000  0.003051
Vp      0.000000  0.000125  0.001082
68
        lwrest    errest    upr errest
Sp      0.000000  0.000000  0.003051
Vp      0.000000  0.000125  0.001082
```

```
0.08 1.5 0.00088 0.00015 10000
0.4 0 0  5 90 0
Sp 0.017480   Vp 0.018537
Sp 0.000587   Vp 0.000000
0
        lwrest    errest    upr errest
Sp      0.023605  0.025760  0.028051
Vp      0.027195  0.027642  0.028107
22
        lwrest    errest    upr errest
Sp      0.008388  0.010478  0.012887
Vp      0.006708  0.007157  0.007661
45
        lwrest    errest    upr errest
Sp      0.000000  0.000000  0.003034
Vp      0.000000  0.000133  0.001005
68
        lwrest    errest    upr errest
Sp      0.000000  0.000000  0.003034
Vp      0.000000  0.000133  0.001005
```

```
0.08 1.5 0.00088 0.00015 10000
0.8 0 0  5 0 0
Sp 0.008679   Vp 0.016362
Sp 0.000587   Vp 0.000000
0
        lwrest    errest    upr errest
Sp      0.130142  0.134823  0.143799
Vp      0.131810  0.144626  0.161901
22
        lwrest    errest    upr errest
Sp      0.000000  0.000000  0.031744
Vp      0.000000  0.000180  0.039618
45
        lwrest    errest    upr errest
Sp      0.000000  0.000000  0.031744
Vp      0.000000  0.000180  0.039617
68
        lwrest    errest    upr errest
Sp      0.000000  0.000000  0.031744
Vp      0.000000  0.000180  0.039618
```

```
0.08 1.5 0.00088 0.00015 10000
0.8 0 0  5 90 0
Sp 0.010250   Vp 0.016362
Sp 0.000587   Vp 0.000000
0
        lwrest    errest    upr errest
Sp      0.011817  0.023389  0.060565
Vp      0.013947  0.019609  0.032803
22
        lwrest    errest    upr errest
Sp      0.000409  0.008275  0.051619
Vp      0.000593  0.003096  0.021340
45
        lwrest    errest    upr errest
Sp      0.000000  0.000000  0.047975
Vp      0.000000  0.000230  0.020193
68
        lwrest    errest    upr errest
Sp      0.000000  0.000000  0.047975
Vp      0.000000  0.000230  0.020195
```

TABLE 8-7e_0

```
0.08 0.014 1.75e-05 0.001 50
0 0 0  5 0 0
Sp 0.001383   Vp 0.000133
Sp 0.001250   Vp 0.000000
0
       lwrest    errest    upr errest
Sp     0.000001  0.000001  0.000253
Vp     0.000723  0.001191  0.001821
22
       lwrest    errest    upr errest
Sp     0.000000  0.000000  0.000253
Vp     0.000000  0.000000  0.000762
45
       lwrest    errest    upr errest
Sp     0.000000  0.000000  0.000253
Vp     0.000000  0.000000  0.000762
68
       lwrest    errest    upr errest
Sp     0.000000  0.000001  0.000253
Vp     0.000723  0.001191  0.001821
```

```
0.08 0.014 1.75e-05 0.001 50
0.4 0 0  5 0 0
Sp 0.001355   Vp 0.000129
Sp 0.001250   Vp 0.000000
0
       lwrest    errest    upr errest
Sp     0.000001  0.000001  0.000218
Vp     0.000698  0.001082  0.001714
22
       lwrest    errest    upr errest
Sp     0.000000  0.000000  0.000218
Vp     0.000000  0.000000  0.000914
45
       lwrest    errest    upr errest
Sp     0.000000  0.000000  0.000218
Vp     0.000000  0.000000  0.000914
68
       lwrest    errest    upr errest
Sp     0.000000  0.000001  0.000219
Vp     0.000698  0.001082  0.001714
```

```
0.08 0.014 1.75e-05 0.001 50
0.4 0 0  5 90 0
Sp 0.001366   Vp 0.000129
Sp 0.001250   Vp 0.000000
0
       lwrest    errest    upr errest
Sp     0.000001  0.000001  0.000226
Vp     0.000000  0.000008  0.000867
22
       lwrest    errest    upr errest
Sp     0.000000  0.000000  0.000226
Vp     0.000000  0.000000  0.000863
45
       lwrest    errest    upr errest
Sp     0.000000  0.000000  0.000226
Vp     0.000000  0.000000  0.000863
68
       lwrest    errest    upr errest
Sp     0.000000  0.000001  0.000227
Vp     0.000000  0.000008  0.000867
```

```
0.08 0.014 1.75e-05 0.001 50
0.8 0 0  5 0 0
Sp 0.001297   Vp 0.000114
Sp 0.001250   Vp 0.000000
0
       lwrest    errest    upr errest
Sp     0.000002  0.000002  0.001740
Vp     0.000000  0.000006  0.038305
22
       lwrest    errest    upr errest
Sp     0.000000  0.000000  0.001739
Vp     0.000000  0.000000  0.038409
45
       lwrest    errest    upr errest
Sp     0.000000  0.000000  0.001739
Vp     0.000000  0.000000  0.038409
68
       lwrest    errest    upr errest
Sp     0.000000  0.000002  0.001740
Vp     0.000000  0.000006  0.038305
```

```
0.08 0.014 1.75e-05 0.001 50
0.8 0 0  5 90 0
Sp 0.001311   Vp 0.000114
Sp 0.001250   Vp 0.000000
0
       lwrest    errest    upr errest
Sp     0.000002  0.000002  0.001703
Vp     0.000000  0.000006  0.019490
22
       lwrest    errest    upr errest
Sp     0.000000  0.000000  0.001703
Vp     0.000000  0.000000  0.019536
45
       lwrest    errest    upr errest
Sp     0.000000  0.000000  0.001703
Vp     0.000000  0.000000  0.019536
68
       lwrest    errest    upr errest
Sp     0.000000  0.000002  0.001704
Vp     0.000000  0.000006  0.019490
```

TABLE 8-7e$_1$

```
0.08 0.014 4.4e-05 0.001 500
0 0 0  5 0 0
Sp 0.003564   Vp 0.000421
Sp 0.003143   Vp 0.000000
0
        lwrest    errest    upr errest
Sp      0.001427  0.001646  0.001875
Vp      0.001941  0.002435  0.003024
22
        lwrest    errest    upr errest
Sp      0.000000  0.000000  0.000258
Vp      0.000000  0.000000  0.000762
45
        lwrest    errest    upr errest
Sp      0.000000  0.000000  0.000258
Vp      0.000000  0.000000  0.000762
68
        lwrest    errest    upr errest
Sp      0.000000  0.000003  0.000260
Vp      0.000716  0.001184  0.001815
```

```
0.08 0.014 4.4e-05 0.001 500
0.4 0 0  5 0 0
Sp 0.003476   Vp 0.000409
Sp 0.003143   Vp 0.000000
0
        lwrest    errest    upr errest
Sp      0.001745  0.001895  0.002059
Vp      0.001759  0.002167  0.002720
22
        lwrest    errest    upr errest
Sp      0.000000  0.000000  0.000224
Vp      0.000000  0.000000  0.000914
45
        lwrest    errest    upr errest
Sp      0.000000  0.000000  0.000224
Vp      0.000000  0.000000  0.000914
68
        lwrest    errest    upr errest
Sp      0.000000  0.000003  0.000226
Vp      0.000699  0.001082  0.001715
```

```
0.08 0.014 4.4e-05 0.001 500
0.4 0 0  5 90 0
Sp 0.003509   Vp 0.000409
Sp 0.003143   Vp 0.000000
0
        lwrest    errest    upr errest
Sp      0.001669  0.001837  0.002017
Vp      0.000782  0.001149  0.001732
22
        lwrest    errest    upr errest
Sp      0.000000  0.000000  0.000232
Vp      0.000000  0.000000  0.000863
45
        lwrest    errest    upr errest
Sp      0.000000  0.000000  0.000232
Vp      0.000000  0.000000  0.000863
68
        lwrest    errest    upr errest
Sp      0.000000  0.000003  0.000234
Vp      0.000000  0.000008  0.000867
```

```
0.08 0.014 4.4e-05 0.001 500
0.8 0 0  5 0 0
Sp 0.003291   Vp 0.000362
Sp 0.003143   Vp 0.000000
0
        lwrest    errest    upr errest
Sp      0.002563  0.002842  0.003773
Vp      0.000000  0.000011  0.038204
22
        lwrest    errest    upr errest
Sp      0.000000  0.000000  0.001804
Vp      0.000000  0.000000  0.038411
45
        lwrest    errest    upr errest
Sp      0.000000  0.000000  0.001804
Vp      0.000000  0.000000  0.038411
68
        lwrest    errest    upr errest
Sp      0.000000  0.000005  0.001805
Vp      0.000000  0.000006  0.038307
```

```
0.08 0.014 4.4e-05 0.001 500
0.8 0 0  5 90 0
Sp 0.003338   Vp 0.000362
Sp 0.003143   Vp 0.000000
0
        lwrest    errest    upr errest
Sp      0.002028  0.002593  0.003724
Vp      0.000000  0.000012  0.019446
22
        lwrest    errest    upr errest
Sp      0.000000  0.000000  0.001802
Vp      0.000000  0.000000  0.019537
45
        lwrest    errest    upr errest
Sp      0.000000  0.000000  0.001802
Vp      0.000000  0.000000  0.019537
68
        lwrest    errest    upr errest
Sp      0.000000  0.000004  0.001803
Vp      0.000000  0.000006  0.019492
```

TABLE 8-7e$_2$

0.08 0.014 5.56e-05 0.001 1000
0 0 0 5 0 0
Sp 0.004567 Vp 0.000596
Sp 0.003971 Vp 0.000000
0

	lwrest	errest	upr errest
Sp	0.003067	0.003291	0.003521
Vp	0.003156	0.003660	0.004231

22

	lwrest	errest	upr errest
Sp	0.000000	0.000000	0.000262
Vp	0.000000	0.000000	0.000762

45

	lwrest	errest	upr errest
Sp	0.000000	0.000000	0.000262
Vp	0.000000	0.000000	0.000762

68

	lwrest	errest	upr errest
Sp	0.000000	0.000004	0.000264
Vp	0.000712	0.001180	0.001811

0.08 0.014 5.56e-05 0.001 1000
0.4 0 0 5 0 0
Sp 0.004444 Vp 0.000579
Sp 0.003971 Vp 0.000000
0

	lwrest	errest	upr errest
Sp	0.003632	0.003788	0.003951
Vp	0.002842	0.003255	0.003772

22

	lwrest	errest	upr errest
Sp	0.000000	0.000000	0.000228
Vp	0.000000	0.000000	0.000914

45

	lwrest	errest	upr errest
Sp	0.000000	0.000000	0.000228
Vp	0.000000	0.000000	0.000914

68

	lwrest	errest	upr errest
Sp	0.000000	0.000004	0.000230
Vp	0.000699	0.001082	0.001715

0.08 0.014 5.56e-05 0.001 1000
0.4 0 0 5 90 0
Sp 0.004490 Vp 0.000579
Sp 0.003971 Vp 0.000000
0

	lwrest	errest	upr errest
Sp	0.003499	0.003672	0.003852
Vp	0.001911	0.002297	0.002808

22

	lwrest	errest	upr errest
Sp	0.000000	0.000000	0.000236
Vp	0.000000	0.000000	0.000863

45

	lwrest	errest	upr errest
Sp	0.000000	0.000000	0.000236
Vp	0.000000	0.000000	0.000863

68

	lwrest	errest	upr errest
Sp	0.000000	0.000004	0.000238
Vp	0.000000	0.000008	0.000867

0.08 0.014 5.56e-05 0.001 1000
0.8 0 0 5 0 0
Sp 0.004181 Vp 0.000512
Sp 0.003971 Vp 0.000000
0

	lwrest	errest	upr errest
Sp	0.002558	0.002842	0.003800
Vp	0.000000	0.000011	0.038205

22

	lwrest	errest	upr errest
Sp	0.000000	0.000000	0.001843
Vp	0.000000	0.000000	0.038413

45

	lwrest	errest	upr errest
Sp	0.000000	0.000000	0.001843
Vp	0.000000	0.000000	0.038413

68

	lwrest	errest	upr errest
Sp	0.000000	0.000006	0.001845
Vp	0.000000	0.000006	0.038309

0.08 0.014 5.56e-05 0.001 1000
0.8 0 0 5 90 0
Sp 0.004247 Vp 0.000512
Sp 0.003971 Vp 0.000000
0

	lwrest	errest	upr errest
Sp	0.002012	0.002593	0.003771
Vp	0.000000	0.000012	0.019447

22

	lwrest	errest	upr errest
Sp	0.000000	0.000000	0.001862
Vp	0.000000	0.000001	0.019538

45

	lwrest	errest	upr errest
Sp	0.000000	0.000000	0.001862
Vp	0.000000	0.000001	0.019538

68

	lwrest	errest	upr errest
Sp	0.000000	0.000005	0.001864
Vp	0.000000	0.000006	0.019492

TABLE 8-7e$_3$

```
0.08 0.014 0.000351 0.001 10000
0 0 0  5 0 0
Sp 0.026972   Vp 0.001901
Sp 0.025071   Vp 0.000000
0
       lwrest    errest    upr errest
Sp     0.019424  0.019669  0.019915
Vp     0.014181  0.014697  0.015231
22
       lwrest    errest    upr errest
Sp     0.000000  0.000000  0.000288
Vp     0.000000  0.000000  0.000763
45
       lwrest    errest    upr errest
Sp     0.000000  0.000000  0.000288
Vp     0.000000  0.000000  0.000763
68
       lwrest    errest    upr errest
Sp     0.007972  0.008219  0.008469
Vp     0.006556  0.007070  0.007622
```

```
0.08 0.014 0.000351 0.001 10000
0.4 0 0  5 0 0
Sp 0.026575   Vp 0.001847
Sp 0.025071   Vp 0.000000
0
       lwrest    errest    upr errest
Sp     0.022442  0.022617  0.022793
Vp     0.016092  0.016502  0.016943
22
       lwrest    errest    upr errest
Sp     0.000000  0.000000  0.000255
Vp     0.000000  0.000001  0.000916
45
       lwrest    errest    upr errest
Sp     0.000000  0.000000  0.000255
Vp     0.000000  0.000001  0.000916
68
       lwrest    errest    upr errest
Sp     0.009281  0.009457  0.009637
Vp     0.006125  0.006540  0.007015
```

```
0.08 0.014 0.000351 0.001 10000
0.4 0 0  5 90 0
Sp 0.026724   Vp 0.001847
Sp 0.025071   Vp 0.000000
0
       lwrest    errest    upr errest
Sp     0.021735  0.021927  0.022121
Vp     0.013465  0.013857  0.014279
22
       lwrest    errest    upr errest
Sp     0.000000  0.000000  0.000263
Vp     0.000000  0.000001  0.000864
45
       lwrest    errest    upr errest
Sp     0.000000  0.000000  0.000263
Vp     0.000000  0.000001  0.000864
68
       lwrest    errest    upr errest
Sp     0.008973  0.009168  0.009365
Vp     0.004214  0.004606  0.005068
```

```
0.08 0.014 0.000351 0.001 10000
0.8 0 0  5 0 0
Sp 0.025737   Vp 0.001635
Sp 0.025071   Vp 0.000000
0
       lwrest    errest    upr errest
Sp     0.027711  0.028234  0.028899
Vp     0.008232  0.015351  0.045312
22
       lwrest    errest    upr errest
Sp     0.000000  0.000000  0.002147
Vp     0.000000  0.000001  0.038425
45
       lwrest    errest    upr errest
Sp     0.000000  0.000000  0.002147
Vp     0.000000  0.000001  0.038425
68
       lwrest    errest    upr errest
Sp     0.010910  0.011344  0.012121
Vp     0.000554  0.004575  0.039838
```

```
0.08 0.014 0.000351 0.001 10000
0.8 0 0  5 90 0
Sp 0.025949   Vp 0.001635
Sp 0.025071   Vp 0.000000
0
       lwrest    errest    upr errest
Sp     0.024887  0.025774  0.026801
Vp     0.010329  0.014862  0.028156
22
       lwrest    errest    upr errest
Sp     0.000000  0.000000  0.002314
Vp     0.000000  0.000002  0.019545
45
       lwrest    errest    upr errest
Sp     0.000000  0.000000  0.002314
Vp     0.000000  0.000002  0.019545
68
       lwrest    errest    upr errest
Sp     0.009514  0.010353  0.011504
Vp     0.000051  0.001865  0.020067
```

9. Discussion

In order to examine the data in a coherent manner, I would like to restate the goals of this dissertation suggested in the introduction. One goal is to assess whether or not it is important to consider frequency dependence in investigations of electromagnetic fields generated by the brain. Another goal is to find peculiarities in electromagnetic field characteristics that would not be predicted by frequency independent models. I will now represent the data in a form suitable for achieving these goals.

9.1 The first goal

Achievement of the first goal is accomplished by considering table 9-1. This table shows maxima extracted from tables 8-7. Notice that all values are from the case $\theta_{FT}=0°$. Is this case physically realizable? $\theta_{FT}=0°$ for all fourier components dictates symmetric or antisymmetric time behavior for the source where the point of symmetry is arbitrary. (The antisymmetric case is included since the same deviations would have been obtained with $\theta_{FT}=90°$.) Even if such time behavior never arises, it seems very likely that at least some fourier components could have $\theta_{FT}= 0$ or $90°$. Regardless, since most of the important fourier components of electromagnetic fields recorded at the scalp are below 50Hz, it can be observed that with repect to the frequency dependent model investigated here, frequency independent models are quite adequate. Data for unbounded conductor models is included to show that, indeed, unbounded conductor models provide conservative estimates for frequency dependence in Φ for frequencies below 10^4Hz.

TABLE 9-1 Maxima of tables 8-7 taken over θ_{FT} and source parameters. Values are reported as percentages; i.e., deviations are multiplied by 10^2.

frequency →		50Hz	500	10^3	10^4
medium	function				
bounded conductors					
CSF	Φ	.0024	.008	.18	13.5
	$\vec{A}$	.11	.11	.22	14.5
SKL		.002	.28	.38	2.8
		.11	.22	.33	1.6
SML		.28	.78	1.3	3.9
		.22	.43	.87	2.7
MED		.28	.57	1.1	4.7
		.22	.44	.94	3.4
LRG		.28	.57	1.4	16.4
		.22	.33	.76	16.9
unbounded conductors					
CSF		.14 (0)	.44 (0)	.62 (0)	2.0 (.06)
		.14 (0)	.43 (0)	.61 (0)	1.9 (0)
SKL		.14 (.12)	.36 (.31)	.46 (.40)	2.7 (2.5)
		.01 (0)	.04 (0)	.06 (0)	1.9 (0)
SML		.28 (.26)	.72 (.65)	1.2 (1.1)	3.6 (3.3)
		.02 (0)	.07 (0)	.10 (0)	.33 (0)
MED		.31 (.26)	.79 (.65)	1.3 (1.1)	4.0 (3.3)
		.05 (0)	.15 (0)	.21 (0)	.66 (0)
LRG		.33 (.26)	.87 (.65)	1.4 (1.1)	4.3 (3.3)
		.07 (0)	.22 (0)	.31 (0)	1.0 (0)

entry format: $e_{im} \neq 0$ value ($e_{im} = 0$ value)

9.2 The second goal

It can be observed from table 9.1 that there are curious differences between the bounded and unbounded data. These differences are clues that there are important peculiarities in frequency dependent fields that cannot be anticipated by frequency independent models nor by comparing frequency dependent and frequency independent solutions of unbounded conductor models. In this section, I will examine how deviations depend on frequency, source location, source orientation, θ_{FT}, R_c, and media type for both unbounded and bounded conductor models. This will clarify the differences between bounded and unbounded conductor models and will lead to achieving the second goal. For trends in deviations associated with $\vec{A}$, central source data is only taken seriously for comparisons within the central source context. This was done because even after 150 iterations of Cimmino's process, it was observed that deviations were still increasing.

9.2.1 Lists of trends in data of tables 8-7

The list for bounded conductor data follows.

1. Deviation dependence on θ_{FT}:

   a. $\theta_{FT}=22°$ and 45° are not resolved[9-1] for all cases of SML, MED, and SKL and for cases 50 to 10^3Hz for LRG.

   b. $\theta_{FT}=45°$ and 68° are not resolved for all cases of CSF and the 10^4Hz case of LRG.

   c. Largest deviations occur, invariably, at $\theta_{FT}=0°$.

2. Deviation dependence on source location: deviation increases with eccentricity.

9-1 A deviation will be labeled unresolvable if the lower bound does not exceed 0.001.

For Φ, of 52 testable cases[9-2], 15 cases contradict the trend where only 1 is significant[9-3]. In contrast, 14 cases consistent with the trend are significant. Contradictions show no obvious dependence on frequency, θ_{FT}, nor source orientation.

For $\vec{A}$, of 43 testable cases, 34 contradict the trend; however, none are significant. In contrast, of the 9 cases consistent with the trend, 5 are significant. The trend is not observed for the SML case and is observed only for $\theta_{FT}=0°$ at 10^3 and 10^4Hz. Taking this into consideration and including central source data in the analysis, source location dependence for $\vec{A}$ might be restated as follows:

a. for $\theta_{FT}=0°$, deviations decrease with increases in eccentricity at low frequencies. The trend gradually changes to deviation increase with eccentricity as frequency is increased.

b. for $\theta_{FT}=22°$ and 45°, deviation decreases with increases in eccentricity.

3. Deviation dependence on source orientation: deviations for radial sources are larger than those for tangential sources.

For Φ, of 50 testable cases, 7 cases contradict the trend with 1 being significant. In contrast, 15 cases consistent with the trend are significant. Contradictions occur, invariably, at eccentricity 0.8.

For $\vec{A}$, of 36 testable cases, 3 cases contradict the trend with 1 being significant. In contrast, 25 cases consistent with the trend are significant. Contradictory cases occur at 10^4Hz.

4. Deviation dependence on frequency: deviations increase with frequency.

For Φ, of 48 testable cases, 5 cases contradict the trend where 3 of these

9-2 I define a ***testable case*** to be one where at least one element of the of the set over which comparisons are to be made is resolvable.

9-3 A trend will be called significant if it is still observed when conservative estimates of the values involved are used, i.e., using one of the two error bounds.

are significant. In contrast, all cases following the trend are significant. Significant contradictions occur when $\theta_{FT}=0°$, sources are centrally located, and media are MED or LRG.

For $\vec{A}$, of 32 testable cases, 1 case contradicts the trend and it is not significant. In contrast, 22 cases consistent with the trend are significant.

5. Deviation dependence on head size: For both Φ and $\vec{A}$,

   a. $\theta_{FT}=0°$, at low frequencies, there is no dependence. As frequency is increased, deviations at lower R_c begin to exceed those at higher R_c. With further increases in frequency, this trend reverses with deviations at larger R_c beginning to exceed those at lower R_c. As eccentricity of the source is increased, the frequency at which this final stage becomes realized is lower. These trends are significant for eccentricities 0 and 0.4 at and above 500Hz. For eccentricity 0.8, significance is achieved only at 10^4Hz.

   b. $\theta_{FT}=22°$, deviations increase with R_c; the trend is resolvable only at 10^4Hz. In addition, at eccentricity 0.8, deviations are resolvable only for $\vec{A}$ but significance is not achieved.

   c. $\theta_{FT}=68°$, at low frequencies there is no dependence. As frequency is increased, deviations at lower R_c begin to exceed those at higher R_c. At lower eccentricities, this stage is achieved at lower frequencies. Significance is achieved for eccentricities 0 and 0.4.

   There are no contradictions to these trends.

6. Deviation dependence on media type: For both Φ and $\vec{A}$,

   a. Up to 10^3Hz, the trend MED>SKL>CSF is significant. Among testable cases, there are no contradictions.

b. At 10^4Hz, CSF is largest at $\theta_{FT}=0°$ and 22° and SKL is largest at $\theta_{FT}=68°$. Both trends are significant. One contradiction occurs at eccentricity 0.8, $\theta_{FT}=0°$, where MED>SKL>CSF. For this case, the trend is not significant.

7. Relationship between Φ and $\vec{A}$ deviations: deviations for $\vec{A}$ are smaller.

Of 106 cases, there are 14 contradictions, 3 of which are significant. In contrast, 26 cases consistent with the trend are significant. Contradictions typically occur at eccentricity 0.4, $\theta_{FT}=0°$. A closer examination reveals that all significant contradictions occur at 10^4Hz in media CSF and LRG. For CSF, of 8 testable cases, 4 contradict the trend with 1 significant case. Of the cases consistent with the trend, 1 is significant. For LRG at 10^4Hz, of 7 testable cases, 4 contradicted the trend with 2 significant cases while of the cases consistent with the trend, 1 is significant. Thus, for these media, it may be that at high frequencies, deviations for $\vec{A}$ exceed those for Φ.

In contrast, here is an analogous list of trends predicted by the unbounded conductor model, $e_{im}\neq 0$:

1. There is no dependence on θ_{FT}.
2. Deviation decreases as source eccentricity increases.
3. For Φ, deviations for radial sources are less than that for tangential sources. For $\vec{A}$, the relationship is an equality.
4. Deviations increase with frequency.
5. Deviations increase with head size.
6. For Φ, deviations for MED are always the largest. For the most part, the order SKL>CSF holds; however, for 500Hz and 10^3Hz at eccentricity 0 and 0.4 and for 10^4Hz at eccentricity 0, the opposite is true.

For $\vec{A}$, the trend CSF>MED>SKL always holds.

7. Deviations for Φ exceed those for $\vec{A}$ for all cases of SML, MED, LRG, and SKL. For CSF, this trend holds for centrally located sources but the converse is true for all other eccentricities.

9.2.2 Discussion of trends

I would like to point out that trends for bounded conductors almost invariably contradict those for unbounded conductors. Only item 4 is in complete agreement although, for bounded conductors, exceptions to the trend that achieve significance do exist. Items 2, 6, and 7 are in partial agreement. It is very difficult to find an explanation for each of these discrepancies. The reason for this is best indicated by this general view of the situation: by comparing the two lists, it can be concluded that both Φ and $\vec{A}$ deviations must turn out to depend on the topology of electromagnetic interference patterns set up in the conductor in addition to depending on properties of fields that would exist in unbounded media (unadulterated fields). In other words, I am claiming that deviations depend not only on the nature of the generated electromagnetic fields but also on how these fields superpose with their reflections at the conductor/insulator interface. Characterizing the net fields is certainly a formidable task and would be a prerequisite for explaining observed trends item by item and making sense of the discrepancies between deviation predictions of bounded and unbounded conductors.

To substantiate the proposed general view, consider the following observations:

1. Deviations for bounded conductors (bounded deviations) strongly depend on θ_{FT} whereas this is not true for unbounded conductors.

2. For LRG, deviations at $\theta_{FT}=22°$ suddenly become resolvable at 10^4Hz at all source eccentricities and orientations except for radial sources at eccentricity 0.8. In addition, deviations at $\theta_{FT}=68°$ suddenly become unresolvable in the same circumstances.

Item 1 can be seen to support the conclusion by noting that θ_{FT} is the phase in fourier sine and cosine transforms. From this, it is clear that if each fourier component of bounded deviations depend on θ_{FT}, each component must depend on the self-superposition of the corresponding fourier component of the electromagnetic field. But then, if this were the case, why would the same phases be unresolvable at each of the frequencies examined? Shouldn't phase dependence be dependent on frequency? A possible explaination is that, because all frequencies examined are low, the effective wavelengths of the electromagnetic fields in question are much longer than the size of the media considered. In other words, for a given medium, if the generated electromagnetic fields have a wave length much larger than the size of the medium, the initial topology of all frequencies studied should be approximately the same. Indeed, wavelength estimates shown in table 9-2 are much larger than the head sizes used.

TABLE 9-2 Wavelength, in meters, predicted by unbounded medium models. Values are to be compared with 0.12m, the largest head size used.

medium ⟶ / frequency ↙	vacuum	skull	brain	cerebral spinal fluid
10Hz	9.0(16)	8.4(3)	2.4(3)	8.1(2)
50	1.8(15)	3.8(3)	1.1(3)	3.6(2)
500	1.8(14)	1.2(3)	3.4(2)	1.2(2)
10^3	9.0(13)	8.4(3)	2.4(2)	8.2(1)
10^4	9.0(12)	2.7(2)	7.6(1)	2.6(1)

These estimates of wavelength were found by considering the solutions to equations 2-25b for the case of unbounded media with the source developed in section 3. In final support of the hypothesis, note that only for LRG does a dramatic change in phase dependence occur as frequency is changed (item 2 above). Furthermore, this change occurs only in increasing frequency from 10^3Hz to 10^4Hz. From this, a possible conclusion is that only for LRG is there a large enough change, as frequency is increased, in the ratio between the effective wavelength of the electromagnetic fields and the size of the conductor. The observation seems quite peculiar since, given estimates of table 9-2, the change in the ratio seems trivial.

Another observation I would like to discuss is the distinct difference between CSF and all other media with respect to dependence on phase. A possible explaination comes from considering the mechanical analogy of a string bound to a post. We all know that the phase of a wave reflected at the post depends on whether the string is tightly bound to the post or is allowed to slip along the post. Using *stiffness* of the conductor/insulator interface to refer to, analogously, how tightly the string is bound to the post, SKL, SML, MED, and LRG must have similar degrees of *stiffness* with respect to the *stiffness* of CSF. Considering the conductivity gradients CSF $\approx 10^4$, SML, MED, and LRG $\approx 10^3$, and SKL ≈ 14, the observation in question seems to be inconsistent with the proposed view. However, considering the unnormalized conductivity values for each medium type (tables 8-7), if the measure of *stiffness* is more dependent on the absolute difference in conductivity between the medium and the surrounding space than on the conductivity gradient, consistency would be achieved. This would be true if generated electromagnetic fields had effective wavelengths much larger than $\Sigma\bar{l}$ for each medium type; I have already substantiated this stipulation. In this regard, the observation being discussed is

another item showing that the proposed general view of the situation has some interpretive power.

9.3 Concluding discussion

It is important to clarify what deviation trends can tell us about the electric and magnetic fields themselves. Note that for frequency independent Maxwell's equations, $\vec{E}$ is independent of $\vec{B}$ but the converse is not true. With this observation, it seems reasonable to interpret the deviation measure as the extent to which $\vec{E}$ depends on $\vec{B}$; we cannot make the corresponding statement for $\vec{B}$. Taking another view of the situation, because of spacial derivatives in equations 2-8, a non-zero deviation for $\vec{A}$ definitely means $\vec{E}$ is perturbed from the ω=0 solution but does not necessarily imply $\vec{B}$ is perturbed. In addition, taking equation 2-10a into consideration, a non-zero deviation for Φ would mean $\vec{E}$ is perturbed from the ω=0 solution. This supports the proposed interpretation and qualification.

With this interpretation in mind, I will now summarize the major results and findings of this dissertation.

1. The relationship between cerebral currents and source terms of Maxwell's model has been clarified.

2. It has been shown that for frequency dependent fields and media considered here, boundary condition techniques cannot be used to derive boundary integral formulations of Maxwell's model.

3. It has been shown that simple continuous models for electromagnetic parameters can be successfully applied to obtain boundary integral formulations.

4. In the circumstances studied, the magnitude of the dependence of $\vec{E}$ on $\vec{B}$

has been found to be small.

5. Evidence has been found to support this hypothesis: the coupling of $\vec{B}$ to $\vec{E}$ depends on electromagnetic interference phenomena within spacially finite conductors even for extremely low frequency fields.

I would like to make a few remarks about item 5. Considering, from table 9-2, that head sizes are much smaller than the estimated wavelength of all frequency components studied, the interpretation summarized in item 5 seems a bit strange. According to estimates of wavelength, superposition effects would have to arise from very small spacial variations in the fields. The estimates also predict that attenuation of the electric field with distance would be dominated by an inverse cubed law. This is to be compared to the attenuation at large distances from the source where exponential attenuation, on the order of a wavelength, is dominant. Comparing the two situations emphasizes that, for frequencies examined here, the size of a typical head occurs within a region about internal sources where reflected energy should make an insignificant contribution to the net field. On the other side of the argument, observations indicating the role of superposition are expected since large differences between wavelengths in a vacuum and wavelengths in the conductors of table 9-2 indicate that most of the electromagnetic energy is internally reflected. I would also like to say that one of the main observations indicating the role of superposition, phase dependence, does not seem to be simply an artifact of applying Cimmino's process; the observed patterns of phase dependence can be observed without using this stage in estimating solutions to equations 5-4. The patterns can be found by examining residuals calculated from using $\omega=0$ solutions in equations 6-9 where $\omega\neq0$. The observations are made based on assuming that large residuals indicate that larger deviations between $\omega=0$ and $\omega\neq0$ solutions exist. The assumption is substantiated by noting that residuals

were observed to increase with frequency as expected. Finally, I would like to note that though reflected electromagnetic energy may be insignificant at most points in the conductors, this may not be so in a locus of points about the conductor/insulator interface. Recall that it is at this interface where deviation measures are evaluated.

What are the implications of these results? Item 4 suggests that frequency dependence can be ignored when modeling bioelectromagnetism. On the other hand, item 5 suggests that there may be special circumstances wherein frequency dependence has an important role in determining the topology of electromagnetic fields in the brain. Might the difference between frequency dependent and frequency independent fields be behaviorally significant? There have been experiments demonstrating that low frequency, low power, externally generated electromagnetic fields can influence behavior [1]. For example, 7-10Hz fields, estimated to result in 10^{-5}Volts/meter electric potential gradients with the brain, have been found to effect the ability of monkeys to estimate duration. It is possible that the strengh of frequency dependent fields differ from that of frequency independent fields on this scale. If deviations of tables 8-7 were assumed to estimate the degree $\nabla\Phi|_{\omega\neq 0}$ differs from $\nabla\Phi|_{\omega=0}$ at the scalp, for a typical auditory evoked source where $\nabla\Phi|_{\substack{\text{exp(imentally)}\\\text{(measured)}}}$ is on the order of $2x10^{-4}$V/m, 10^{-5}V/m is achieved with a deviation of approximately 10%. At the cortex, for a typical visually evoked source where $\nabla\Phi|_{exp}$ is on the order of $7x10^{-3}$V/m, 10^{-5}V/m is achieved with a deviation below 1%. Given this analysis, data of tables 8-7 indicate a slight chance for behavioral significance. Theoretical results should be generally applicable to model electromagnetic fields in bounded conductors with internal sources. Experimental results for the brain may suggest how to efficiently explore these equations for other circumstances.

Regarding future investigations suggested by this work, electrolytic tank experiments must be performed to test the validity of the calculations presented. The major problem for future investigation suggested by this work is the problem of finding a simple model for Φ and $\vec{A}$ that would be consistent with the experimental data. Only with such a model will we be able to understand how spacial frequencies of $\vec{E}$ and $\vec{B}$ depend on ω, source parameters, and parameters of the conductor. Given a model with an explicit parameter for spacial frequency, we must derive predictions for interference patterns that would arise within the conductor. Only then could we begin to understand how interference phenomena can force $\vec{E}$ to have a large or negligible dependence on $\vec{B}$.

10. References

[1] Adey W.R., "Tissue interactions with nonionizing electromagnetic fields", *Phys. Rev.*, v61, n2, Apr., 1981, p435-514.

[2] Aidley D.J., *The Physiology of Excitable Cells*, Cambridge University Press, 1978.

[3] Anselone P.M., "Convergence and error bounds for approximate solutions of integral and operator equations" in *Error in Digital Computation vII*, ed. Rall L.B., John Wiley and Sons, 1965.

[4] Anselone P.M., Opfer G., "Numerical integration of weakly singular functions" in *Numeriche Integration v1 n7*, ed. Herausgegeben von G. Hamonerlin, M., Birkhauser Verlag, 1979.

[5] Anselone P.M., "Singularity subtraction in the numerical solution of integral equations", *J. Austral. Math. Soc. Series B*, v22, 1981, p408-418.

[6] Atkinson K.E., "The numerical solution of Fredholm integral equations of the second kind", *SIAM J. Num. Anal.*, v4, n3, 1967, p337-348.

[7] Atkinson K.E., "The solution of non-unique linear integral equations", *Num. Math.*, v10, 1967, p117-124.

[8] Atkinson K.E., "The numerical solution of Fredholm integral equations of the second kind with singular kernels", *Num. Math.*, v19, 1972 p248-259.

[9] Atkinson K.E., *A Survey of Numerical Methods for the Solution of Fredholm Integral Equations of the Second Kind*, Society for Industrial and Applied Mathematics, 1976.

[10] Atkinson K.E., *An Introduction to Numerical Analysis*, John Wiley and Sons, 1978, p268-279.

[11] Atkinson K.E., "Numerical integration on the sphere", *J. Austral. Math. Soc. Series B*, v23, 1982, p332-347.

[12] Atkinson K.E., "Addendum to numerical integration on the sphere", Preprint.

[13] Atkinson K.E., "The numerical solution of Laplace's equation in three dimensions", *SIAM J. Num. Anal.*, v19, n2, Apr., 1982, p263-274.

[14] Atkinson K.E., "An integral equation program for Laplace's equation in three dimensions",*ACM Trans. Math. Software*, v11, n2, 1985, p85-96.

[15] Atkinson K.E., "The numerical evaluation of particular solutions for Poisson's equation", Preprint.

[16] Baker C.T.H., *The Numerical Treatment of Integral Equations*, Oxford University Press, 1977.

[17] Balchin M.J., Davidson J.A.M., "Numerical method for calculating magnetic-flux and eddy-current distributions in three dimensions", *IEEE Proc. Part A*, v127, n1, Jan., 1980, p46-53.

[18] Baldwin A.F., Rush S., "Comparison of theoretical with measured forward ECG solutions: a progress report", *Compu. and Biomed. Res.*, v15, 1982, p485-501.

[19] Barnard A.C.L., Duck I.M. Lynn M.S., "The application of electromagnetic theory to electrocardiology: I. derivation of the integral equations", *Biophys. J.*, v7, 1967, p443-462.

[20] Barnard A.C.L., Duck I.M. Lynn M.S., Timlake W.P., "The application of electromagnetic theory to electrocardiology: II. numerical solution of the integral equations", *Biophys. J.*, v7, 1967, p463-491.

[21] Barnes W.J., Davey K.R., "Magnetic field calculation of time varying vertical and horozontal electric current dipoles in a conducting half space via the T-Ω method", *IEEE Trans. Mag.*, v19, n6, Nov., 1983, p2710-2714.

[22] Basar E., *EEG Brain Dynamics*, North Holland Biomedical Press, 1980.

[23] Biddlecombe E.A., Heighway E.A., Simkin J., Trowbridge C.W., "Methods for eddy current computation in three dimensions", *IEEE Trans. Mag.*, v18, n2, Mar., 1982, p492-497.

[24] Bodewig E., *Matrix Calculus*, North Holland, 1959.

[25] Brody L.A., Terry F.H., Ideker R.E., "Eccentric dipole in a spherical medium: generalized expression for surface potentials", *IEEE Biomed. Eng.*, v1, Mar., 1973, p141-143.

[26] Caldwell J. "Computational methods for solving the Dirichlet problem via Fredholm integral equations", *J. Appl. Phys.*, v53, n7, Jul., 1982, p4567-4570.

[27] Carpenter C.J. "Finite-element network models and their application to eddy-current problems", *IEE Proc.*, v122, n4, Apr., 1975, p455-462.

[28] Carpenter C.J. "Comparison of alternative formulations of 3-dimensional magnetic-field and eddy-current problems at power frequencies", *Proc. IEE*, v124, n11, Nov., 1977, p1026-1034.

[29] Clapp R.E. "Zipper transition in an alpha-helix: a mechanism for gating of voltage-sensitive ion channels in a biological membrane", *J. Theoret. Biol.*, v104, 1983, p137-158.

[30] Cohen D., Hosaka H., "Magnetic field produced by a current dipole part II", *J. Electrocard.*, v9, n4, 1976, p409-417.

[31] Cohen D., Cuffin B.N., "Demonstration of useful differences between magnetoencelphalogram and electroencephalogram", *EEG Clin. Neurophys.*, v56, 1983, p38-51.

[32] Courant R., Hilbert D., *Methods of Mathematical Physics vI*, Interscience Publishers, Inc., 1953, p358.

[33] Craven P., Wahba G., "Smoothing noisy data with spline functions", *Num. Math.*, v31, 1979, p177-403.

[34] Cuffin B.N., Cohen D., "Magnetic fields produced by models of biological current sources", *J. App. Phys.*, v48, n9, Sept., 1977, p3971-3980.

[35] Cuffin B.N., Cohen D. "Comparison of the magnetoencephalogram and electroencephalogram", *EEG Clin. Neurophys.*, v47, 1979, p132-146.

[36] Darcey T.M., *Methods for Localization of Electrical Sources in the Human Brain and Applications to the Visual System*, Ph.D. Dissertation, California Institute of Technology, 1979.

[37] Davey, K.R., Barnes W.J., "Three-dimensional eddy current problems using the T-Ω method and Fredholm integral equations", *IEEE Trans. Mag*, v19, n2, Mar. 1983, p120-125.

[38] Davidson J.A.M., Balchin M.J., "Three-dimensional eddy-current calculations using loop variables to represent magnetic vector potential in conducting regions", *IEE Proc. Part A*, v131, n8, Nov., 1984, p577-583.

[39] Eriksen J.K., *Biophysical Modeling of some Exogenous and Endogenous Components of the Human Event Related Potential*, Ph.D. Dissertation, California Institute of Technology, 1984.

[40] Feldstein A., Miller R.K. "Error bounds for compound quadrature of weakly singular integrals", *Math. Computa.*, v25, n115, Jul. 1971, p505-520.

[41] Feynman R.P., Leighton R.B., Sands M., *The Feynman Lectures on Physics II: Mainly Electromagnetism and Matter*, Addison-Wesley, 1964.

[42] Frank E., "Electric potential produced by two point current sources in a homogeneous conducting sphere", *J. Appl. Phys.*, v23, n11, Nov., 1952, p1225-1229.

[43] Freeman W.J., *Mass Action in the Nervous System*, Academic Press, 1975.

[44] Gardner-Medwin A.R., "The migration of potassium produced by electric current through brain tissue", *Proc. Physiol. Soc.*, Mar., 1977, p32P-33P.

[45] Gardner-Medwin A.R., "Measurements of extracellular potassium and calcium concentration during passage of current across the surface of the brain", *Proc. Physiol. Soc.*, Nov., 1977, p66P-67P.

[46] Gardner-Medwin A.R., "The amplitude and time-course of extracellular potassium concentration changes during potassium flux through brain tissue", *Proc. Physiol. Soc.*, Jul., 1978, p38P-39P.

[47] Gardner-Medwin A.R., "The mechanism of potassium dispersal in brain tissue", *Proc. Physiol. Soc.*, Apr., 1979, p37P-38P.

[48] Gastinel N., *Linear Numerical Analysis*, Hermann Press, 1970, p160-162.

[49] Geddes L.A., Baker L.E., "The specific resistance of biological material-- a compendium of data for the biomedical engineer and physiologist", *Med. Biol. Eng.*, v5, 1967, p271-293.

[50] Geselowitz D.B., "The concept of an equivalent cardiac generator", in *Biomedical Sciences Instrumentation v1* ed. Alt F., Plenum Press, 1963, p325-329.

[51] Geselowitz D.B., "On bioelectric potential in an inhomogeneous volumn conductor", *Biophys. J.*, v7, 1967, p1-11.

[52] Geselowitz D.B., "On the magnetic field generated outside and inhomogeneous volumn conductor by internal current sources", *IEEE Trans. Mag.*, v6, n2, Jun. 1970, p346-347.

[53] Grynszpan F., Geselowitz D.B., "Model studies of the magnetocardiogram", *Biophys. J.*, v13, 1973, p911-925.

[54] Gulrajani R.M., Mailloux G.E. "A simulation study of the effects of torso inhomogenaities on electrocardiographic potentials using realistic heart and torso models", *Circula. Res.*, v52, n1, Jan., 1983, p45-56.

[55] Heringa A., Stegeman D.F., Uijen G.J.H., De Weerd J.P.C., "Solution methods of electical field problems in physiology", *IEEE Trans. Biomed. Eng.*, v29, n1, Jan., 1982, p34-42.

[56] Hodgkin A.L., Rushton W.A.H., "The electrical constants of a crustacean nerve fiber", *Proc. Roy. Soc. London Series B*, v133, 1946, p444-479.

[57] Hodgkin A.L., Huxley A.F., "A quantitative description of membrane current and its application to conduction and excitation in nerve", *J. Physiol. London*, v117, 1952, p500-544.

[58] Hosek R.S., Sances A., Jodat R.W., Larson S.J., "The contributions of intracerebral currents to the EEG and evoked potentials", *IEEE Biomed. Eng.*, v25, n5, Sept., 1978, p405-413.

[59] Houstis E.N., Papatheodorou T.S., "A collocation method for Fredholm integral equations of the second kind", *Math. Computa.*, v32, n141, Jan., 1978, p159-173.

[60] Humphrey D.R., "Re-analysis of the antidromic cortical response: I potentials evoked by stimulation of the isolated pyramidal tract", *EEG Clin. Neurophys.*, 1968, p116-129.

[61] Humphrey D.R., "Re-analysis of the antidromic cortical response: II on the contribution of cell discharge and PSPs to the evoked potentials", *EEG Clin. Neurophys.*, 1968, p421-442.

[62] Isaacson E., Keller H., *Analysis of Numerical Methods*, John Wiley and Sons, 1966, chap. 7.

[63] Kammerer W.J., Nashed M.Z., "Iterative methods for best approximate solutions of linear integral equations of the first and second kinds", *J. Math. Anal. Appl.*, v40, 1972, p547-573.

[64] Kantorovich L.V., Krylov V.I., *Approximate Methods of Higher Analysis*, Interscience Publishers, Inc., 1958.

[65] Kel'zon A.A., "Interpolation on a sphere", *Izvestiya VUZ. Matematika*, v19, n11, 1975, p41-46.

[66] Kosterich J.D., Foster K.R., Pollack S.R., "Dielectric permittivity and electrical conductivity of fluid saturated bone", *IEEE Trans. Biomed. Eng.*, v30, n2, Feb., 1983, p81-86.

[67] Kriezis E.E., Cangellaris A.K., "An integral equation approach to the problem of eddy currents in cylindrical shells of finite thickness with infinite or finite length", *Archiv Elektrotechnik*, v67, 1984, p317-324.

[68] Kuffler S.W., Nicholls J.G., Orkland R.K., "Physiological properties of glial cells in the central nervous system of amphibia", *J. Neurophys.*, 1966, p268-787.

[69] Kuffler S.W., Potler D.D., "Glia in the leech central nervous system: physiological properties and neuron-glia relationship", *J. Neurophys.*, v27, 1966, p290-320.

[70] Kuffler S.W., Nicholls J.G. , *From Neuron to Brain*, Sinauer Associates, Inc., 1977.

[71] Levin M., "On the evaluation of double integrals", *Math. Computa.*, v39, n159, Jul., 1982, p173-177.

[72] Lin T.C. "The numerical solution of Helmholtz's equation for the exterior Dirichlet problem in three dimensions", *SIAM J. Num. Anal.*, v22, n4, Aug., 1985.

[73] Lubinsky D.S., Rabinowitz P., "Rates of convergence of Gaussian quadrature for singular integrands", *Math. Computa.*, v43, n167, Jul., 1984, p219-242.

[74] Lynn M.S., Timlake W.P., "The numerical solution of singular integral equations of potential theory", *Num. Math.*, v11, 1968, p77-98.

[75] Lynn M.S., Timlake W.P., "The use of multiple deflations in the numerical solution of singular systems of equations, with applications to potential theory", *SIAM J. Num. Anal.*, v5, n2, Jun., 1968, p303-322.

[76] Mayergoyz I.D., "Boundary integral equations of minimum order for the calculation of three-dimensional eddy current problems", *IEEE Trans. Mag.*, v18, n2, Mar., 1982, p536-539.

[77] Mitzdorf U., Singer W., "Prominent excitatory pathways in the cat visual cortex (A17 and A18): a current source density analysis of electrically evoked potentials", *Exp. Brain Res.*, v33, 1978, p371-394.

[78] Morisue T., "Magnetic vector potential and electric scalar potential in 3-dimensional eddy current problem", *IEEE Trans. Mag.*, v18, n2, Mar., 1982, p531-535.

[79] Nakayama K., "The relationship of visual evoked potentials to cortical physiology" in *Ann. N.Y. Acad. Sci. v388*, ed. Wollner B., p21-34.

[80] Nicholls J.G., Kuffler S.W., "Extracellular space as a pathway for exchange between blood and neurons in the central nervous system of the leech: ionic composition of glial cells and neurons", *J. Neurophys.*, v27, 1964, p645-671.

[81] Nicholson C., Freeman J.A., "Theory of current source density analysis and determination of conductivity tensor for anuran cerebellum", *J. Neurophsy.*, v38, 1975, p356-368.

[82] Nunez P., *Electric Fields of the Brain*, Oxford University Press, 1981.

[83] Penman J., Fraser J.R., "Unified approach to problems in electromagnetism", *IEE Proc. Part A*, v131, n1, Jan., 1984, p55-61.

[84] Pickard W.F., "Generalizations of the Goldman-Hodgkin-Katz equation", *Math. Biosci.*, v30, 1976, p99-111.

[85] Pickard W.F., Lettvin J.Y., "A physical model for the passage of ions through an ion-specific channel -- I. the sodium-like channel", *Math. Biosci.*, v32, 1976, p37-50.

[86] Pickard W.F., Lettvin J.Y., "A physical model for the passage of ions through an ion-specific channel -- I. the potassium-like channel", *Math. Biosci.*, v32, 1976, p51-61.

[87] Pilkington T.C., Morrow M.N., Stanley P.C., "A comparison of finite element and integral equation formulations for the calculation of electrocardiographic potentials", *IEEE Trans. Biomed. Eng.*, v32, n2, Feb., 1985, p166-173.

[88] Plonsey R., *Bioelectric Phenomena*, McGraw Hill, Inc., 1969.

[89] Polgorzelski W., *Integral Equations and their Application Vol. I*, Permagnon Press, 1966.

[90] Preston T.W., Reece A.B.J., "Solution of 3-dimensional eddy current problems: the T-Ω method", *IEEE Trans. Mag.*, v18, n2, Mar. 1982, p486-491.

[91] Rall W., "Electrophysiology of a dendritic neuron model", *Biophys. J.*, v2, n2, 1962, p145-166.

[92] Rall W., Shepherd G.M., "Theoretical reconstruction of field potentials and dendrodendritic synaptic interactions in olfactory bulb", *J. Neurophys.*, v31, 1968, p884-915.

[93] Rall W., "Dendritic neuron theory and dendrodendritic sysnapses in a simple cortical system", in *Neurosciences 2 sup nd Study Program*, 1970, p552-565.

[94] Rall W., "Core conductor theory and cable properties of neurons" in *Handbook of Physiology Sec. 1 Vol. 1*, Sec. ed. Brookhart J.M., Mountcastle V.B., Vol. ed. Kandel E.R., Exec. ed. Geiger S.R., 1977.

[95] ed. Rektorys K., *Survey of Applicable Mathematics*, MIT University Press, 1969.

[96] Rodger D., "Finite-element method for calculating power frequency 3-dimensional electromagnetic field distributions", *IEE Proc. Part A*, v1130, n5, Jul., 1983, p233-238.

[97] Rush S., Driscoll D.A., "Current distribution in the brain from surface electrodes", *Anasthe. Analge.*, v47, 1968, p717-723.

[98] Rush S., "On the independence of magnetic and electric body surface recordings", *IEEE Trans. Biomed. Eng.*, v22, n3, May, 1975, p157-167.

[99] Salu Y., "Implementing a consistency criterion in numerical solution of the bioelectric forward problem", *IEEE Trans. Biomed. Eng.*, v27, n6, Jun., 1980, p338-341.

[100] Schwan H.P., "Electrical properties of tissue and cell suspensions", *Advan. Biol. Med. Phys.*, v5, 1957, p147-209.

[101] Schwan H.P., Kay C.F., "The conductivity of living tissues", *Ann. N.Y. Acad. Sci.*, v65, 1957, p1007-1013.

[102] Simkin J., "A comparison of integral and differential equation solutions for field problems", *IEEE Trans. Mag.*, v18, n2, Mar., 1982, p401-405.

[103] Smith D.B., Sidman R.D., Henke J.S., Flanigin H., Labiner D., Evans C.N., "Scalp and depth recordings of induced deep cerebral potentials", *EEG Clin. Neurophys.*, v55, 1983, p145-150.

[104] ed. Spector W.S., *Handbook of Biological Data*, W.B. Saunders Co., 1956.

[105] Stoy R.D., Foster K.R., Schwan H.P., "Dielectric properties of mammalian tissues from 0.1 to 100MHz: a summary of recent data", *Phys. Med. Biol.*, v27, n4, 1982, p501-513.

[106] Tikhonov A.N., Arsinin V.Y., *Solutions of Ill-posed Problems*, John Wiley and Sons, 1977.

[107] Vainikko G., Pedas A., "The properties of solutions of weakly singular integral equations", *Austral. Math. Soc. Series B*, v22, 1981, p419-430.

[108] Van Oostrom A., Strackee J., "The solid angle of a plane triangle", *IEEE Trans. Biomed. Eng.*, v30, n2, Feb., 1983, p125-126.

[109] Vaughan H.G., "The neural origins of human event related potentials" in *Annals N.Y. Academy of Sciences Vol. 388*, ed. Wollner B., 1982, p125-138.

[110] Wahba G., "Spline interpolation and smoothing on the sphere", *SIAM J. Sci. Stat. Comput.*, v2, n1, Mar., 1981, p5-16.

[111] Wahba G., "Erratum: spline interpolation and smoothing on the sphere", *SIAM J. Sci. Stat. Comput.*, v3, n3, Sept., 1982, p385-386.

[112] Wikswo J.P., "Cellular action currents" in *Biomagnetism*, eds. Williamson S.J., Romani G.L., Kaufman L., Modena I., 1983.

[113] Williamson S.J., Kaufman L., "Biomagnetism", *J. Magnetism Magnetic Mater.*, v22, n2, 1981, p129-201.

[114] Witwer J.G., Trezek G.J., Jewett D.L., "The effect of media inhomogenaities upon intracranial electric fields", *IEEE Trans. Biomed. Eng.*, v19, n5, Sept., 1972, p352-362.

[115] Wood C.C., Allison T., "Interpretation of evoked potentials: a neurophysiological perspective", *Canad. J. Psychol. Rev. Canad. Psychol.*, v35, n2, 1981, p113-135.